N° d'ordre: 41712

Université Lille 1

Centre de Recherche en Informatique, Signal
et Automatique de Lille, UMR 9189
Ecole Doctorale Sciences de l'Ingénieur de Lille EDSPI 072

Thèse de doctorat

Présentée en vue d'obtenir le grade de docteur
Spécialité automatique et informatique industrielle
par

Xian ZHANG

Fault-tolerant Control Scheme for Linear Systems with Input Constraints and Actuator Faults

Soutenue publiquement le 30/03/2015 devant le jury composé de

Composition du jury

Rapporteurs :	**Didier Theilliol**	Professeur, Université de Lorraine
	Steven Ding	Professeur, University of Duisburg-Essen
Examinateurs :	**Olivier Sename**	Professeur, ENSE3 Grenoble
	Laurentiu Hetel	Chargé de Recherche, CNRS Lille
	Rochdi Merzouki	Professeur, Université Lille1
Directeur :	**Vincent COCQUEMPOT**	Professeur, Université Lille 1

" All good things must come to an end. And this too, Shall pass away. "

King Solomon

Acknowledgements

I would like to express my gratitude to all those who helped me during my PhD study in France.

My deepest gratitude goes first and foremost to Professor Vincent COCQUEMPOT, my supervisor, for his constant encouragement, valuable guidance and instructive suggestions on my thesis. I am deeply grateful of his help in my study here and in the completion of this thesis.

My thanks would go to my beloved family, for their loving considerations and great confidence all through these three years. I really thank them for supporting my choice of studying PhD in France at the beginning. And through the process of researching and writing thesis, they also tolerate a lot of my complains.

I would also like to thank Severus Costantin OLTEANU for his very help during my study. My thanks also go to the entire group in laboratory, for their numerous conversations and help.

Also many thanks to my Chinese friends in Lille, Paris, Nantes, Lyon and Marseille, for their accompany during my life in France.

Finally, I want to express my acknowledge to Professor Steven DING, University of Duisburg-Essen (Germany) and Professor Didier THEILLIOL, University of Lorraine (France) who accepted to review this manuscript, and also to Professor Olivier Sename, ENSE3 Grenoble (France), Dr. Laurentiu Hetel, CNRS Lille (France) and Professor Rochdi Merzouki, University of Lille 1 (France) who attended my oral defence and gave useful comments to this thesis.

Thank you!

To my loved parents Anying WU and Jinxiang ZHANG

To my loved Lu WANG

Contents

List of Figures

List of Tables

Acronyms

FTC	**F**ault-tolerant **C**ontrol
FTCS	**F**ault-tolerant **C**ontrol **S**ystems
PFTCS	**P**assive **F**ault-tolerant **C**ontrol **S**ystems
LQG	**L**inear **Q**uadratic **G**aussian
AFTCS	**A**ctive **F**ault-tolerant **C**ontrol **S**ystems
GS	**G**ain **S**cheduling
SISO	**S**ingle **I**nput **S**ingle **O**utput
MIMO	**M**ultiple **I**nput **M**ultiple **O**utput
LQR	**L**inear **Q**uadratic **R**egulartor
PIM	**P**seudo-**I**nverse **M**ethod
GS	**G**lobal **S**tabilization
SGS	**S**emi-**G**lobal **S**tabilization
MPC	**M**odel **P**redictive **C**ontrol
LMI	**L**inear **M**atrix **I**nequality
ISS	**I**put to **S**tate **S**tability
IMU	**I**nertial **M**easurement **U**nit
AFD	**A**ctive **F**ault **D**iagnosis
FDI	**F**ault **D**iagnosis and **I**dentification

Abstract

Because of the growing demands for reliability and maintainability, a lot of significant researches on fault-tolerant control systems have been conducted in the past decades. Among these researches, few involve input constraints for actuators. If saturation effects are not taken into account in control design, severe performance degradation or even instability may result. In order to guarantee the system's stability under nominal and faulty situations while providing an acceptable performance, it has a great meaning to study FTC design methods for systems with actuator saturation.

In this thesis, we deal with the FTC design problem for a linear system with both input constraints and actuator faults.

For the nominal system, a low-high gain controller is designed based on the Lyapunov stability theory and the solution of LMI. An iterative Ricatti equation algorithm is given to find such controller. Based on the designed controller, with the analysis of the linear system subject to actuator saturation, the invariant ellipsoids of attraction and performance regions are calculated. For the case that the initial state is not within the attraction region, a novel methodology based on the reference adjustment technique is proposed in the thesis to achieve large-region stabilization.

For the system with certain actuator faults, the fault's influence is analysed first, its size and the time when it happens will decide whether the system is stable or not and will influence the system's performance. Then two main FTC design methods (PFTC and AFTC) are used to cope with faults and actuator saturation together. The proposed PFTC and AFTC methods have both their restrictions when dealing with the input saturation problem : Since the passive fault-tolerant controller is designed for presumed faults, it can guarantee that the system operates with degraded performance in a small stability region which is decided by the worst fault case. For the AFTC method, the degraded performance caused by faults will be recovered by designing an observer to obtain the fault information. However, its control capability will be reduced due to the fault, and it is hard to analyse the system's stability region. Based on the existing performance analysis principle and the implementation results of PFTC and AFTC, a novel fault-tolerant control scheme based on the reference adjustment technique is proposed to guarantee the system's performance in an acceptable region.

Several academic examples are taken all along the thesis to illustrate the methods. Finally, the methodology is applied to the path tracking problem of an electric vehicle (EV) which has four electromechanical wheel-driven (4WD vehicle) systems under normal and faulty conditions. With considering wheel slip constraints and certain faults, a controller based on low-high gain control is developed to maintain the system's stability and guarantee the acceptable tracking performance. Then based on the designed controller, a simple active fault diagnosis approach is introduced for this typical over-actuated system to isolate and to evaluate faults more precisely. With the diagnosed information, an accommodated fault-tolerant controller is designed to maintain the tracking performance as best as possible.

Keywords: Fault-tolerant control; Fault diagnosis; Actuator saturation; Actuator fault; Domain of attraction; Domain of performance; Reference adjustment Technique; Low-high-gain control;

Notations

Throughout this thesis, A' or A^T denotes the transpose of the matrix A, A^- denotes the inverse matrix of the matrix A, A^+ denotes the pseudo inverse matrix of the matrix A, $\lambda(A)$ denotes the set of eigenvalues of the matrix A, $\lambda_{min}(A)$ and $\lambda_{max}(A)$ denote, respectively, the minimal and maximal eigenvalues of the matrix A, I_r denotes the identity matrix of dimension $r \times r$, $\|x\|$ denotes the Euclidean norm of $x \in R^n$.

Chapter 1

LITERATURE REVIEW, MOTIVATIONS AND OBJECTIVES OF THE THESIS

Contents

Abstract In this chapter, a review of the existing fault-tolerant control (FTC) approaches and of the current literatures on FTC with actuator saturation is provided. The motivations and objectives of this thesis are also given.

1.1 Fault-tolerant Control Systems

1.1.1 Needs of fault-tolerant control systems

Modern technological systems rely on sophisticated control systems to meet increased performance and safety requirements [1]. For such systems where security and reliability requirements are critical, one tiny fault may have catastrophic consequences not only on the system itself but also on its environment. Several incidents had occurred that motivate the development of efficient diagnosis methods and control approaches to tolerate potential faults while maintaining the systems' stability and performance properties. Examples of such incidents are the following:

On December 2nd, 1984, a gas leak incident occurred at the Union Carbide India Limited (UCIL) pesticide plant in Bhopal, India. This disaster caused a total of 3,787 deaths and 558,125 injuries. It is considered as the world's worst industrial disaster.

From August, 1998 to May, 1999, the Americans' carrier rockets *Hercules*, *Athena* and *Delta* had five launch failures in a short period of 10 months, resulting in the economic loss of more than 30 billions which forced NASA to stop all commercial launch plans for the US space programs.

On December 12th, 2002, only three minutes after launching, the *Ariane*-5 rocket exploded and two satellites crashed into the Atlantic. On February 1st, 2003, the space shuttle *Columbia* exploded, all seven astronauts abroad died in this disaster.

Designing fault-tolerant control systems (FTCS) drew more and more attention in industry and research laboratories. Many application areas where security, safety

and reliability must be guaranteed, are concerned as for instance communication, railway transport, energy, electric power, nuclear power plant and aerospace.

Improving the fault tolerance ability of control systems is a hot topic for researchers now. The key methods vary from improving the reliability of components and of the system itself, to implementing fault diagnosis and fault-tolerant control algorithms. In the following, we will mainly focus on fault-tolerant control algorithms.

1.1.2 Fault-tolerant control systems

Fault-tolerant techniques are mainly developed for computer systems to continue a fully, perhaps a degraded operation when some partial failures occur. Introducing this concept to control systems leads to the idea of fault-tolerant control (FTC)[2].

A fault-tolerant control enables a system to continue its original mission when some components of the system fail, possibly with degraded performance. If the closed-loop system is maintained stable with an acceptable performance in faulty situations, this system is called a fault-tolerant control system (FTCS)[3].

1.1.2.1 Classification of fault-tolerant techniques

Fault-tolerant techniques can be divided into two types: system architecture based fault-tolerant technique and fault-tolerant control methods.

1. **System architecture based fault-tolerant technique**. This technique is mainly based on hardware redundancy. This redundancy technique is applied on control units, actuators and sensors. When some of the actuators, sensors or key components fail, in order to maintain the same or degraded performance (within a specified level), the failed parts will be isolated by a monitoring system and they will be replaced by their redundant components. This technique improves the reliability by increasing the number of components with the direct consequence of increasing the cost of the whole system. In many applications, it is impossible to implement a huge number

of redundancies for all the system units, therefore other techniques based on software tools arise.

2. **Fault-tolerant control methods**. This technique relies on software. Software programes including different control laws and control strategies are implemented in control unit. The main purpose is to reconfigure the existing hardware or software when faults occur. When some components fail, in order to maintain the system within the acceptable performance region, the other unfailed components which can have the same effect to the system are used to replace the faulty ones. The fault-tolerant reconfiguration control, as a kind of switching control, is one important method. Based on the fault information from fault diagnosis system, it can reconfigure the structure of the controller in order to achieve fault-tolerant capability. Another used method is fault accommodation where the estimated fault is used in the control law, such that the closed loop faulty system maintains acceptable performance.

1.1.2.2 Characteristics of fault-tolerant control systems

One can improve the reliability of a system through hardware redundancies or reconfiguration control methods. A typical FTCS includes a control unit, actuators and sensors. The role of the control unit is not only to calculate the control law, but also to implement other algorithms as estimation or monitoring functions.

A FTCS has the following characteristics:

1. A FTCS is more complex than a classical control system. The structure with hardware and software redundancies is more complex than a single-channel system which can achieve the same operation. Besides, after detecting and isolating the failed part, the system structure will change, which makes the design of the control law much more difficult.

2. Hardware and software are interrelated. Since hardware and software are functionally interrelated, they must be coupled with each other when faults occur. Usually, a hardware or software fault may spread and cause a fault in other parts. Thanks to the development of computer technology, some

functions of the control system can be realized through either hardware or software components. For example, a state observer may be used instead of a physical sensor and is sometimes called as a soft or virtual sensor.

1.1.3 Fault-tolerant control methodology

Generally speaking, FTCS can be classified into two types: passive (PFTCS) [4] and active (AFTCS) [5]. In PFTCS, controllers are fixed and they are designed to be robust against a class of presumed faults. In contrast to PFTCS, AFTCS react actively to the system failures which are detected, isolated and identified by a diagnosis module, by reconfiguring the control law so that the stability and acceptable performance of the faulty system can be maintained [1].

1.1.3.1 Passive fault-tolerant control

PFTC method can also be called as robust fault-tolerant control. Classically, robustness in control theory refers to the capability of a system in achieving good performance and/or stability under uncertain parameters, uncertainties and disturbances or modeling errors. Robust fault-tolerant control is based on the same concept, that is to design a fixed controller to meet the requirements for the control system, with considering the parameters or structure changes caused by faults.

Examples of PFTC methods are given below:

1. **Reliable stabilization**. Reliable stabilization was firstly introduced by Siljak in [6] for the control design in presence of actuators's faults . He adopted several compensators to stabilize one object. When one compensator failed, the others can work normally to stabilize the object. Cho et al. [7] used together one regular controller and a redundant adaptive controller. This design guarantees the system's asymptotic stability and zero-steady error tracking under certain fault modes. In [8], a stable controller was divided into two dynamic compensators and a method to design these compensators was also proposed. Sebe et al. [9] gave a sufficient condition for the existence of the solution of the reliable stabilization problem using the coprime

factorization of polynomials. A solution which can be used for non-strong stabilizable systems by adopting several parallel dynamical compensators was proposed in this paper.

2. **Reliable control**. Reliable control consists in designing one controller to stabilize the system and to ensure its performance under a given actuator and sensor fault sets [10]. Ackermann [11] proposed a graphical method to choose the control gain of the state-feedback controller, this method can ensure that the system achieves asymptotically stability even when sensor faults occur. Joshi [12] decomposed the input matrix into two parts corresponding to the normal and loss-effectiveness actuators, then a LQG state-feedback controller was designed.

3. **Integrity control**. If, after the occurrence of actuator/sensor faults, the closed-loop system is still stable, then the control system has integrity feature. Shimemura and Fujita in 1985 [13], in order to obtain a better dynamic feature, proposed to assign the system's poles based on a Riccati equation. Shieh [14] used Lyapunov equation to replace Riccati equation since Riccati equation has the drawback that the parameters need to be adjusted during the controller design process. Wang [15] investigated the control design problem that satisfies the constraints of integrity and a robustness H_∞ criterion together.

4. **Simultaneous stabilization**. The simultaneous stabilization problem was studied in 1982 by Seaks and Murray [16]. In paper [16], for n linear time-invariant systems $P_1, ..., P_N$, one fixed controller K was designed to stabilize all N systems. The simultaneous stabilization has two main advantages: Firstly to maintain stability for the system when faults happen; Secondly, the linearization for nonlinear systems often works at one working point. The linear models change with different working points, therefore, designing one controller to stabilize all these linear models has better control effect on the real system.

The advantage of the PFTC is that the controller is designed off-line and is identical in normal and faulty situations. It does not change when faults occur,

therefore there doesn't exist instability problems caused by the time-delays of the diagnosis systems. However, since the controller is fixed, it is designed only to tolerate a class of presumed faults, and it can generally not fully compensate the degraded performance.

1.1.3.2 Active fault-tolerant control

AFTCS typically include four sub-systems [1]: (1) a reconfigurable controller which can be designed on-line or off-line; (2) a fault detection and diagnosis (FDD) scheme; (3) a controller reconfiguration mechanism and (4) a command/reference generator. Fig. 1.1 shows an overall structure of a typical AFTCS.

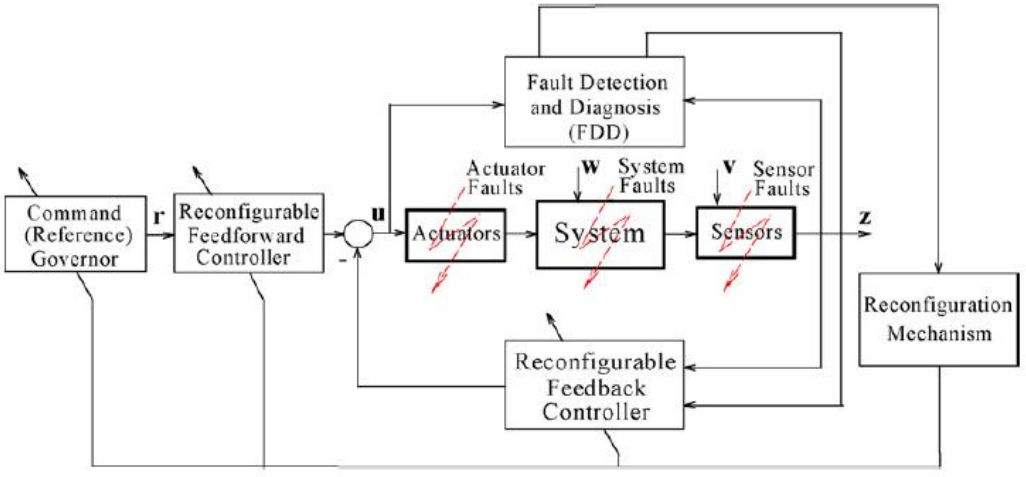

FIGURE 1.1: An Overall Structure of AFTCS [1]

The design of AFTCS mainly includes controller reconfiguration and controller reconstruction. Many methods are proposed in the literature as in [1] (see. Fig. 1.2), such as gain scheduling, linear quadratic regulator, model reference adaptive control, eigenstructure assignment, pseudo inverse method, model following, intelligent control and so on. We will briefly introduce these methods in the following.

1. **Gain Scheduling (GS)**. Gain scheduling was proposed by Aström in 1989 [17]. In this work, the nonlinear system is linearized at different working

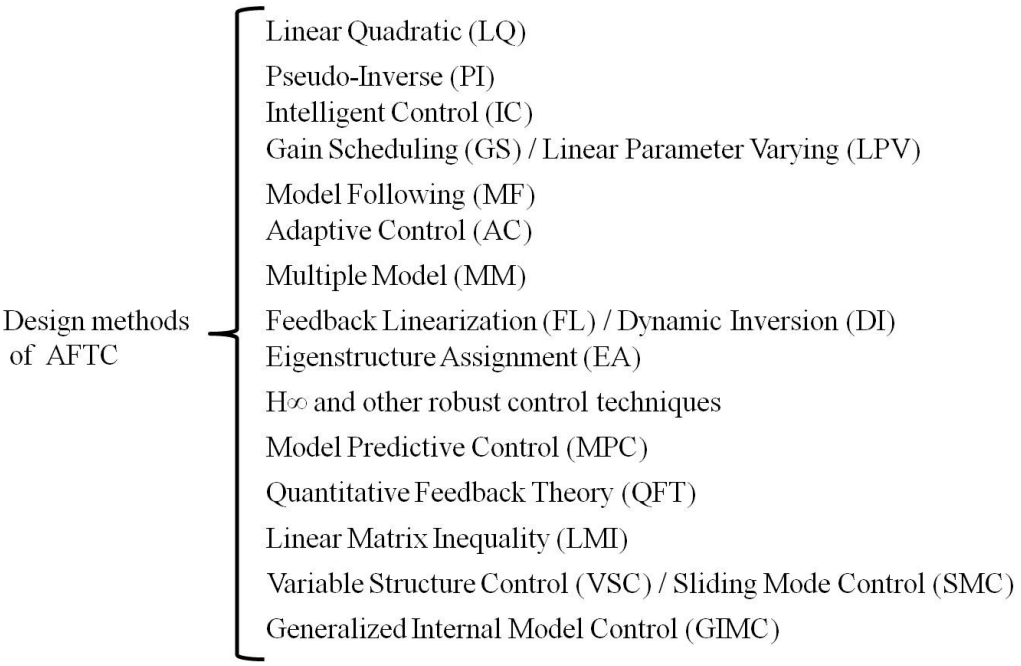

FIGURE 1.2: Design Methods of AFTC [1]

points and, for each linear model system, the feedback control gain is designed off-line. When the fault information is obtained, one proper gain is chosen to get the fault tolerant control law. The advantage is that it can handle nonlinear systems with linear control methods. However, it is difficult to choose the proper parameter. Shamma et al. [18] and Lawrence et al. [19] studied the nonlinear gain scheduling problem. Kaminer et al. [20] proposed an algorithm to choose the feedback control gain for nonlinear systems.

2. **Linear Quadratic Regulator (LQR)**. This method uses optimal control techniques, using a quadratic cost function, to design a new feedback control gain matrix for the system when faults are diagnosed. Looze et al. [21] solved the optimal control problem with a feedback controller. Huang [22] proposed an implicit model-following method based on LQ control.

3. **Model Reference Adaptive Control**. AFTCS relies on FDD, but FDD is not perfect. Missed detection, time-delay and false alarms may influence the controller's fault-tolerant capability. To cope with this problem, the model reference control was proposed. After a fault occurs, the control law is adjusted to track the reference model. Hu [23] used a fault detection filter

to detect and to estimate the fault gain, and designed the model reference controller to ensure the stability for a flight system.

4. **Eigenvalue/Eigenvector Assignment**. Jiang [24] proposed a control reconfiguration method based on eigenstructure assignment in order to possibly recover the change of eigenvalues of the closed-loop system.

5. **Pseudo-Inverse Method (PIM)**. Pseudo-inverse method, which is quite easy to apply, was proposed by Caglayan [25], where a new feedback gain is calculated by using the pseudo inverse of the control matrix. In Gao [26], an improved MPIM method was adopted. By transferring the control reconfiguration problem to a constrained extreme value problem, one can get the optimal solution for a SISO system and also a solution for a MIMO system.

6. **Intelligent Control**. Intelligent control method is a class of control techniques that use various AI computing approaches like neural networks, Bayesian probability, fuzzy logic, machine learning, evolutionary computation and genetic algorithms. Guo et al. [27] designed a new FTC structure based on an intelligent PID algorithm to solve the tracking problem for an unknown nonlinear MIMO system. Ichalal et al. [28] and Shen et al. [29] proposed a FTC method for actuator failure in a nonlinear system where the nonlinear system is represented by a TS multi-model.

One of the key functions of AFTCS is FDD. Based on the general concepts in [30],[31] and [32], FDD methods can be classified into five types:

1. **Knowledge-based Fault Diagnosis Methods**. These methods do not need a quantitative mathematic model, they are mainly based on: Neural Network [33][34], Rough Set Theory [35], Fault Tree and Expert System [36], Pattern Recognition [37].

2. **Data Driven Fault Diagnosis Methods**. These methods rely on all measurable signals (input or output) and their change trends. Based on the statistical dependence of these signals, one can characterize the normal and

faulty behaviors in a given data space [38] [39]. Many statistical techniques have been developed: wavelet analysis [40], principal component analysis (PCA) [41][42], Kullback information criterion [43], Kernel methods [44][45] and so on.

3. **Analytical Redundancy-based Fault Diagnosis Methods**. These methods are based on checking analytical redundancy relations (ARR) that exist among system inputs and outputs to achieve fault diagnosis [46] [47]. Parity space method was initially investigated for linear systems [48][49], it was also extended to bi-linear [50], state affine systems [51], non-linear systems [52] and to hybrid systems [53]. Three techniques are considered to eliminate the unknown state and generate the ARR: elimination theory [54], Gröebner bases [55] and characteristics sets [56].

4. **Observer-based Fault Diagnosis Methods**. These methods generally compare the actual system's measurements with the estimated outputs which are obtained from observers. The output estimation errors are taken as residuals [57] [58] [59] [60]. The commonly used observers include Luenberger observers [61], Kalman filters [62], sliding mode observers [63][64], unknown-input observers (UIO) [65] and adaptive observers [29] [66] [67].

5. **Parameter Identification-based Fault Diagnosis Methods** . These methods can handle faults which will result in time dependent parameter drifts [68]. The fault identification can be framed as a parameter estimation problem, using online fast parameter estimation methods, such as least-squares techniques [69], instrumental variables and estimation [70].

1.2 Fault-tolerant Control with Actuator Saturation

1.2.1 Motivation

Because of the growing demands for reliability and maintainability, a lot of significant researches on fault-tolerant control systems (FTCS) have been conducted in the past decades and many theoretical results have been published [1]. However,

practical control design methods which can fit with practical applications are still a challenging issue for researchers and engineers. One of these challenges in the field of FTCS is how to deal with the actuator saturation problem in presence of actuator faults [71].

Every physical system subject to control is limited by actuators' amplitude and rate constraints in practice. In some cases, the control design techniques that ignore these actuator limits may lead to actuator damage or serious performance degradation. Therefore, a lot of attention has been focused on the stability requirements for systems with saturating actuators. Keerthi and Gibert [72], Aström and Rundowist [73], S. Tarbouriech and G. Garcia et al. [74] and T. Hu and Z. L. Lin [75] investigated the control problem for systems with actuator saturations (input constraints). Gutman and Hagander [76] also did researches considering constraints both on actuators and on states.

It is of prime importance to take into account the input constraints in the FTCS design, especially when actuator faults are considered. For example, if some of the actuators fail during operation, the remaining healthy actuators have to compensate for the lost of control effectiveness, which may lead to actuator saturation. If the actuator saturation effects are not taken into account, then severe system performance degradation or even instability may result, hence, many researches were dedicated to this topic.

1.2.2 Literature review on control systems design with actuator saturation

Every physical system has input constraints in practice. Because of the actuator physical limits, it is impossible to apply unlimited control signals. However, many designed controllers presented in the literature do not consider this common feature. Such controllers may incur actuator damage or serious performance sacrifice in some situations. Therefore, control systems subject to input constraints need to be studied. Various control methods have been proposed.

Generally speaking, there are two ways to handle the saturation problem:

1. Designing first the controller without considering the saturation problems, then using simple saturation filters when applying the designed controller. However, since the saturation is omitted in the control design method, the stability of the system can not be guaranteed.

2. To ensure the system's stability, it is necessary to consider the saturation influence in the whole controller design process. Many algorithms are proposed to design such controllers. Anti-windup compensation method is one of the common used methods [77][78], see Fig. 1.3. This method consists in designing the controller without considering saturation in the first step, then based on the input and output signals, a compensator is designed to eliminate the saturation influence. Other methods, as adaptive neural network [79], H_∞ control [80], sliding mode [81], adaptive robust control [82] and etc, have also been applied into saturated control systems with great success.

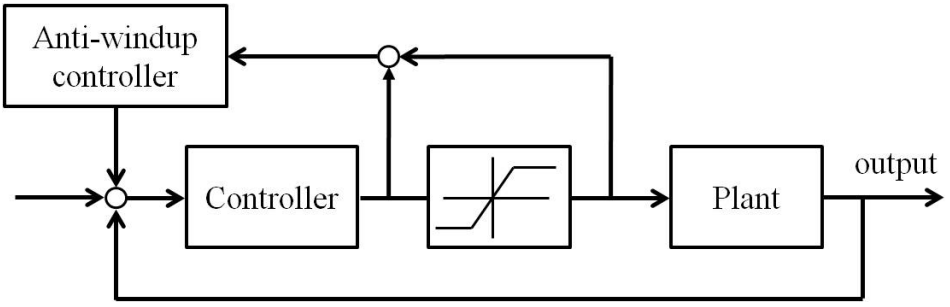

FIGURE 1.3: The Structure of Anti-windup Control

1.2.2.1 Stability analysis for control systems with actuator saturation

To analyze the stability for control systems with actuator saturation, one way is to use the Lyapunov stability theory with the invariant set on time-domain; the other way is to use the circle criterion on frequency domain. In the following, three analysis methods on time-domain are discussed, i.e. the global stabilization (GS), semi-global stabilization (SGS) and local stabilization (LS).

1. **GS/SGS for Null Controllable Systems with Bounded Controls**. Sontag and Sussmann [83] pointed out that for linear control systems with input constraints, the necessary condition for its global stabilization is that

all eigenvalues of the open-loop system are in the left-half plane. The early works on control designs with saturations were almost based on this condition. In general, the linear feedback control cannot achieve global asymptotic stabilization for linear systems with input saturation. But by using a nonlinear feedback controller with a condition that the open-loop system is asymptotically null controllable with bounded controls (ANCBC) [84], the linear system can achieve global asymptotic stabilization.

However, with the notion of semi-global stabilization of linear systems subject to input saturation, that is the system has an asymptotically stable equilibrium point whose domain of attraction includes *a priori* given bounded set, one can achieve semi-global stabilization for linear systems with linear feedback laws. Lin and Saberi [85] proposed a linear feedback controller for null controllable systems to achieve semi-global stabilization. In this paper, the reasons for choosing semi-global stabilization were given: since a plant's model is usually valid in some region of the state space, from the engineering view, relaxing the requirement of global stabilization to semi-global stabilization makes sense. Such relaxation gives us simple linear control laws and stronger stability property for the closed-loop system.

In [85], a low gain control design method was proposed for globally stabilization control objective. Based on Riccati Equation, Lin [86] designed a low gain controller to semi-global stabilize the discrete systems. In order to provide the best performance, Lin [84] and Jose [87] proposed a low-high gain control design method: a low gain is designed first; then a high gain - based on the low gain and a proper Lyapunov function - is constructed to improve the performance.

2. **Local Stabilization : Invariant Set Theory**. GS and SGS have strict constraints for the eigenvalues of the systems in open loop. If the open-loop system is exponentially stable, the designed controller can achieve GS and SGS; if the open-loop system is unstable, then any feedback control law can only guarantee local stabilization. Since in practical situation, the working area for a system is limited in one region, therefore, the local stabilization is more deserving to be studied.

The invariant set theory plays a very important role in the control theory. Paper [88] gives a bibliographical review on the invariant set applications. Usually, only giving one asymptotically stable point is not sufficient, the estimation of the attraction region around this point is needed. The invariant set theory is widely used to estimate the attraction region with ellipsoid set [89] and polyhedron (convex) set [90].

According to the Lyapunov stability theory, if there exists a Lyapunov function $V(x)$ such that $\dot{V} \leq 0$, then the system is asymptotically stable for any given initial state. If for all states $x \in C$, one has a set defined as $\Omega = \{x \in R^n : V(x) \leq c\} \subseteq C$, then Ω is an ellipsoid set which is the attraction region. It can guarantee the states exponentially attenuation within the given set. By choosing the Lyapunov function in a quadratic form, this problem can be easily transferred to a LMI problem. Therefore, using the invariant ellipsoid set to present the attraction region based on a Lyapunov function in a quadratic form has become a standard tool to solve stabilization problem with saturation [89].

Different from the ellipsoid invariant set with quadratic Lyapunov function, the polyhedron invariant set adopts another Lyapunov form. By using state feedback control, estimating the attraction region is transferred to a problem of pole assignment/eigenstructure assignment [91][92].

The feedback control design for linear systems with input constraints is an important research topic. Recently, two main problems are studied for saturated linear system with feedback control: one is to estimate the nearest approximate attraction domain or invariant set of the saturating system under a given feedback control matrix; the other is to design the feedback control matrix in order to obtain a bigger attraction domain based on the relationship between control matrix and attraction domain.

1.2.2.2 Control methodology for control systems with actuator saturation

Here we briefly present two methods to deal with the actuator saturation problem:

1. **Model Predictive Control (MPC)**. Model Predictive Control (MPC), also referred as Receding Horizon Control or Moving Horizon Optimal Control, has been widely adopted in industry as an effective mean to deal with multi-variable constrained control problems [93]. At each sampling instant, treating the current states as initial values, the control signal is obtained by solving a finite horizon optimal control problem. An optimal control sequence is yield and the first one is applied to the plant. Different from many traditional control laws, MPC is an on-line controller while the latter ones are off-line designed.

   Designing a MPC is actually an optimal control problem. It finds the optimal input trajectory that minimizes the difference between the predicted plant behavior and the desired one. Different from other optimal control methods, it is solved on-line with the current state, rather than off-line [94]. The robust stability for MPC was also studied by many researchers. Lee [95] pointed out that the local optimality can not guarantee the system's stability . In order to stablize the system, the commonly used method is to constraint the terminal value or to add a weighted matrix for each state in the objective function. Besides, the robust MPC also gets a lot of attention. Campo and Morari proposed in [96] to design the controller by minimizing the worst cost function ; Zheng [97] proposed a MPC algorithm to optimize performance subject to stability constraints for linear systems with mixed constraints, then extended the algorithm to a robust case. Wan and Kothare [98] proposed a MPC algorithm by using output feedback with solving LMIs.

2. **Robust Control with Input Constraints**. The optimization-based problem of designing control laws for the linear systems with controller constraints can be transferred to a resolution of linear matrix inequalities (LMI). LMI is obtained in different types of control problems, such as stabilization, H_∞ control, L_∞ control, LQG control and so on. Since the controller designed by LMIs can satisfy both stability and performance requirements, LMIs are often used to solve multi-objectives problem .

   Consider a function in the form $F(x) \triangleq F_0 + \sum_{i=1}^{m} x_i F_i$ (where $x \in R^m$ is the variable and $F_i = F_i^T \in R^{n \times n}$ are symmetric matrices). The $F(x) > 0$

inequality describes a a strict LMI. Many constraint problems of x, especially for linear inequalities, convex quadratic inequalities, matrix norm inequalities and also the constraints problems for controllers design referring to Lyapunov, convex quadratic matrix inequalities and so on [99] can be expressed as LMI. Some convex nonlinear inequalities can also be transformed to LMI by using the Schur complement [100]. Now, LMI becomes the most used method in modern control theory.

1.2.3 Literature review on FTC design with actuator saturation

The significant progress of FTC researches has emerged in a large number of publications [1]. However, few researches on FTC involve saturation constraints for actuators. In practice, one can avoid saturation by two ways: one is letting control signals far away from its limitation, but this method will limit the system's capability and the other is to use more efficient actuators which can provide more forces, however, this way costs more than using classical actuators.

Since the closed-loop control system under bounded control can generally reach local stability, when faults happen, its region of attraction under the original controller may change, and the system's performance also can not be guaranteed. Usually, the controller must be designed for the system to meet given performance specifications. These objectives are usually expressed in terms of energy cost, time constraints, transient and steady state characteristics, and are related to [101]

1) system stability;

2) preciseness : error between the reference and the output;

3) robustness against disturbance or parameter uncertainties and variations;

4) fault tolerance ability.

For the first objective, a saturated system's stability can be analyzed by estimating the system's attraction domain or its invariant set.

However, its invariant set is not strictly invariant because the disturbances and the states are not guaranteed to converge to the origin. Certain measurements of

the disturbance rejection are proposed, which is also described by an ellipsoidal invariant set. In [102], the authors pointed out that for saturated systems with a suitable designed controller, all trajectories starting from the system's attraction domain will enter its disturbance rejection domain. From the viewpoint of system performance, this disturbance rejection domain should be as small as possible. Therefore, the disturbance rejection can be used to analyzed the system's performance for the second and third objectives. Some researchers studied the optimization of the system's attraction domain using LMIs or nonlinear programming method, to make sure that the system still stays inside the domain when actuator saturation and certain actuator faults occur [71][102][103]. In [102], the authors also proposed to maximize the attraction domain and to minimize the disturbance rejection domain.

Some researchers focus on the stability problems of FTCS under control input constraints. These FTCS design techniques fall into one of the following approaches: robust control [71][102][103], adaptive control [104][105], variable structure and sliding mode control [106][107], observer-based approach [108], fault-hiding approach [109], control allocation [110], model predictive control [111] and hybrid approach [112]. As for the effect of the disturbances to the system, although various approaches guarantee the stability for the FTCS in faulty situations, the states are generally not guaranteed to converge to the origin because of the faults. When faults are considered, the controllers which have smaller control gains may avoid saturation as soon as the states exceed some threshold. However, it can not provide better performance in comparison with higher gains controllers. The effect of the saturation on the control system performance, which is caused by the system's physical restriction itself or the faults, depends on the range of the required control action relative to the saturation bounds [87].

Normally, after fault occurrence, if one tries to achieve the pre-fault performance, this may require the system's actuators to provide extra efforts to compensate for the changes caused by faults, especially during the initial fault recovery period. This will lead to actuator saturation in many situations. Therefore, recovering the original performance fully or accepting a degraded performance is a worth considering choice. In a typical control system, the stability, the desired time

response and the minimal steady-state errors are the main performance objectives. However, one should notice that system behaviors in normal and faulty situations may be significantly different. In presence of fault, the robustness of the system to fault and how the system survives become important issues [113].

Rather than obtaining optimization parameters to maximize the attraction domain, designing a controller for systems under input constraints to guarantee a safe and stable plant with acceptable degraded performance is more practical. Few attention has been paid to study the saturation effects and faults inference on the system's performance. Only some works come to the aspect of the system's performance, and study on the topic of reference management for FTC design with saturation problems. Several contributions were focus on how to avoid the occurrence of such controller saturation. For example, a design concept and procedure for FTCS design to explicitly incorporate possible graceful performance degradation was proposed by Zhang and Jiang [113]. Along this line, some other researchers have also studied the FTCS with actuator saturation using reference management techniques. Zhang and Jiang [113] adjusted on-line the command input to avoid potential actuator saturation after faults happen. Boussaid et al. [101] [114] proposed a fault recovery approach using a reference modification method, the fault accommodation based on reference management techniques modifies the references and adds an offset to the control input after fault occurrence.

1.3 Objectives and Contributions of the Thesis

In this thesis, we are going to study the FTCS design problem for linear tracking control systems with actuator saturation. As stated in Section 1.2.3, few research handles the saturation constraints of actuators when designing fault tolerant control. Among these researches on FTC with actuator saturation, the strategy using reference management techniques guarantees that the system operates with acceptable degraded performance.

The following issues need to be considered for linear tracking control systems under actuator saturation:

(1) How to estimate the controllable region for the control system taking into account the actuator's capability? how to maximize this region?

(2) Under faulty situation, how will the controllable region be influenced? how will the performance degrade due to different faults scenarios?

(3) What are the advantages and disadvantages of using traditional FTC methods for faulty systems with actuator saturation ?

(4) How the reference management technique is adopted when handling faulty systems with actuator saturation?

Owing to the significant results on the stability property of system under input constraints, the stability region and the performance region of the system can be described in the form of invariant sets. Issue (1) could be considered from this point of view; For Issue (2), obviously, according to a variety and severity of faults that may affect the system with input saturation, stability and performance domains would be different. It is not easy to generate extra control signals by using traditional FTC methods to compensate the degraded performance, the reference management technique could be considered to generate the control signal far away from its limitation. This technique could be used to cope with Issue (3) and Issue (4). The details on how to solve these problems will be presented in the next chapters.

The thesis is divided into five chapters. In Chapter 1, we have provided a review of existing fault-tolerant control approaches and of current researches results on FTC with actuator saturation. In this chapter, we also have posed the motivations and objectives of this thesis. Chapter 2 deals with the controller design for linear systems with actuator saturation. The invariant set theory is applied to estimate the attraction region and the performance region for the tracking system with the designed controller. The reference adjustment technique will be first used here in order to enlarge the attraction region. This chapter lays strong basis for the other chapters. In Chapter 3, the fault-tolerant control methods for the linear tracking system with actuator saturation and certain faults are considered. The influence of happened faults is discussed first, two main methods (PFTC and AFTC) in FTC design will be studied. A fault-tolerant control scheme based on

the reference adjustment technique is proposed to improve the PFTC method and the AFTC method. In Chapter 4, an application for the path tracking of a 4WD electric vehicle will be presented to test and verify in simulation the proposed fault-tolerant control scheme. In Chapter 5, conclusions and future researches are given.

Chapter 2

CONTROL DESIGN FOR LINEAR SYSTEMS WITH INPUT CONSTRAINTS

Contents

Abstract A controller based on the low-high gain control technique is designed for linear systems with actuator saturation. The invariant set theory is applied to estimate the attraction region and the performance region for the system with the designed controller. For the case that the initial state is not within the attraction region, a new algorithm based on the reference adjustment technique is proposed with the same designed controller to achieve large-region stabilization.

2.1 Control Design with Actuator Saturation

The primary purpose of control is to force the system keeping the desired behavior in one environment under disturbances. Regulating control and tracking control are fundamental control issues [115]. For a given system, we are often interested not in regulating the system's states to zero, but also in following a nonzero reference signal. An important problem is to design a dynamic controller such that the output of the resulting closed-loop system can track (or converge to) *a priori* given reference, i.e. if $r(t)$ is the reference input, the output $y(t)$ should track $r(t)$ asymptotically, which means $(y(t) \to r(t))$ as $(t \to +\infty)$. Three methods are used to include the reference input into the control design [116]: (1) Internal model controller; (2) Incorporating reference in state space control system; (3) Feedforward control design.

In addition, every physical systems subject to control involve actuators' amplitude and rate limitations, and it is of prime importance in practice to take these constraints into account in the control design. Before getting into the tracking problem, let first define the saturation function.

Definition 2.1. *[84] A function* $\sigma(s) = [\sigma_1(s), ..., \sigma_m(s)]^T : R^m \to R^m$ *with element* $\sigma_i(s)$ $(i = 1, 2, ..., m)$ *is called a saturation function if*

1) σ_i *is locally Lipschitz.*

2) $s\sigma_i(s) > 0$ *whenever* $s \neq 0$.

3) $min\{\lim_{s\to 0^+}\frac{\sigma_i(s)}{s}, \lim_{s\to 0^-}\frac{\sigma_i(s)}{s}\} > 0$.

4) $\liminf_{|s|\to\infty} |\sigma_i(s)| > 0$.

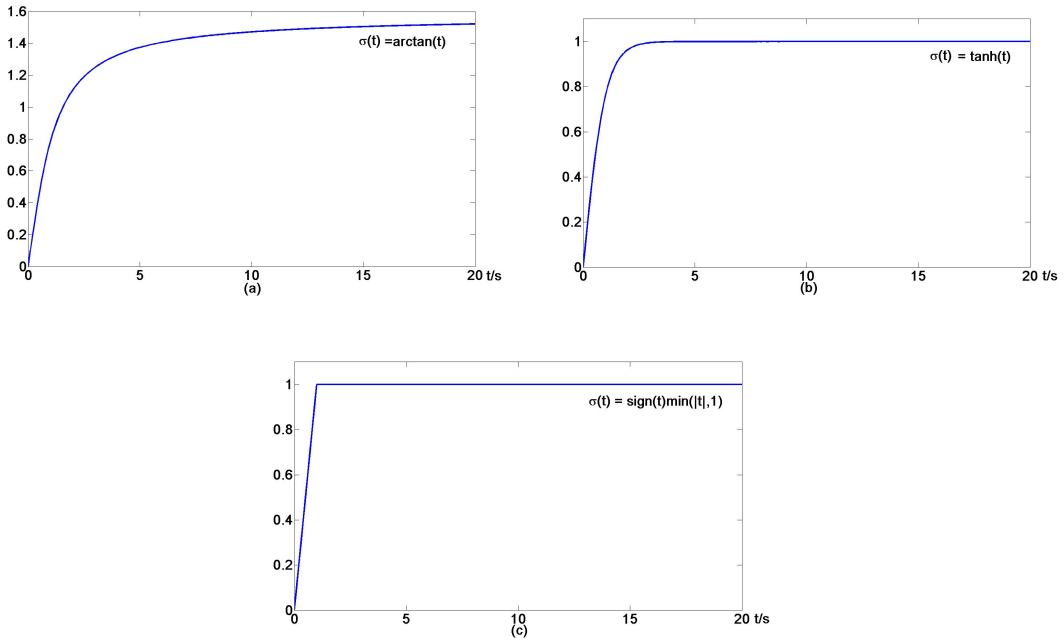

FIGURE 2.1: Saturation Functions: (a). $\sigma(t) = \arctan(t)$; (b). $\sigma(t) = \tanh(t)$; (c). $\sigma(t) = sign(t)\min\{|t|, 1\}$

The functions $\sigma(t) = \arctan(t)$, $\sigma(t) = \tanh(t)$ and $\sigma(t) = sign(t)\min\{|t|, 1\}$, see Fig. 2.1 are all saturation functions that satisfy the definition 2.1.

Let us consider the following general tracking problem.

Giving the following linear system Σ_0

$$\Sigma_0 : \begin{cases} \dot{x} = Ax + B\sigma(u(t)) + E\omega(x,t) \\ y = Cx \end{cases} \tag{2.1}$$

where $x \in R^n$, $u \in R^m$ are the state and control input vectors, $\omega \in R^n$ represents the uncertainty and the disturbance, A, B, C, E are matrices with appropriate dimensions, and $\sigma(u)$ is a saturation function, satisfying $\sigma(u) : R^m \to R^m$,

$$\sigma(u) = [\sigma_1(u_1), ..., \sigma_m(u_m)]^T \tag{2.2}$$

where $\sigma_i(u_i) = sign(u_i)\min\{|u_i|, 1\}$, $i = 1, 2, ..., m$.

Problem 1. *For the given linear system Σ_0, $r(t)$ is the reference input, design a control law to make $y(t) \to r(t)$ $(t \to +\infty)$.*

2.1.1 Controller design

For the system Σ_0, the following assumptions are first given:

Assumption 2.1. *Assume that the full state x is available $(C = I)$, and (A, B) is controllable.*

Assumption 2.2. *The norm of $\omega(x,t)$ is bounded by a known function*

$$\|\omega(x,t)\| \leq \omega_0 \quad \forall (t,x) \in R^+ \times R^n \tag{2.3}$$

Assumption 2.3. *Assume that the reference $r(t)$ is a step input $r(t) = x_d$ as $t \to +\infty$.*

Remark 2.1. *For the general tracking problem with certain time-varying references $r(t)$, Problem 1 can also be approached as a regulation problem, that is to design a dynamic controller such that the tracking error converges to 0, i.e., $((y(t) - r(t)) \to 0)$.*

The following control law is designed to achieve the regulation mission [114], see Fig. 2.2.

$$u(t) = -Kx + K_r x_d \tag{2.4}$$

where K is the state feedback gain such that $(A - BK)$ is stable, and K_r is the feedforward control gain.

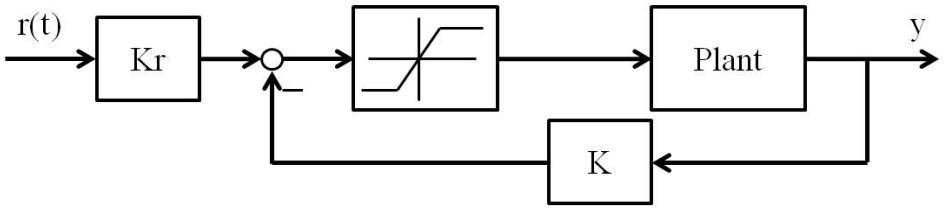

FIGURE 2.2: The Control Structure

To obtain K_r, the desired steady state equation is considered. Define $u_d(x_d)$ as the constant solution for the system Σ_0

$$Ax_d + Bu_d(x_d) = 0 \tag{2.5}$$

Based on Eq. 2.4 and Eq. 2.5, we have $u_d = -Kx_d + K_r x_d$ with $K_r = ((BK - A)^{-1}B)^+$.

For Eq. 2.5, the following assumption 2.4 is made.

Assumption 2.4. *For any $x_d \in R^n$, assuming that there exists one and only one constant solution $u_d(x_d) \in R^m$ for Eq. 2.5.*

Define $e = x - x_d$, then the Problem 1 is transferred to a regulation problem of the error equation Σ_e

$$\Sigma_e : \dot{e} = Ae + B\sigma(u(t)) - Bu_d(x_d) + E\omega(x,t) \tag{2.6}$$

with

$$\begin{cases} u = -Kx + K_r x_d = u_e + u_d = -Ke + (K_r - K)x_d \\ K_r = ((BK - A)^{-1}B)^+ \end{cases} \tag{2.7}$$

The linear feedback controller does not work well when the input is subject to a magnitude constraint. Large gains enhance performance but the states will violate the input constraints easily including those which are small. Smaller gains can ensure that the input magnitude constraints are respected but will lead to reduced performance [117]. In regard to the feedback control, it is often been formulated into an optimal control problem which specifies some performance objective functions. Linear quadratic (LQ) optimal control is often used to resolve these issues [118]. A low-and-high gain technique was introduced in [87] , [119] and [120] for the regulation problem: a low gain is designed first to guarantee the input constraints, then a high gain - based on the low gain - is constructed to improve the performance [87]. This technique presented in [120] achieves robust semi-global stabilization in the presence of actuator saturation, additive bounded uncertainties and additive bounded disturbances.

One similar sub-optimal control law can be designed [87]

$$\begin{cases} K = (1+\rho)B'P \\ K_r = ((BK - A)^{-1}B)^+ \end{cases} \tag{2.8}$$

where ρ is a positive constant to be chosen and P is a positive semi-definite and symmetric solution of the following LMI

$$A'P + PA - PBB'P + \frac{1}{\mu}PEE'P + \mu\omega_0^2 P < 0 \tag{2.9}$$

The controller design process will be presented and be improved in the next subsection 2.1.2.

2.1.2 Stability analysis

Generally, a system with input constraints cannot achieve global asymptotic stabilization by using a linear feedback law, unless by using nonlinear feedback with condition that the system without input constraints is globally null controllable [121]. The notion of semi-global stabilization of linear systems subject to input saturation was introduced in the foundational work [85][86]. It is shown that linear feedback laws can achieve semi-global stabilization for both discrete and continuous linear systems under some appropriate conditions. However, global stabilization (SG) and semi-global stabilization (SGS) all have strict constraints for the eigenvalues of the systems' open-loop. If the open-loop system is exponentially stable, the designed controller can achieve GS and SGS, else any feedback control law can only guarantee local stabilization.

Definition 2.2. *The local stabilization consists in finding a feedback law such that the closed-loop system satisfies that, for a given bounded set $\Omega \subset R^n$ and a given small bounded set $\Omega_0 \subset R^n$ containing the origin, any trajectory starting in Ω will enter Ω_0 and remain in Ω_0 thereafter.*

Lemma 2.1. *[102] Consider a linear system*

$$\dot{\xi} = A\xi + E\omega(\xi, t) \tag{2.10}$$

where $\xi \in R^n$ *and* $\|\omega(\xi, t)\| \leq \omega_0$.

An ellipsoidal set centered at the origin is denoted by $\Omega(P, 1) = \{\xi \in R^n | \xi^T P \xi \leq 1, P^T = P > 0\}$. *If there exists a symmetric and positive definite matrix* P, *and a positive scalar* μ *such that*

$$A'P + PA + \frac{1}{\mu} PEE'P + \mu\omega_0^2 P \leq 0 \tag{2.11}$$

Then the ellipsoid $\Omega(P, 1)$ *is an invariant set for the closed-loop system 2.10.*

Proof: Consider a quadratic Lyapunov function $V = \xi^T P \xi$, the derivative of V along the system trajectories is given by

$$\dot{V} = \xi'(A'P + PA)\xi + 2\xi' PE\omega$$

Based on Assumption 2.2, since

$$2\xi' PE\omega \leq \frac{1}{\mu}\xi' PEE'P\xi + \mu\omega_0^2$$

then

$$\dot{V} \leq \xi'(A'P + PA + \frac{1}{\mu} PEE'P)\xi + \mu\omega_0^2$$

It follows from Eq. 2.11 that

$$\begin{aligned} \dot{V} &\leq -\mu\omega_0^2 \xi' P\xi + \mu\omega_0^2 \\ &= \mu\omega_0^2(1 - \xi' P\xi) \end{aligned}$$

Obviously, $\Omega(P, 1)$ is an invariant set which means that all the trajectories starting from $\Omega(P, 1)$ will still remain inside it. This ends the proof. □

The local stabilization stated in Definition 2.2 requires to design a control law such that for the closed-loop system, its domain of attraction Ω is *a priori* given bounded set which includes an asymptotically stable equilibrium [84]. Various methods for estimating the domain of attraction have been developed by applying the absolute stability analysis tools, such as the circle criterion and Popov criterion

[122] [123]. Enlarging the domain of attraction based on the model predictive method and anti-windup design is also achieved in [124] [125].

A less conservative way different from the above researches for calculating the domain of attraction in which the stability is guaranteed for the system Eq. 2.6 with the control law Eq. 2.7 with Eq. 2.8 is presented in the following theorem 2.1.

Assumption 2.5. *Assume that each element of the constant control solution* $u_d(x_d)$ *for system* Σ_0 *satisfies*

$$\|u_{di}(x_d)\| \leq 1 - \delta_i \quad \delta_i \in [0, 1] \tag{2.12}$$

This assumption implies that the tracking objective x_d is within the controller's capability.

Theorem 2.1. *Consider Problem 1, for the system 2.6 satisfying Assumption 2.1, Assumption 2.2 and Assumption 2.5, under the control law 2.7 with 2.8*

$$\begin{cases} K = (1+\rho)B'P \\ K_r = ((BK - A)^{-1}B)^+ \end{cases}$$

where ρ *is a positive constant that has to be chosen and* P *is a positive semi-definite and symmetric solution of the following condition*

$$A'P + PA - PBB'P + \frac{1}{\mu}PEE'P + \frac{\mu}{\varrho}\omega_0^2 P < 0 \tag{2.13}$$

with

$$\varrho = \min_i \frac{4\delta_i^2}{B_i' P B_i} \tag{2.14}$$

If the symmetric and positive definite matrix P *and a positive scalar* μ *exist for Eq. 2.13, then* $\Omega(P, \varrho)$ *as the domain of attraction for system 2.6 is an invariant set. For all* $x \in \Omega(P, \varrho)$ *and all* $\delta_i \in (0, 1]$*, the system can achieve local stabilization and the tracking mission.*

Proof: For system 2.6 with the controller 2.7, one has

$$\begin{aligned}\dot{e} &= Ae + B\sigma(u(t)) - Bu_d(x_d) + E\omega(x,t)\\ &= Ae + B\sigma(u(t)) - B(K_r - K)x_d + E\omega(x,t)\\ &= Ae + B\sigma(u(t)) - BK_r x_d + BKx_d - BKx + BKx + E\omega(x,t)\\ &= (A - BK)e + B(\sigma(u(t)) - u) + E\omega(x,t)\end{aligned}$$

Define $V(e) = e'Pe$, consider the derivative of $V(e)$ along the trajectory of the closed-loop system 2.6, we obtain

1. Case 1: The controller is not saturated, i.e, $u(t) = u$.

$$\dot{e} = (A - BK)e + E\omega(x,t) \tag{2.15}$$

Substituting it into $\dot{V}$ with $K = (1+\rho)B'P$, we have

$$\begin{aligned}\dot{V} &= e'((A - BK)'P + P(A - BK))e + 2e'PE\omega(x,t)\\ &= e'(A'P + PA)e - 2(1+\rho)e'PBB'Pe + 2e'PE\omega(x,t)\end{aligned}$$

Based on Eq. 2.13, then

$$\dot{V} \leq -(2\rho+1)e'PBB'Pe - \frac{1}{\mu}e'PEE'Pe - \frac{\mu}{\varrho}\omega_0^2 e'Pe + 2e'PE\omega(x,t) \tag{2.16}$$

since

$$2e'PE\omega(x,t) \leq \frac{1}{\mu}e'PEE'Pe + \mu\omega_0^2 \tag{2.17}$$

then one has

$$\begin{aligned}\dot{V} &\leq -(2\rho+1)e'PBB'Pe - \frac{\mu}{\varrho}\omega_0^2 e'Pe + \mu\omega_0^2\\ &\leq -\frac{\mu}{\varrho}\omega_0^2 e'Pe + \mu\omega_0^2\\ &\leq \mu\omega_0^2(1 - \frac{V}{\varrho})\\ &\leq \frac{\mu}{\varrho}\omega_0^2(\varrho - V)\end{aligned} \tag{2.18}$$

$\Omega(P,\varrho)$ is thus the invariant set for system 2.6.

2. Case 2: The controller is saturated. Based on Eq. 2.7 and Assumption 2.5, let define

$$\bar{\sigma}(u_e) = \sigma(u(t)) - u \tag{2.19}$$

and $\bar{\sigma}_i = \delta_i$. Then we have

$$\dot{e} = Ae + B\bar{\sigma}(u_e) + E\omega(x,t) \tag{2.20}$$

Substituting it into $\dot{V}$, we have

$$\dot{V} = e'(A'P + PA)e + 2e'PB\bar{\sigma}(-Ke) + 2e'PE\omega(x,t) \tag{2.21}$$

With Eq. 2.13 and Eq. 2.17, $\dot{V}$ becomes

$$\dot{V} \leq e'PBB'Pe - \frac{\mu}{\varrho}\omega_0^2 e'Pe + \mu\omega_0^2 + 2e'PB\bar{\sigma}(-Ke) \tag{2.22}$$

Defining $u_{Le} = -B'Pe$, then

$$\dot{V} \leq \mu\omega_0^2(1 - \frac{V}{\varrho}) + \sum_{i=1}^{m}(u_{Lei}^2 - 2|u_{Lei}|\delta_i) \tag{2.23}$$

Within the region $|B_i'Pe| \leq 2\delta_i$, we have

$$\dot{V} \leq \mu\omega_0^2(1 - \frac{V}{\varrho}) \tag{2.24}$$

Based on Eq. 2.14, Eq. 2.24 can be satisfied. Thus, based on Lemma 2.1, $\Omega(P,\varrho)$ is the invariant set for system 2.6. This ends the proof. □

$\Omega(P,\varrho)$ is an invariant set defined as the region of attraction for the system under the given control law. From the proof, we found that $\forall x \in \Omega(P,\varrho)$, the system with the given controller 2.7 can achieve local stability for the tracking system Σ_0.

Remark 2.2. *Based on Assumption 2.5 and Eq. 2.14, the value of the tracking point x_d which can be tracked with decides the size of the ellipsoid $\Omega(P,\varrho)$. $\Omega(P,\varrho)$ is larger with a bigger δ_i, and is consequently reduced with a smaller δ_i.*

Remark 2.3. *The stability region $\Omega(P,\varrho)$ which is obtained by Theorem 2.1 is not the optimal one for system 2.6. Some researches studied the optimization*

of the system's attraction region by using LMIs, nonlinear programming method [71][102][103][126] or by solving the convex optimization problems [127].

The condition Eq. 2.13 is very difficult to be solved, because the parameter ϱ is also a function of P, therefore, a simpler way to obtain the solution of P is proposed in 3 steps:

Step 1: The control gain K (see Eq. 2.8) is designed as a low-high-gain controller as in [120]. Based on this special feature, firstly consider $K = (1+\rho)B'P$, where P is the solution of the following Algebraic Riccati Equation (ARE)

$$A'P + PA - PBB'P + Q = 0 \tag{2.25}$$

with Q a positive definite matrix.

Remark 2.4. *The low-high gain control law is simply formed by adding together the low-gain control and the high-gain control.*

$$u_e = Ke = u_{Le} + u_{He} = -B'Pe - \rho B'Pe \tag{2.26}$$

This is actually an optimal design for the linear system in the absence of input saturation and the tracking mission with appropriately chosing $R_n = I/(1+\rho)$ *and* $Q_n = Q + \rho PBB'P$*, and* P *is the solution to the ARE*

$$A'P + PA - PBR_n^{-1}B'P + Q_n = 0$$

Step 2: Then the solution P of Eq. 2.25 is used to obtain ϱ from Eq. 2.14.

Step 3: For the following inequality

$$\frac{1}{\mu}PEE'P + \frac{\mu}{\varrho}\omega_0^2 P < Q \tag{2.27}$$

If μ exists to make Eq. 2.27 valid, then combining Eq. 2.25 and Eq. 2.27, it is shown that the condition Eq. 2.13 is satisfied.

If Eq. 2.27 cannot be satisfied by any positive μ, then a new Q should be chosen for Eq. 2.25 to get a new solution P. □

2.1.3 Performance analysis

The controller is designed for the system to meet given performance. Usually, the performance objectives that we consider are related to [101]

• the system stability, which has already been discussed in section 2.1.2. An LMI Eq. 2.13 is solved to compute the attraction region.

• the error between the reference signal and the output signal.

• the robustness against disturbances or system uncertainty.

• the fault tolerance capability.

The fault tolerance capability will be discussed in the next chapter 3.

Here, for the system Σ_0 (see Eq. 2.1), we will analyze the second and the third objectives. Because of the disturbances, the state trajectories are not guaranteed to converge to the reference x_d.

In the proof of Theorem 2.1, we have the following equation 2.18 in Case 1

$$\dot{V} \leq -(2\rho+1)e'PBB'Pe - \frac{\mu}{\varrho}\omega_0^2 e'Pe + \mu\omega_0^2 \tag{2.28}$$

Define $Q_{BP} = PBB'P = M \times P$ with $M = Q_{BP}P^{-1}$, then $\dot{V}$ satisfies

$$\begin{aligned} \dot{V} &\leq -(2\rho+1)\lambda_{min}(M)V - \frac{\mu}{\varrho}\omega_0^2 V + \mu\omega_0^2 \\ &\leq \mu\omega_0^2(1 - s^{-1}V) \end{aligned}$$

where

$$s = \frac{\mu\omega_0^2\varrho}{(2\rho+1)\lambda_{min}(M)\varrho + \mu\omega_0^2} \tag{2.29}$$

Obviously, $\Omega(P, s)$ is also an invariant set for system 2.6.

It implies that under the given control law, any trajectory which starts from $\Omega(P, \varrho)$ will enter $\Omega(P, s)$ and will stay within it [102].

Based on the proof of Theorem 2.1, we found that, similar as the analysis of the low-high gain controller in [120], the control law 2.8 can maintain the system's

stability in the region $\Omega(P, \varrho)$. The closed-loop system is stabilized by the low-gain control u_{Le} and the high-gain control u_{He} with ρ and u_d is constructed to improve the tracking performance within $\Omega(P, s)$.

Remark 2.5. *By choosing ρ larger, $\Omega(P, s)$ will become smaller. However, large ρ will increase the chattering situation.*

Let choose s^* such that $e^T P e \leq s^*$, and s^* is the minimal performance error that we can accept. Based on Eq. 2.29, we can find ρ^* which satisfies

$$s^* = \frac{\mu\omega_0^2\varrho}{(2\rho^* + 1)\lambda_{min}(M)\varrho + \mu\omega_0^2} \tag{2.30}$$

Then we can conclude that any trajectory will enter and remain in $\Omega(P, s^*)$ in a finite time.

To sum up, under the above given assumptions, based on the stability analysis in section 2.1.2 and the performance analysis in section 2.1.3, the designed control Eq. 2.7 with and Eq. 2.8 in Theorem 2.1 can ensure that the system whose initial state belongs to $\Omega(P, \varrho)$ will achieve local stabilization and track into $\Omega(P, s)$ which includes the tracking objective x_d .

The designing process will be illustrated by one example in section 2.1.4.

2.1.4 Illustrative example

In this subsection, one example is presented to illustrate the above proposed theories.

The system Σ_0 with input constraints (see Eq. 2.1) is defined by

$$A = \begin{bmatrix} 0.1 & -0.1 \\ 0.1 & 0.3 \end{bmatrix}, B = \begin{bmatrix} 25 & 0 \\ 0 & 2 \end{bmatrix},$$

$$C = \begin{bmatrix} 1 & 0 \\ 0 & 1 \end{bmatrix}, E = \begin{bmatrix} 1 \\ 1 \end{bmatrix}, \omega(x, t) = sin(t)$$

Then for Assumption 2.2, $\omega_0 = 1$. Consider Assumption 2.5, for simplicity, one tracking point is set as

$$x_d = \begin{bmatrix} 0 \\ 0 \end{bmatrix}$$

To design the control law Eq. 2.7 with Eq. 2.8, Eq. 2.14 should be solved. Following the given method in pages 27, based on Eq. 2.25, by choosing

$$Q = \begin{bmatrix} 0.001 & 0 \\ 0 & 0.1 \end{bmatrix}$$

we can get

$$P = \begin{bmatrix} 0.0022 & 0.0106 \\ 0.0106 & 0.187 \end{bmatrix}$$

Based on Eq. 2.14 in theorem 2.1, one can get $\varrho = 2.8659$. Substituting P, ϱ with Q into Eq. 2.27, suppose $\mu = 0.9$, Eq. 2.27 is satisfied.

The minimal performance error that we can accept s^* is given as 0.05. Let fix $\rho = 30$, based on Eq. 2.29, we can also get $s = 0.0324 < s^*$.

The invariant sets $\Omega(P, \varrho)$ and $\Omega(P, s)$ are both obtained, as shown in Fig. 2.3. To verify the proposed theories, a randomly selected point $x_0 = [-40; 1]^T$ on the boundary of $\Omega(P, \varrho)$ is taken as the initial state, by running the closed-loop system with the designed controller 2.8, the phase trajectory can be obtained as shown in Fig. 2.3. It is obvious that the trajectory starting from x_0 in $\Omega(P, \varrho)$ enters $\Omega(P, s)$ and remains inside it. The actuator control signals are also shown in Fig. 2.4.

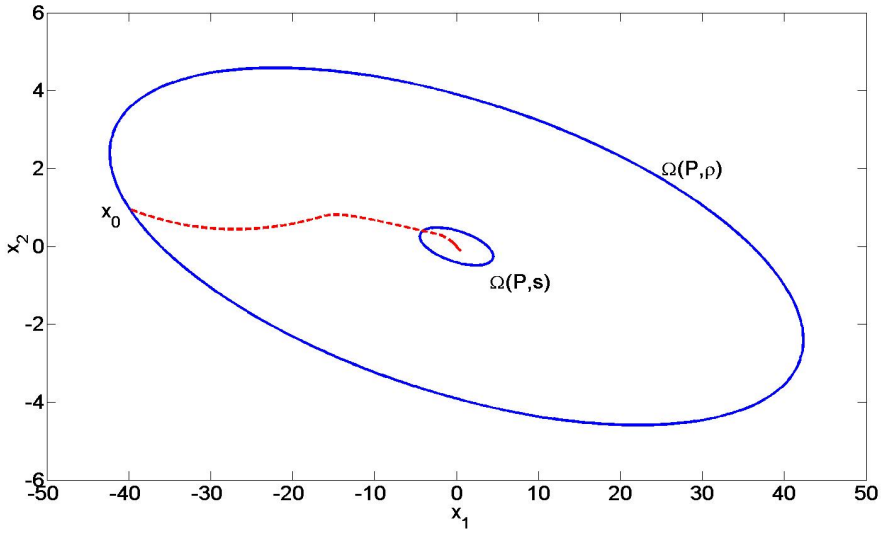

FIGURE 2.3: Invariant Ellipsoid and State Response

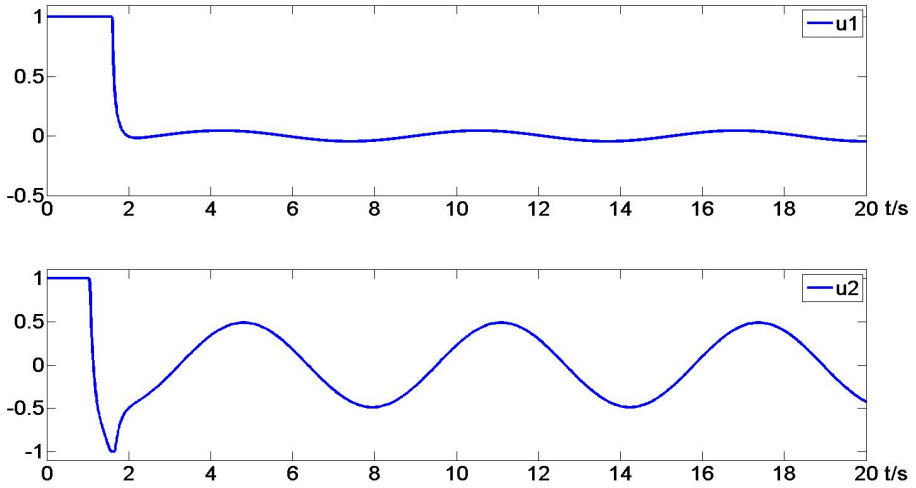

FIGURE 2.4: Actuator Control Signals

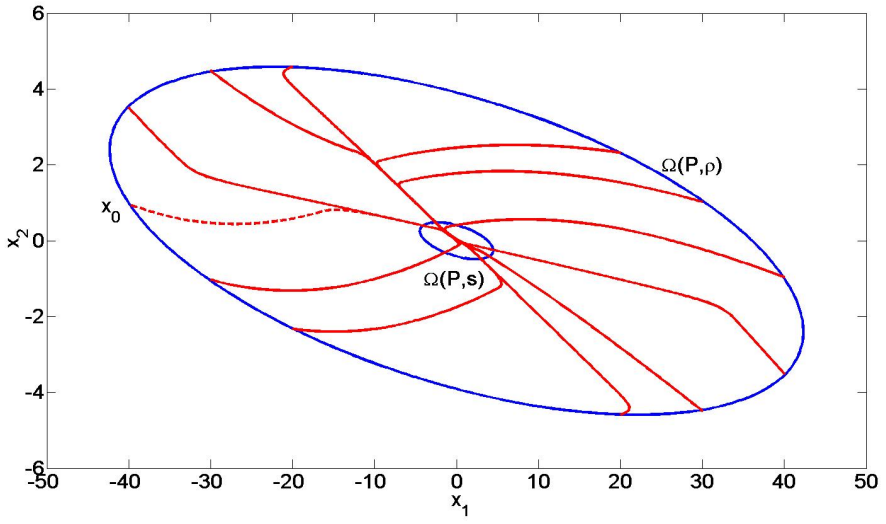

FIGURE 2.5: Convergence Demonstration of Trajectories with Different Initial States

Both invariant sets $\Omega(P, \varrho)$ and $\Omega(P, s)$ can be verified by changing the initial states on the boundary of $\Omega(P, \varrho)$, as seen in Fig. 2.5.

4 different initial states: $x_0 = [-40; 1]^T$, $x_{01} = [-40; 3.5]^T$, $x_{02} = [-30; -1]^T$ and $x_{03} = [40; -1]^T$ are chosen to verify the invariance of the set $\Omega(P, s)$, see Fig. 2.6. These trajectories enter $\Omega(P, s)$ and remain inside it.

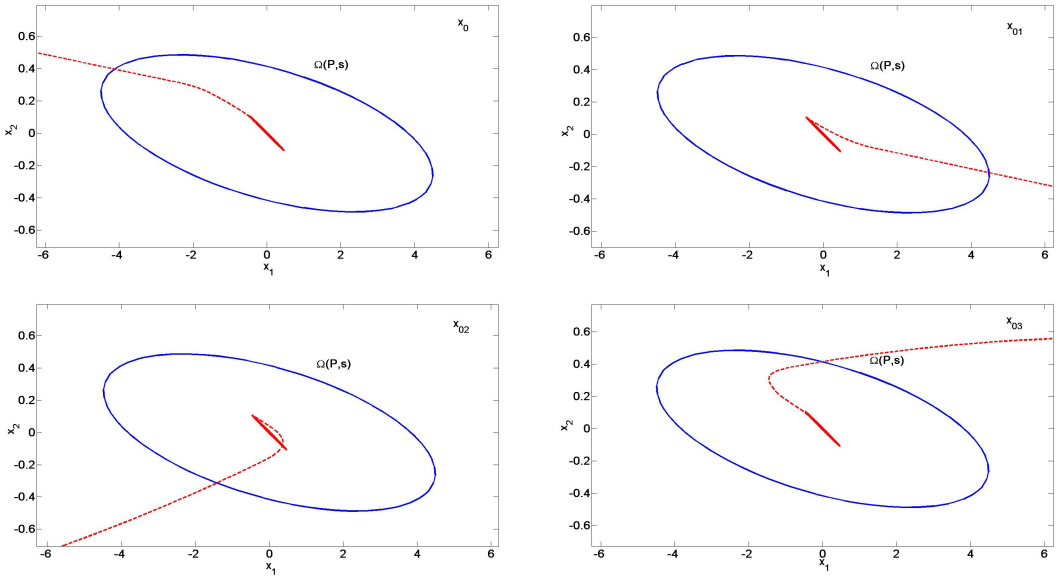

FIGURE 2.6: State Trajectories with Different Initial Conditions

Define $\Omega(P, s_3)$ with $\rho = 200$. Choosing the initial state as $x_{03} = [40; -1]^T$, Fig. 2.7 shows the trajectory with $\rho = 30$ and Fig. 2.8 the trajectory with $\rho = 200$, we can see that by choosing ρ larger, $\Omega(P, s)$ will become smaller, however, the chattering situation will become more serious, as what we stated in subsection 2.1.3.

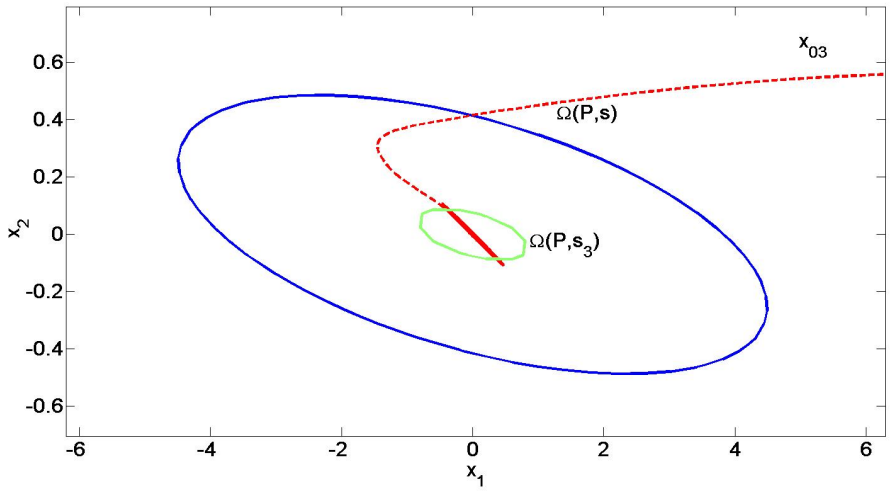

FIGURE 2.7: Trajectory of x_{03} with $\rho = 30$

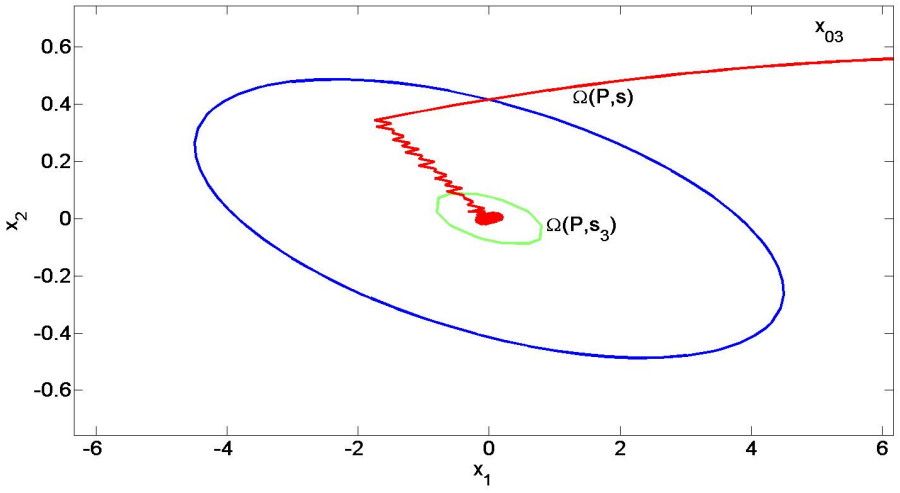

FIGURE 2.8: Trajectory of x_{03} with $\rho = 200$

2.2 Large-region Stabilization Realization

In section 2.1.2, we studied how to estimate the domain of attraction for the tracking system Σ_0 with a constant reference $r = x_d$ in Problem 1. Based on Theorem 2.1, the estimated invariant set $\Omega(P, \varrho)$ is given for the tracking objective x_d. For all $x \in \Omega(P, \varrho)$, the system can achieve semi-global stabilization and track into $\Omega(P, s)$ which includes the tracking objective x_d. However, if $x \notin \Omega(P, \varrho)$, obviously, the tracking mission can not be completed or even the stability of the tracking system can not be guaranteed by the proposed controller Eq. 2.7 and Eq. 2.8. In order to cope with this situation, the large-region stabilization problem will be studied in the following.

Let us recall the error equation 2.6 of the system Σ_0

$$\Sigma_e : \dot{e} = Ae + B\sigma(u(t)) - Bu_d(x_d) + E\omega(x, t)$$

where $u_d(x_d)$ is the constant solution for the objective x_d, see Eq. 2.5; $e = x - x_d$, A, B, E are matrices with appropriate dimensions, $\sigma(u(t))$ is a saturation function, see Eq. 2.2, the controller $u(t)$ is designed based on Theorem 2.1, taking the form of Eq. 2.7 with Eq. 2.8.

For the tracking objective x_d with the designed controller Eq. 2.7 with Eq. 2.8, the system's attraction region $\Omega(P, \varrho)$ can be calculated based on Eq. 2.14 and also the performance region $\Omega(P, s)$ from Eq. 2.29. For all $x \in \Omega(P, \varrho)$, the system can enter into $\Omega(P, s)$ which includes the tracking objective x_d.

Assumption 2.6. *Assume (A, B) is stabilizable and A has all its eigenvalues in the closed left-half plane, i.e., the given system is asymptotically null controllable with bounded control (ANCBC) [128].*

Lemma 2.2. *Let assume $u_d(x_d)$ satisfies Assumption 2.5, and the initial state $x_0 \notin \Omega(P, \varrho)$, that means the actuator output should be larger than the maximal control of which the saturated controller can afford, then*

If the system Eq. 2.6 with small disturbances can satisfy Assumption 2.6, the system can be stable at

$$x(t \to +\infty) = x_d + e_{ss} \tag{2.31}$$

where $e_{ss} = A^{-1}B\Delta$ *is the tracking error,* $\Delta = (I - u_d) + B^{-1}E\omega$.

Else the system Eq. 2.6 is unstable.

Proof: If the system Eq. 2.6 satisfies Assumption 2.6, and the initial state $x_0 \notin \Omega(P, \varrho)$, then based on the saturation case proof in Theorem 2.1, the tracking mission will not be achieved. However, since the open-loop of the system is stable, Eq. 2.20 in the proof of Theorem 2.1 can be rewritten as

$$\dot{e} = Ae + B(I - u_d) + E\omega(x, t) \tag{2.32}$$

when the system is stable, i.e., $\dot{e} = 0$, the state will be stabilized at $x = (x_d + e_{ss})$ with a constant error e_{ss}.

If the system Eq. 2.6 does not satisfy Assumption 2.6, then for Eq. 2.32, the system will become unstable. This ends the proof. □

$x_0 \notin \Omega(P, \varrho)$ for two reasons: one is that the value of x_0 is too large; the second reason is that the size of the set $\Omega(P, \varrho)$ is too small, as what was stated in Remark 2.6. From Assumption 2.5 and Eq. 2.14, we can see that if the set-point which needs to be tracked with is too large, then δ_i will become small (see Assumption 2.5), the ellipsoid $\Omega(P, \varrho)$ which has relationship with δ_i, see Eq. 2.14, is small.

How to guarantee the tracking system's stability and the tracking mission for a saturated system even if the open-loop system is not stable? To solve this problem, a lot of researches focus on the control design under input constraints, by maximizing the domain of attraction. Another method to avoid potential actuator saturation is to accept a performance degradation. A well known example of performance degradation is the integrator windup phenomenon in a PID controller [129]. Another solution is the reference governor approach. By using reference management techniques [101][114], we can prevent the control input from entering the saturation region. The reference governor is an auxiliary system to the

controller, which is already designed to stabilize the system and track the reference, therefore this approach is effective especially when the opened-loop plant is unstable [130].

In this section, we will discuss the case when $x_0 \notin \Omega(P, \varrho)$, and by using the controller designed in section 2.1.2, a algorithm based on the reference management technique is proposed to achieve the tracking mission and also the system's stability.

2.2.1 The reference management technique

For the control objective x_d, using the designed control law Eq. 2.7 with Eq. 2.8, we have that any trajectory starting from $\Omega(P, \varrho_d)$ (see Eq. 2.14) will enter $\Omega(P, s_d)$ (see Eq. 2.29) and will remain inside it. If the initial state $x_0 \notin \Omega(P, \varrho_d)$, then an iterative methodology could be applied. The principle is to change adequately, at each step, the reference to follow such that the stability is guaranteed. Step by step, the trajectory will converge to x_d.

For the initial state $x_0 \notin \Omega(P, \varrho_d)$, first, another reference x_{d1} has to be found such that it can make sure $x_0 \in \Omega(P, \varrho_{d1})$. The trajectory starting by x_0 will enter $\Omega(P, s_{d1})$ whose origin is x_{d1}. If $\Omega(P, s_{d1}) \not\subset \Omega(P, \varrho_d)$, then another reference x_{d2} could be found such that it can make sure $\Omega(P, s_{d1}) \subset \Omega(P, \varrho_{d2})$, the trajectory starting with x_{d1} will enter $\Omega(P, s_{d2})$ whose origin is x_{d2}. If $\Omega(P, s_{d2}) \notin \Omega(P, \varrho_d)$, another reference could be found and so on, until we find $\Omega(P, s_{dk})$ whose origin is x_{dk} such that $\Omega(P, s_{dk}) \subset \Omega(P, \varrho_d)$, see Fig. 2.9. So that after adopting the original tracking point x_d, the designed controller can guarantee the tracking objective.

Remark 2.6. *It should be noted that the new chosen tracking point* $x_{d(i)}, i = 1, 2, ..., k$ *should also satisfy Assumption 2.5.*

The proposed algorithm based on the reference management technique here is designed off-line. Let us consider the following k sets of tracking points $x_{d(i)}, i =$

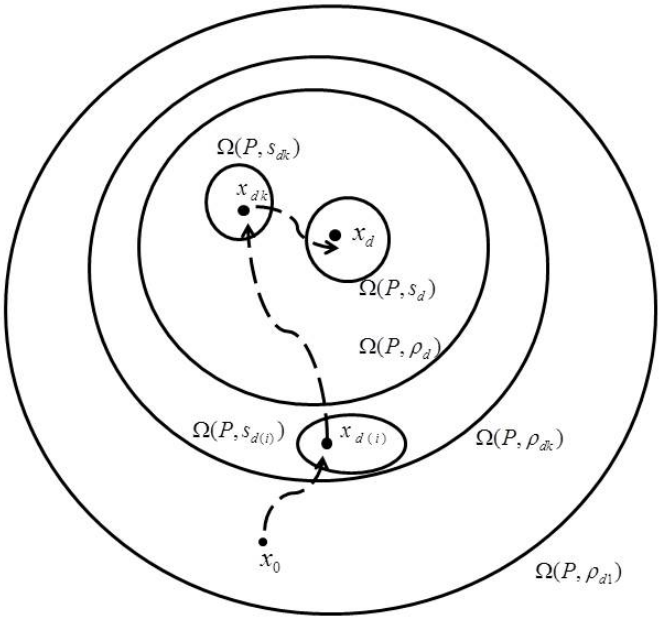

FIGURE 2.9: The Successive Stabilization Process

$1, 2, ..., k$ with their two invariant sets $\Omega(P, \varrho_{d(i)})$ and $\Omega(P, s_{d(i)})$:

$$\begin{aligned} x_{d1} &: \{\Omega(P, \varrho_{d1}), \Omega(P, s_{d1})\} \\ x_{d2} &: \{\Omega(P, \varrho_{d2}), \Omega(P, s_{d2})\} \\ &\vdots \\ &\vdots \\ x_{dk} &: \{\Omega(P, \varrho_{dk}), \Omega(P, s_{dk})\} \end{aligned} \tag{2.33}$$

Within the reference points which satisfy Assumption 2.5, the combination of the chosen k points has many possibilities. Here, one requirement is given to choose k reference points. They should satisfy the following Assumption 2.7:

Assumption 2.7. *Assume that k sets of tracking points x_{dk} are constructed off-line, and they satisfy*

$$\Omega(P, s_{d(i)}) \subset \Omega(P, \varrho_{d(i+1)}), i = 1, 2..., (k-1) \tag{2.34}$$

$$\Omega(P, s_{d(i)}) \bigcap \Omega(P, \varrho_{d(i+2)}) = \varnothing, i = 1, 2..., (k-1) \tag{2.35}$$

and

$$\Omega(P, s_{dk}) \subset \Omega(P, \varrho_d) \tag{2.36}$$

$$\Omega(P, s_{dk}) \bigcap \Omega(P, s_d) = \varnothing \tag{2.37}$$

Remark 2.7. *The number of the chosen reference points k is not a fixed number. It depends on how large the stabilization we want to achieve and other specific requirements on these reference points. Since these reference points are chosen off-line, k should also be adjustable to meet different requirements. If the chosen set point $x_{d(i)}$ could satisfy that $\Omega(P, s_{d(i)})$ is very close to the boundary of $\Omega(P, \varrho_{d(i+1)})$, then it could be helpful to reduce the number of set points to chose.*

Remark 2.8. *For each $x_{d(i)}, i = 1, 2, ..., k$, with the designed controller Eq. 2.7 with Eq. 2.8, their invariant sets $\Omega(P, \varrho_{d(i)})$ and $\Omega(P, s_{d(i)})$ can be calculated based on Eq. 2.14 and Eq. 2.29.*

Based on Assumption 2.7, let us assume that k reference points are chosen. Then the following reference management algorithm is given. The overall structure of the reference governor is depicted in Fig. 2.10.

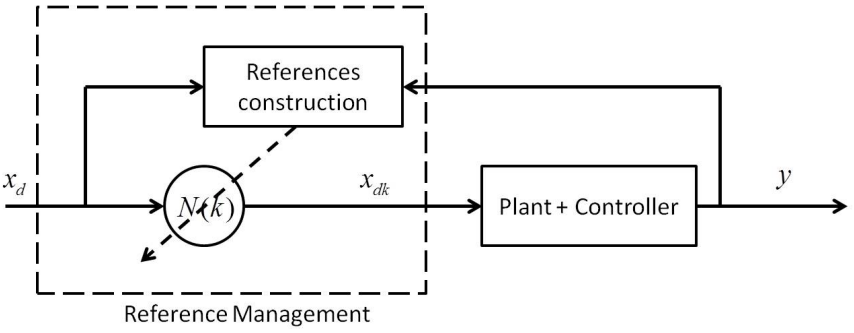

FIGURE 2.10: The Overall Structure of The Proposed Reference Governor

For the initial state $x_0 \notin \Omega(P, \varrho_d)$, firstly, the given initial state x_0 is compared with the set $\Omega(P, \varrho_d(i))$ of tracking points $x_{d(i)}(i = 1, 2, ..., k)$ to find the initial tracking objective $x_{d(i)}$ that the saturated controller can achieve, i.e, $x_0 \in \Omega(P, \varrho_d(i))$, this process is achieved by the initial reference algorithm, see Fig. 2.11.

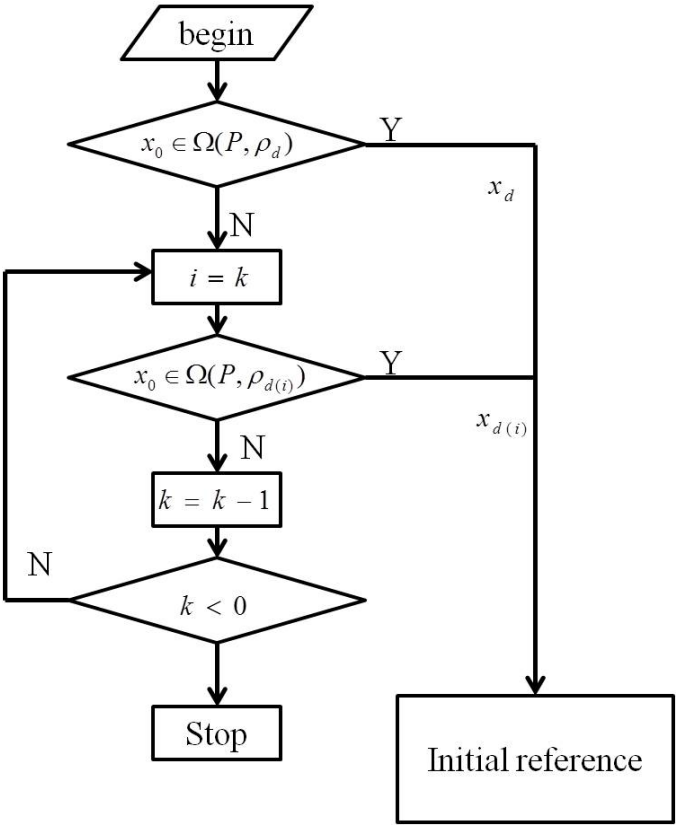

FIGURE 2.11: The Proposed Initial Reference Algorithm

If $x_{d(i)}$ is chosen as the initial objective, as soon as the system achieves this goal, i.e., the trajectory enters $\Omega(P, s_{d(i)})$, then the objective is changed to $x_{d(i+1)}$ such that the trajectory can enter $\Omega(P, s_{d(i+1)})$, continuing until x_d is set, see Fig. 2.12.

If the original objective x_d is the choosing point, then the whole reference management (see Fig. 2.12) does not need to be applied.

Remark 2.9. *Since each $x_{d(i)}$ is within the controller's capability, the whole control process will be stable, and x_d will be reached finally with the given controller.*

2.2.2 Illustrative example

In this subsection, the same example as in section 2.1.4 is presented to illustrate the above proposed theories.

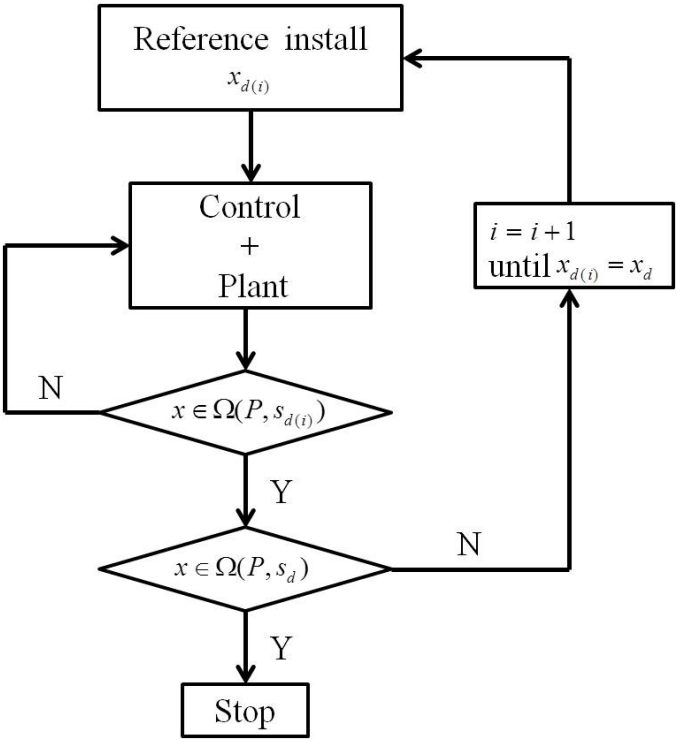

FIGURE 2.12: The Control Process with Reference Management Technique

The system Σ_0 (see Eq. 2.1) is defined by

$$A = \begin{bmatrix} 0.1 & -0.1 \\ 0.1 & 0.3 \end{bmatrix}, B = \begin{bmatrix} 25 & 0 \\ 0 & 2 \end{bmatrix}, C = \begin{bmatrix} 1 & 0 \\ 0 & 1 \end{bmatrix}, E = \begin{bmatrix} 1 \\ 1 \end{bmatrix}$$

$$\omega(x,t) = 0.2sin(t)$$

The given system does not satisfy Assumption 2.6. And for Assumption 2.2, $\omega_0 = 0.2$.

The tracking objective x_d and the following chosen new references $x_{d(i)}$ should satisfy Assumption 2.5. The tracking points in the area which is surrounded by the four lines in Fig. 2.13 satisfy Assumption 2.5. The tracking objective here is set as

$$r = x_d = \begin{bmatrix} 18 \\ 0 \end{bmatrix}$$

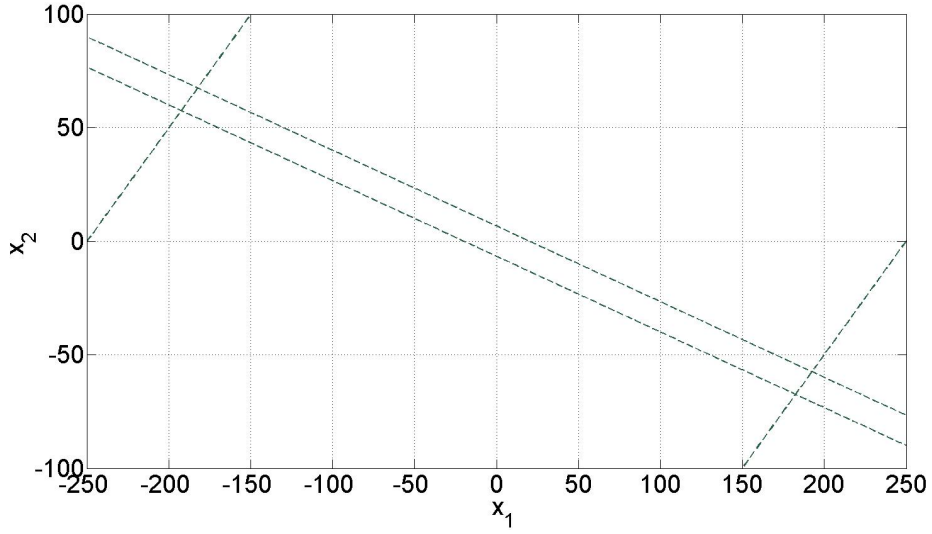

FIGURE 2.13: The Area of Tracking Points Which Satisfy Assumption 2.5

At first, the controller is designed based on Theorem 2.1 in Chapter 2.1.2. By giving

$$Q = \begin{bmatrix} 1 \times 10^{-6} & 0 \\ 0 & 1 \times 10^{-6} \end{bmatrix}$$

we can get

$$P = \begin{bmatrix} 0.0012 & 0.0035 \\ 0.0035 & 0.0151 \end{bmatrix}$$

Based on theorem 2.1, one can get $\varrho = 0.6623$. Substituting P, ϱ with Q into Eq. 2.27, choosing $\mu = 0.2$, Eq. 2.27 is satisfied.

The minimal performance error s^* that we can accept is given as 0.005. Let fix $\rho = 50$, based on Eq. 2.29, we can also get $s = 0.0044 < s^*$.

The invariant sets $\Omega(P, \varrho)$ and $\Omega(P, s)$ are both obtained. Since the tracking point x_d is near the boundary of the area which is defined in Fig. 2.13, the acceptable performance error s^* is chosen small in order to avoid $\Omega(P, s)$ exceeding this area, see Fig. 2.14.

A randomly selected point $[0; -2]^T$ near the boundary of $\Omega(P, \varrho)$ is taken as the initial state, as shown in Fig. 2.14. By running the closed-loop system with the designed controller 2.8, the phase trajectory can be obtained as shown in Fig. 2.14.

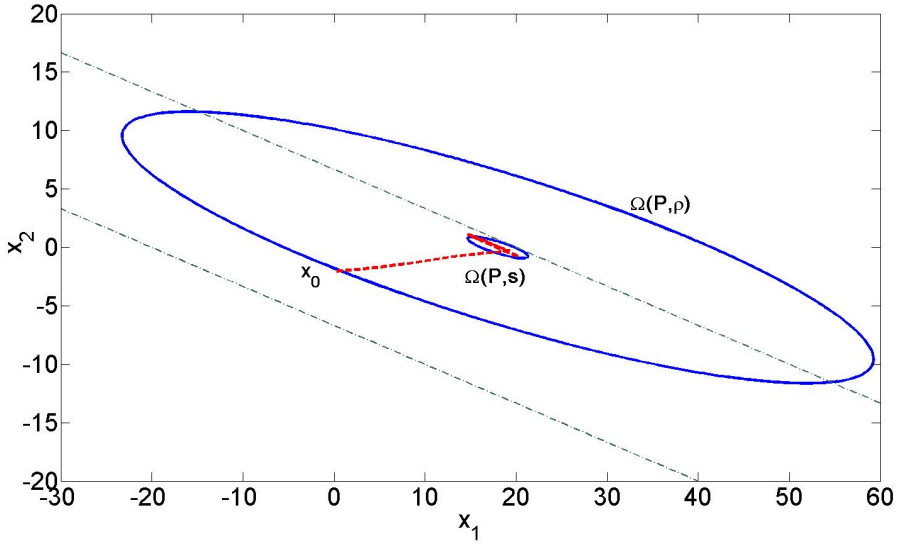

FIGURE 2.14: Invariant Ellipsoid and State Response

From Fig. 2.14 we can see that any trajectory starting from $\Omega(P, \varrho)$ will enter $\Omega(P, s)$. However, for initial states $x_0 \notin \Omega(P, \varrho)$, the proposed algorithm which is based on reference adjustment technique should be adopted.

Let assume that one additional requirement is given for choosing the new reference points: $x_{d(i)}(2) = 0$. In the proposed algorithm, $k = 1$ is chosen for simplicity. Only one set of tracking point $x_{d(1)}$ is chosen off-line as

$$x_{d1} = \begin{bmatrix} 0 \\ 0 \end{bmatrix}$$

to satisfy Assumption 2.7.

With the same controller for x_d, the invariant sets $\Omega(P, \varrho_{d1})$ and $\Omega(P, s_{d1})$ of $x_{d(1)}$ can be obtained: $\varrho_{d1} = 5.3885$ and $s_{d1} = 0.0044$, see Fig. 2.15.

With the proposed algorithm, the system's attraction region is extended from $\Omega(P, \varrho_d)$ to $\Omega(P, \varrho_{d1})$. For obtaining larger attraction region, different k and reference points should be chosen.

The initial state is set as $x_0 = [-100; 33]^T$. Since $x_0 \notin \Omega(P, \varrho_d)$, without adopting the proposed algorithm, the trajectory starting with x_0 can not enter $\Omega(P, s)$, see Fig. 2.16.

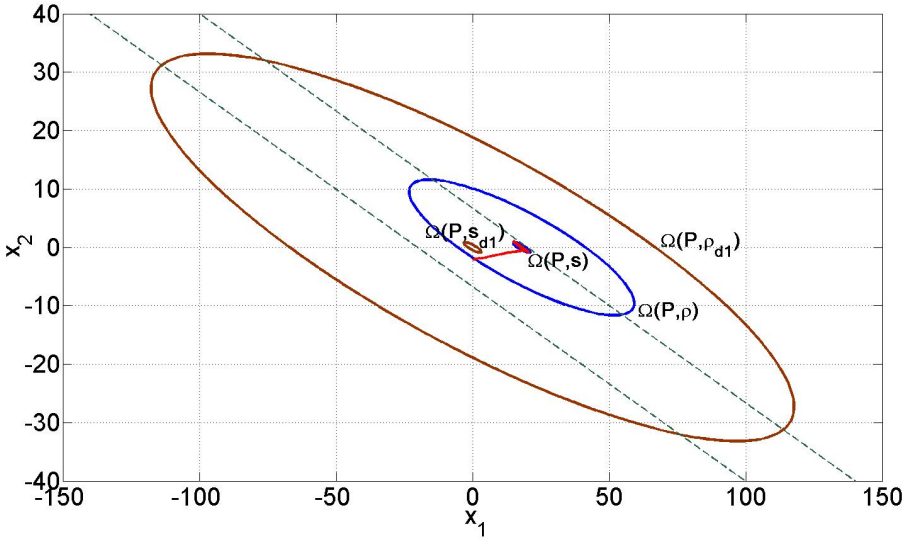

FIGURE 2.15: Invariant Ellipsoid for x_d and x_{d1}

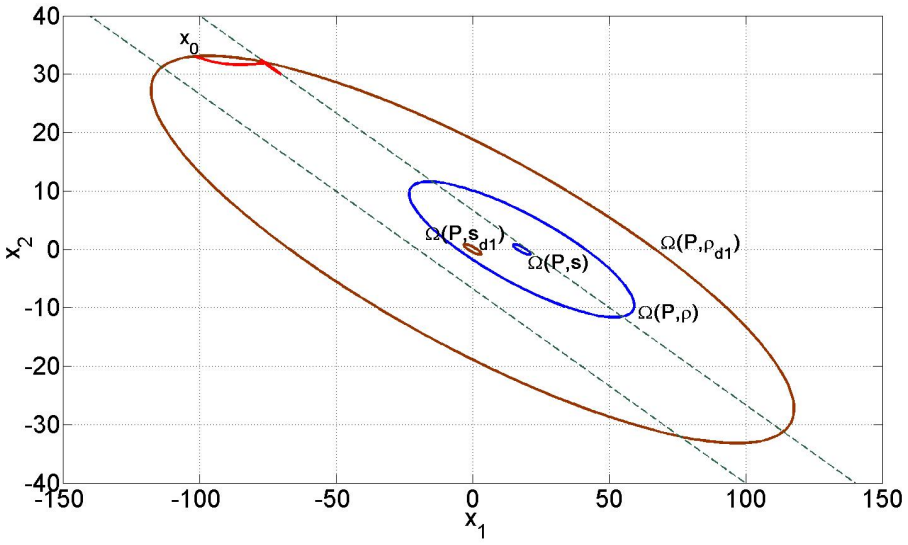

FIGURE 2.16: State Trajectory with $x_0 \notin \Omega(P, \varrho_d)$

In order to achieve the tracking mission, the proposed algorithm is adopted. At the beginning the initial reference algorithm is applied. Based on Fig. 2.11, we find that $x_0 \in \Omega(P, \varrho_{d1})$, therefore x_{d1} is set as initial tracking point at first.

When the trajectory starting from x_0 enters $\Omega(P, s_{d1})$, based on Fig. 2.12, the real objective x_d is installed. Since $\Omega(P, s_{d1}) \in \Omega(P, \varrho_d)$, thus the objective can finally be achieved in the end, see Fig. 2.17.

The sequence is shown in Fig. 2.18.

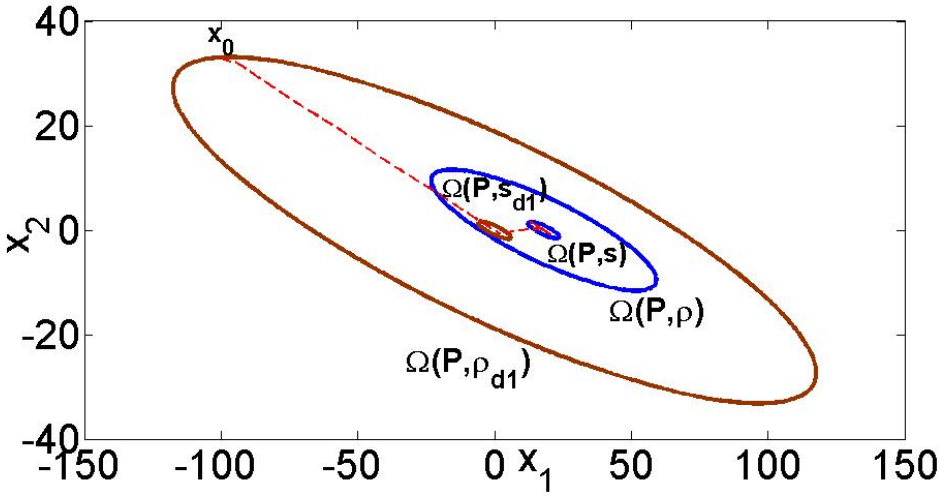

FIGURE 2.17: State Trajectory with Proposed Reference Adjustment Algorithm

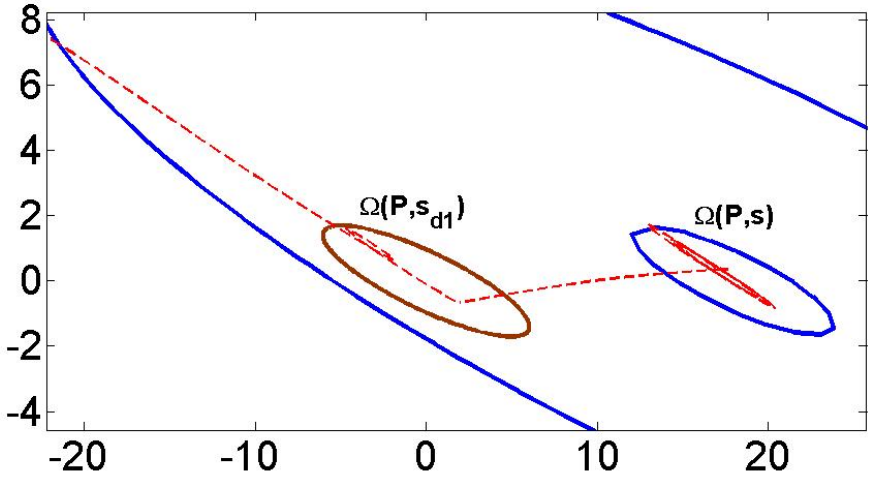

FIGURE 2.18: Sequence of State Trajectory in Fig. 2.17

The actuator control signals are also shown in Fig. 2.19.

The whole control process in Fig. 2.17 and Fig. 2.18 shows that the tracking system with reference adjustment technique is stable, and based on the proposed algorithm, x_d will be reached finally with the given controller.

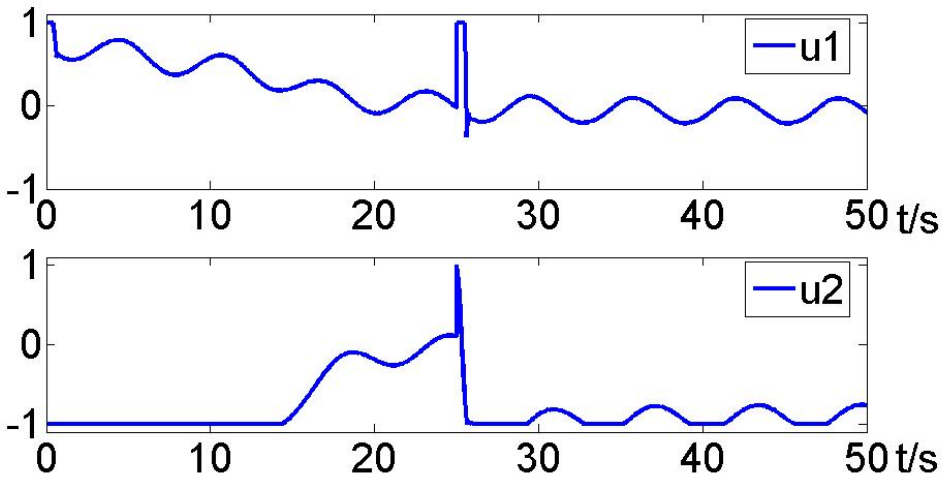

FIGURE 2.19: Actuator Control Signals

2.3 Conclusion

In Chapter 2, the tracking control design for a linear system with disturbances and actuator saturation is studied. First, the tracking problem for linear systems is proposed in Problem 1. Based on the given assumptions (Assumption 2.1, Assumption 2.2 and Assumption 2.5), a controller (Eq. 2.7, Eq. 2.8) based on the low-high-gain control technique is designed for the tracking mission.

Then the invariant set theory is applied to estimate the attraction region for the tracking system with the designed controller. The stability region $\Omega(P, \varrho)$ (Eq. 2.14) and the tracking performance region $\Omega(P, s)$ (Eq. 2.29) can be calculated. For the tracking system with the designed controller, any trajectory starting from $\Omega(P, \varrho)$ will enter $\Omega(P, s)$ and remain inside it.

The performance region $\Omega(P, s)$ (Eq. 2.29) is described as a function of the high-gain ρ in the designed tracking controller Eq. 2.8, thus the tracking performance region can be adjusted by choosing different values of ρ in the tracking controller Eq. 2.8.

For the case that the state $x_0 \notin \Omega(P, \varrho)$, if the open-loop system is stable, the tracking system can be stabilized and will have a tracking error, else the tracking system will become unstable. Considering this problem, a new algorithm based on

a reference adjustment technique is proposed with the same designed controller to achieve large-region stabilization.

k sets of tracking points $x_{d(i)}$ are chosen off-line. Since each x_{di} satisfies Assumption 2.7 and is within the controller's capability expressed by Assumption 2.5, the whole control process will be stable, and the objective x_d will be reached finally even the initial state x_0 is not in the stability region $\Omega(P, \varrho)$ of x_d.

The same example is simulated by using MATLAB in section 2.1 and section 2.2. The simulation results in section 2.1.4 and 2.2.2 show the effectiveness of the designed controller and the proposed algorithm for large-region stabilization.

New contributions of the studies in this chapter are:

1. Most of the researches related to the control design with actuator saturation are aiming at regulating the system's state near zero. In this chapter, we considered the tracking problem that is to follow a nonzero constant reference command signal. The methods and algorithms proposed here can be easily extended to the former case by setting reference as zero.

2. The low-high-gain controller is widely used for systems control with actuator saturation, see [87][120]. Many researchers analyze the stability region for systems with low-high-gain controller, different from these analyses, we adopted the invariant set theory with the Lyapunov function to estimate the stability region. The stability region estimated for the low-high-gain controller with our method has less conservatism. The result is the same as in [120] which also used another less conservative way to estimate the stability region. Besides, our method can not only be used to estimate the stability region but also can give the performance region (called as disturbance rejection region in [102]).

3. Many researchers aimed at using the invariant set theory to analyze the control systems with actuator saturations. A lot of studies focus on getting the controller by solving LMI or BMI problems, and by using optimisation tools to maximize the domain of attraction and minimize the disturbance

rejection region [102][121]. Different from these papers, we adopted the low-high-gain control technique directly to get an optimal controller. Although at first we proposed to design the controller as a solution of a LMI (BMI) problem, then a new design method is proposed to reduce the LMI problem to a Riccati-equation solving problem. By choosing appropriate parameters, the sub-maximized stability region can also be obtained by our method for the low-high-gain controller.

4. A lot of the existing researches focus on maximizing the domain of attraction to solve the large-region stabilization problem for systems with actuator saturation. Only few uses the reference adjustment technique. The former way actually has a lot of limitations comparing to the reference adjustment technique. Different from [101][114] which also adjusted the reference when meeting the saturation problem, a new algorithm is designed in our thesis to realize large-region stabilization, and the proposed algorithm and method can also be systematically expressed by the invariant sets.

Chapter 3

FAULT-TOLERANT CONTROL DESIGN FOR LINEAR SYSTEMS WITH INPUT SATURATION

Contents

Abstract In this chapter, fault-tolerant control methods for linear systems with actuator saturation and certain faults are considered. The fault's influence on the system's attraction region and on the performance region is analyzed first, then two main FTC design methods (PFTC and AFTC) are used to cope with faults and actuator saturation together. Finally based on the implementation results of PFTC and AFTC, a fault-tolerant control scheme based on the reference adjustment technique is proposed to guarantee the system's performance in an acceptable region.

With increasing requirements for systems' reliability and safety, a lot of significant researches on FTCS design have been conducted in the past several decades [1]. However, few of them takes the actuator saturation/input constraints into consideration during the FTCS design process. How to deal with the actuator saturation problem in the presence of faults is still a challenging issue.

Since the closed-loop system with saturated control can generally achieve local stability, in Chapter 2, the invariant set theory is used to estimate the attraction region of the system with one designed controller. When designing the controller for healthy system, the objective is not only to achieve the objective (the performance region should be as small as possible), but also to enlarge the stability region (the attraction region should be as large as possible). If faults happen, the attraction region might change, therefore the stability and also the performance may not be guaranteed anymore.

Therefore it has a great meaning to study fault tolerant controller design methods for systems with actuator saturation.

3.1 Problem Statement

Let us recall the linear system Σ_0 (see Eq. 2.1) in Chapter 2.

$$\dot{x} = Ax + B\sigma(u(t)) + E\omega(x,t) \tag{3.1}$$

where $x \in R^n$, $u \in R^m$ are the state and control input vectors, $\omega \in R^n$ represents the uncertainties and disturbances, A, B, E are matrices with appropriate dimensions, and $\sigma(u)$ is a saturation function of $u(t)$. We suppose that Assumption 2.1, Assumption 2.2 and Assumption 2.3 is still satisfied.

The faults may be: actuator faults; sensor faults or component faults. They can be presented under additive form and multiplicative form [131]. Here, actuator faults which will bring changes in the control matrix B are considered.

The considered faulty system can be modeled as [131]

$$\dot{x} = Ax + B\bar{\Gamma}_f\sigma(u(t)) + E\omega(x,t) \tag{3.2}$$

where $\bar{\Gamma}_f = diag(\gamma_1, \gamma_2, ..., \gamma_m) \in R^{m\times m}$ and each element $\gamma_i \in [0,1], i = 1, 2, ..., m$. In this way $\gamma_i = 0$, $\gamma_i = 1$ and $\gamma_i = \varepsilon \in (0,1)$ represent a complete failure, nominal operation and partial loss effectiveness respectively of the i-th actuator.

Remark 3.1. *The faults that we considered here are in the multiplicative form. They are modelled as* $\sigma^f(u) = \bar{\Gamma}_f\sigma(u(t))$, *rather than* $\sigma^f(u) = \sigma(\bar{\Gamma}_f u(t))$ *in [102].*

The tracking problem for the faulty system Eq. 3.2 with input saturation is proposed as follows:

Consider the following linear faulty system Σ_f

$$\Sigma_f : \dot{x} = Ax + B\bar{\Gamma}_f\sigma(u(t)) + E\omega(x,t)$$

where $\sigma(u) = [\sigma_1(u_1), ..., \sigma_m(u_m)]^T$, where $\sigma_i(u_i) = sign(u_i)\min\{|u_i|, 1\}$, $\bar{\Gamma}_f = diag(\gamma_1, \gamma_2, ..., \gamma_m)$ with $\gamma_i \in [0,1]$ represents the actuator fault gain matrix.

Problem 2. *If Assumption 2.3 is satisfied, let* $r = x_d$ *be a constant reference. For system* Σ_f, *design a control law* $u(t)$ *to make* $x(t) \to x_d$ $(t \to +\infty)$.

3.2 Influence of Faults

The following control law is designed to achieve the tracking mission as in Chapter 2 , see Eq. 2.7.

$$u(t) = -Kx + K_r x_d \tag{3.3}$$

where K is the state feedback gain and K_r the feedforward control gain.

Define $u_{df}(x_d)$ as the constant solution for System Eq. 3.2 when achieving x_d

$$Ax_d + B\bar{\Gamma}_f u_{df}(x_d) = 0 \tag{3.4}$$

with $u_{df} = (K_r - K)x_d$.

Based on Eq. 3.4 and Eq. 2.5, we can see that for the tracking objective x_d that even the faulty system can achieve, $u_{df}(x_d)$ and $u_d(x_d)$ should satisfy

$$u_d(x_d) = \bar{\Gamma}_f u_{df}(x_d) \tag{3.5}$$

Assumption 3.1. *Assume that each element of u_{df} satisfies*

$$\|u_{dfi}(x_d)\| \leq 1 - \delta_{fi} \quad \delta_{fi} \in [0, 1] \tag{3.6}$$

This assumption requires that γ_i should be larger than u_{di} (the constant solution of System Eq. 3.1,see Eq. 2.5).

This assumption implies that the controller has the capability to achieve x_d even if the fault happens. Supposing that the plant dynamics is corrupted by unpredictable fault events which alter the nominal behavior of System Eq. 3.1.

The same controller which is used in Chapter 2 is adopted here to analyze the influence of the fault. Giving $K = (1 + \rho)B'P$ where P is a positive semi-definite and symmetric solution of Eq. 2.13. Let define $e = x - x_d$, then the error equation of system 3.2 is given by

$$\dot{e} = Ae + B\bar{\Gamma}_f \sigma(u(t)) - B\bar{\Gamma}_f u_{df}(x_d) + E\omega(x, t) \tag{3.7}$$

Consider $V(e) = e'Pe$ as a quadratic Lyapunov function candidate. The derivative of $V(e)$ along the trajectory of the closed-loop system is

$$\dot{V} = 2e^T P(Ae + B\bar{\Gamma}_f \sigma(u(t)) - B\bar{\Gamma}_f u_{df}(x_d) + E\omega(x,t))$$

Assume that when a fault happened, the following condition is satisfied

$$A'P + PA - PB\bar{\Gamma}_f B'P + \frac{1}{\mu}PEE'P + \frac{\mu}{\varrho_f}\omega_0^2 P < 0 \tag{3.8}$$

where

$$\varrho_f = \min_i \frac{4(1-|u_{dfi}|)^2}{B_i' P B_i} \tag{3.9}$$

Similar as the proof of Theorem 2.1 in Chapter 2, for the saturation case, by defining $u_{Le} = B'Pe$, with Eq. 3.9 we get

$$\dot{V} \leq \mu\omega_0^2(1 - \frac{V}{\varrho_f}) + \sum_{i=1}^{m} \gamma_i(u_{Lei}^2 - 2(1-|u_{dfi}|)|u_{Lei}|) \tag{3.10}$$

Then, one can conclude that $\Omega(P, \varrho_f)$ is an invariant set for system 3.7.

Comparing $\Omega(P, \varrho_f)$ with $\Omega(P, \varrho)$ (see Theorem 2.1 in Chapter 2), we can see that the fault will reduce the size of the system's stability region.

Let us assume that the stability is not affected by the fault, that is to say the system is still stable even if the fault happens, now the tracking performance is analyzed.

Under the unsaturation case, $\dot{V}(e)$ becomes

$$\dot{V}(e) = e'(PA + A'P)e - 2(1+\rho)e'PB\bar{\Gamma}_f B'Pe + 2BPE\omega(x,t))$$

By substituting Eq. 3.8, $\dot{V}(e)$ becomes

$$\begin{aligned}
\dot{V}(e) &\leq e'PB\bar{\Gamma}_f B'Pe - 2(1+\rho)e'PB\bar{\Gamma}_f B'Pe - \frac{\mu}{\varrho_f}\omega_0^2 e'Pe + \mu\omega_0^2 \\
&= -(2\rho+1)e'PB\bar{\Gamma}_f B'Pe - \frac{\mu}{\varrho_f}\omega_0^2 e'Pe + \mu\omega_0^2 \\
&\leq -(2\rho+1)\lambda_{min}(M)V - \frac{\mu}{\varrho_f}\omega_0^2 V + \mu\omega_0^2 \\
&= \mu\omega_0^2(1 - s_f^{-1}V)
\end{aligned} \tag{3.11}$$

where $M_f = Q_{BPf}P^{-1}$ with $Q_{BPf} = PB\bar{\Gamma}_f B'P$ and

$$s_f = \frac{\mu\omega_0^2\varrho_f}{(2\rho+1)\lambda_{min}(M_f)\varrho_f + \mu\omega_0^2} \tag{3.12}$$

Comparing $\Omega(P, s_f)$ with $\Omega(P, s)$ in Eq. 2.29, we can see that the fault will enlarge the size of the system's performance region.

Remark 3.2. *The above analysis is mainly based on Eq. 3.8. However, if the fault is more severe, Eq. 3.8 may not be found, then substituting Eq. 2.13 into* $\dot{V}$*, one can get*

$$\varrho_f = \min_i \frac{4\gamma_i^2(1-|u_{dfi}|)^2}{B_i'PB_i} \tag{3.13}$$

and

$$s_f = \frac{\mu\omega_0^2\varrho}{(2\rho+1)\lambda_{min}(M)\varrho + \mu\omega_0^2 - \lambda_{max}(N)\varrho} \tag{3.14}$$

where $M = Q_{BP}P^{-1}$ *with* $Q_{BP} = PBB'P$ *and* $N = Q_{BPf}P^{-1}$ *with* $Q_{BPf} = PB(I-\bar{\Gamma}_f)B'P$.

Comparing Eq. 3.9 (Eq. 3.13) with Eq. 2.14 and Eq. 3.12 (Eq. 3.14) with Eq. 2.29, we can see that the more severe the fault is, the more the stability region will reduce and the performance region will enlarge.

$\Omega(P, \varrho)$ and $\Omega(P, s)$ can be calculated based on Eq. 2.14 and Eq. 2.29 for System 3.1, $\Omega(P, \varrho_f)$ and $\Omega(P, s_f)$ from Eq. 3.9 and Eq. 3.12 for System 3.2, the size of the fault and also the time when it happens will influence the stability and the tracking performance of our system.

One illustrative example of the same system (A, B) using the same controller in section 2.2.2 is treated here. The fault $\bar{\Gamma}_f = diag(0.2, 0.5)$ is considered. $\Omega(P, \varrho)$ and $\Omega(P, s)$, $\Omega(P, \varrho_f)$ and $\Omega(P, s_f)$ are presented in Fig. 3.1 and Fig. 3.2. The dotted line represents the trajectory starting with initial state $x_0 = (40, -2.8)^T$ without considering faults.

If the fault happens at $t_f = 1s$, that is to say, before the trajectory enters $\Omega(P, \varrho_f)$, the stability will be destroyed, see Fig. 3.3.

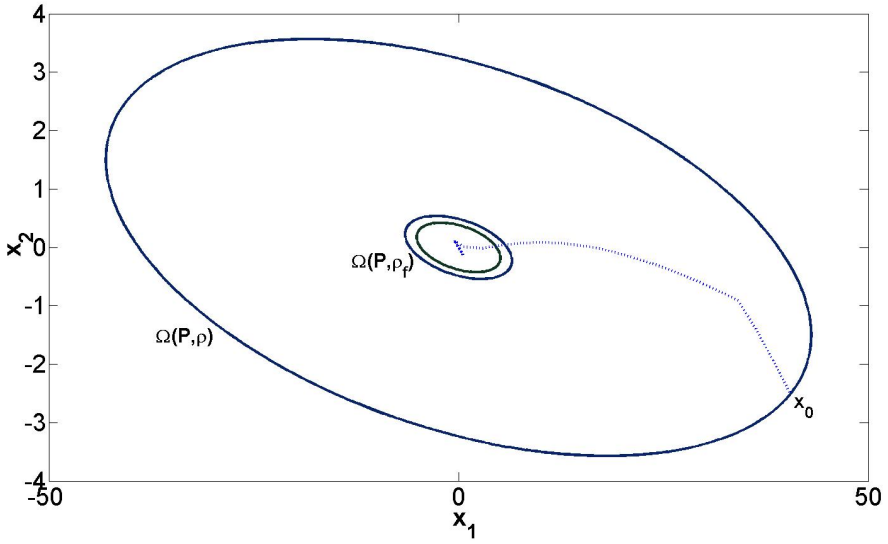

FIGURE 3.1: Invariant Ellipsoid and State Response

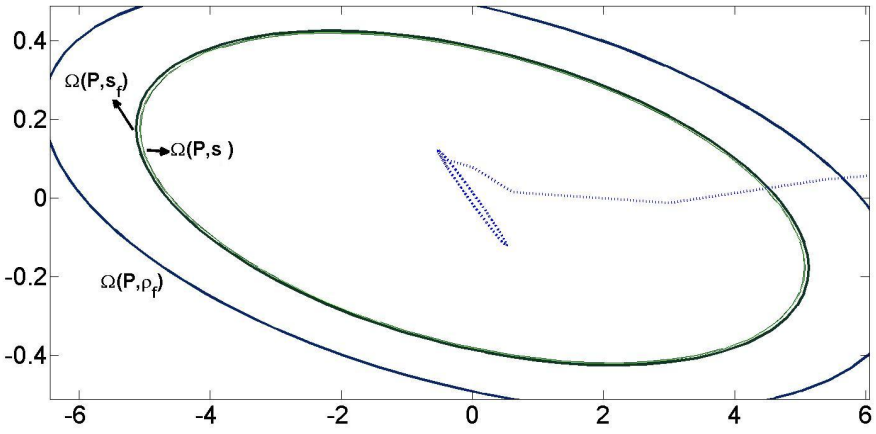

FIGURE 3.2: Invariant Ellipsoid

If the fault happens at $t_f = 1.6s$, i.e., the trajectory has already entered $\Omega(P, \varrho_f)$, then the stability will be guaranteed but the performance is degraded, see Fig. 3.4.

Through the analysis above, one can see that the size of the fault will influence the attraction and performance regions, and the time when the fault happens will also decide whether the tracking system will be stable or not. However, in practice, $\bar{\Gamma}_f$ and t_f are unknown parameters, therefore, designing a fault-tolerant controller is necessary in order to handle the possible faults.

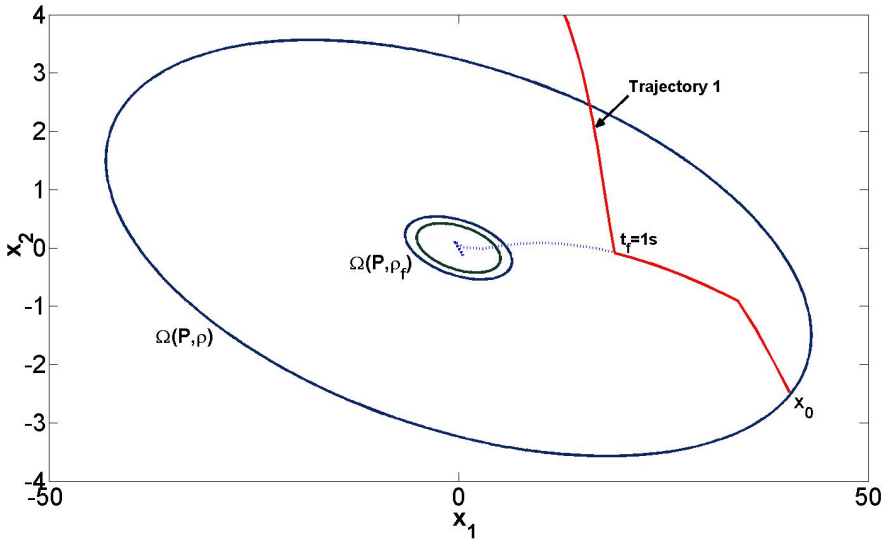

FIGURE 3.3: The Trajectory 1 of State Response with A Fault Occurring at $t_f = 1s$

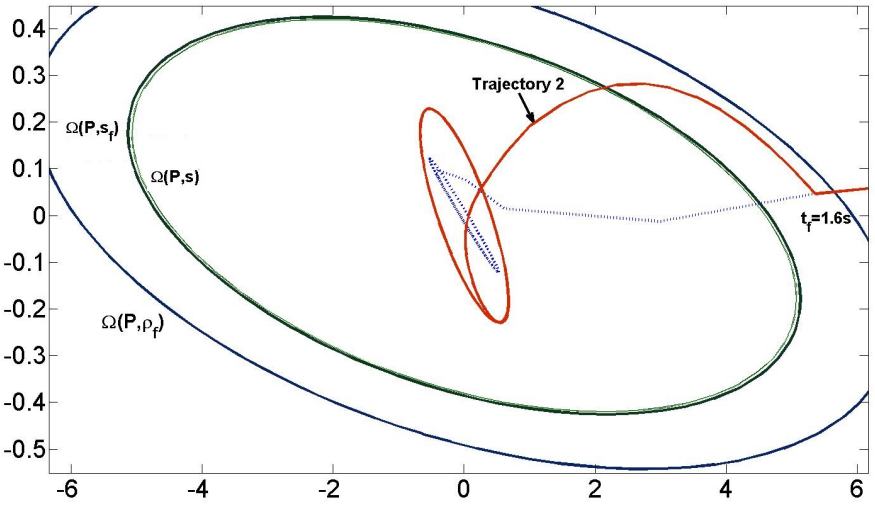

FIGURE 3.4: The trajectory 2 of State Response with A Fault Occurring at $t_f = 1.6s$

3.3 Fault-tolerant Control Design for Systems with Input Constraints

Fault-tolerant control (FTC) is the most popular method applied to systems in the case of unexpected faults. Passive and active FTC approaches may be used.

3.3.1 Passive fault-tolerant control method

The main idea of passive FTC approaches is to design a fixed controller that is robust against faults and uncertainties. Hence, when faults occur, the controller is able to maintain the stability of the system with an acceptable degraded performance, and it does not require the fault diagnosis and detection (FDD) subsystem and the control reconfiguration mechanism. At present, numerous research results are available for the passive fault-tolerant control design with different approaches, such as LMI scheme, $H\infty$ theory, and sliding mode control. Also these results are applied with considering actuator saturation. In most situations, LMI-based method and model predictive control (MPC) are mostly used to deal with actuator saturation.

3.3.1.1 Passive fault-tolerant controller design

Assume that Λ is a set of k possible faults, i.e., $\Lambda = \{\bar{\Gamma}_{f1}, ..., \bar{\Gamma}_{fk}\}$, where $\bar{\Gamma}_{fj} = diag(\gamma_{j1}, \gamma_{j2}, ..., \gamma_{jm})$ with $\gamma_{ji} \in [0, 1]$ $(i = 1, 2, ..., m)$,$(j = 1, 2, ..., k)$.

Let us consider the tracking system with possible faults as stated in Problem 2

$$\dot{x} = Ax + B\bar{\Gamma}_{fj}\sigma(u(t)) + E\omega(x, t)$$

where $x \in R^n$, $u \in R^m$ are the state and the control input vectors, $\omega \in R^n$ represents the uncertainty and the disturbance, A, B, E are matrices with appropriate dimensions. $\sigma(u)$ is the saturation function, $\sigma(u) = [\sigma_1(u_1), ..., \sigma_m(u_m)]^T$, where $\sigma_i(u_i) = sign(u_i)\min\{|u_i|, 1\}$. $\bar{\Gamma}_{fj}$ is one fault in the set Λ.

Define x_d as the reference for tracking system with possible faults that satisfy Assumption 3.1. The error equation can be obtained

$$\dot{e} = Ae + B\bar{\Gamma}_{fj}\sigma(u(t)) - B\bar{\Gamma}_{fj}u_{df}(x_d) + E\omega(x,t) \tag{3.15}$$

The controller takes the form as Eq. 2.7 in Chapter 2

$$\begin{cases} u = u_e + u_d = -Kx + K_r x_d = -Ke + (K_r - K)x_d \\ K_r = ((BK - A)^{-1}B)^{+} \end{cases}$$

Definition 3.1. *[71] Ω is a set that includes the stable point. If any initial state that starts from Ω will converge to the stable point, no matter what kind of faults happen during this period, then Ω is called as a fault-tolerant attraction region.*

Definition 3.2. *[71] Based on Definition 3.1, if all states are inside Ω , then Ω is called as an invariant set of faulty system, noted as Ω_0.*

Based on the above definitions, the following theorem can be presented.

Theorem 3.1. *For the possible faults set Λ, if there exist a symmetric and positive definite matrix P, a matrix K and a positive scalar μ satisfying*

$$A'P + PA - PB\bar{\Gamma}_{fj}K + \frac{1}{\mu}PEE'P + \mu\omega_0^2 P < 0 \tag{3.16}$$

and if a positive scalar m can be found as the minimal value that satisfies

$$A'P + PA - PB\bar{\Gamma}_{fj}K + \frac{1}{\mu}PEE'P + \frac{\mu\omega_0^2}{m}P < 0 \tag{3.17}$$

if $\varrho > m$ with

$$\varrho = \min_i(4(1 - |u_{dfi}|)^2\lambda_{min}(P_K)) \tag{3.18}$$

where $P_K = (K'K)^{-1}P$.

then $\Omega(P,\varrho) = \{e : e'Pe < \varrho\}$ is an invariant set of the faulty system when the controller $u = -Ke + (K_r - K)x_d$ is used.

Proof: Define $V(e) = e'Pe$, consider the derivative of $V(e)$ along the trajectory of the closed-loop system, we obtain

$$\begin{aligned}\dot{V} &= e^TPAe + e^TA'Pe + 2e^TPB\bar{\Gamma}_{fj}\sigma(u(t)) - 2e^TPB\bar{\Gamma}_{fj}u_{df}(x_d) + 2e^TPBE\omega(x,t)) \\ &= e^TPAe + e^TA'Pe + 2e^TPB\bar{\Gamma}_{fj}\bar{\sigma}(-Ke) + 2e^TPBE\omega(x,t))\end{aligned}$$

where $\bar{\sigma}_i = sign(-u_{ei})\min\{|u_{ei}|, 1 - |u_{dfi}|\}$.

Combining Eq. 3.17 and the condition $\varrho > m$, we get

$$A'P + PA - PB\bar{\Gamma}_{fj}K + \frac{1}{\mu}PEE'P + \frac{\mu\omega_0^2}{\varrho}P < 0 \tag{3.19}$$

1. Case 1: The controller is not saturated, i.e., $\bar{\sigma}(-Ke) = -Ke$, then with Eq. 3.19

$$\begin{aligned}\dot{V} &= e^TPAe + e^TA'Pe - 2e^TPB\bar{\Gamma}_{fj}Ke + 2e^TPBE\omega(x,t)) \\ &\leq -e^TPB\bar{\Gamma}_{fj}Ke - \frac{1}{\mu}e'PEE'Pe - \frac{\mu}{\varrho}\omega_0^2e'Pe + 2e'PE\omega(x,t) \end{aligned} \tag{3.20}$$

   Since

$$2e'PE\omega(x,t) \leq \frac{1}{\mu}e'PEE'Pe + \mu\omega_0^2$$

   then one has

$$\begin{aligned}\dot{V} &\leq -e^TPB\bar{\Gamma}_{fj}Ke - \frac{\mu}{\varrho}\omega_0^2e'Pe + \mu\omega_0^2 \\ &\leq \mu\omega_0^2(1 - \frac{V}{\varrho})\end{aligned}$$

   then one concludes that $\Omega(P, \varrho)$ is an invariant set for Eq. 3.15.

2. Case 2: The controller is saturated. Based on Eq. 3.19, $\dot{V}$ becomes

$$\begin{aligned}\dot{V} &= e^TPAe + e^TA'Pe - 2e^TPB\bar{\Gamma}_{fj}(1 - |u_{dfi}|) + 2e^TPBE\omega(x,t)) \\ &\leq e^TPB\bar{\Gamma}_{fj}(Ke - 2(1 - |u_{dfi}|)) - \frac{\mu}{\varrho}\omega_0^2e'Pe + \mu\omega_0^2 \\ &\leq e^TPB\bar{\Gamma}_{fj}(Ke - 2(1 - |u_{dfi}|)) + \mu\omega_0^2(1 - \frac{V}{\varrho})\end{aligned}$$

Thus, based on Theorem 3.1, $\Omega(P, \varrho)$ is the invariant set for system 3.15. That ends the proof. □

The performance region can be estimated by a different way with Eq. 3.12 in section 3.2.

Since P, K and μ can be obtained by Eq. 3.16, there must exist a scalar s that satisfies

$$A'P + PA - 2PB\bar{\Gamma}_{fj}K + \frac{1}{\mu}PEE'P + \frac{\mu\omega_0^2}{s}P < 0 \tag{3.21}$$

Submitting Eq. 3.21 into Eq. 3.20, one gets

$$\begin{aligned} \dot{V} &\leq -\frac{\mu\omega_0^2}{s}e'Pe + \mu\omega_0^2 \\ &\leq \mu\omega_0^2(1 - \frac{V}{s}) \end{aligned}$$

then $\Omega(P, s)$ is the estimation of the performance region for system 3.15.

Remark 3.3. *In order to solve Eq. 3.16 in Theorem 3.1, let* $Q = P^{-1}$, $Y = -KQ$, *Eq. 3.16 can be transformed as follows*

$$A^TQ + QA - \frac{1}{2}B\bar{\Gamma}_{fj}Y - \frac{1}{2}Y^T\bar{\Gamma}_{fj}^TB^T + \frac{1}{\mu}EE^T + \mu\omega_0^2Q \leq 0$$

then based on Schur-Complement Lemma, it can be rewritten as

$$\begin{bmatrix} A^TQ + QA - \frac{1}{2}B\bar{\Gamma}_{fj}Y - \frac{1}{2}Y^T\bar{\Gamma}_{fj}^TB^T + \frac{1}{\mu}EE^T & \omega_0^2I \\ Q & -\frac{1}{\mu}I \end{bmatrix} \leq 0$$

then it can be solved by YALMIP tool or matlab LMI toolbox.

Also for Eq. 3.17, we have

$$A^TQ + QA - \frac{1}{2}B\bar{\Gamma}_{fj}Y - \frac{1}{2}Y^T\bar{\Gamma}_{fj}^TB^T + \frac{1}{\mu}EE^T + \frac{\mu\omega_0^2}{m}Q \leq 0$$

then the minimal m *can be obtained.*

Remark 3.4. *The number of LMIs that need to be solved is* k, *it depends on the set of the possible faults* $\Phi = \{\bar{\Gamma}_{fj}\}$ $(j = 1, 2, ..., k)$.

Remark 3.5. *Different from the classical method that uses the convex combination in [102][103], the proposed method also gets the estimation of the attraction region and it is not limited only in the linear part of the controller.*

3.3.1.2 Illustrative example for PFTC

In this subsection, one example is presented to illustrate the above proposed theory.

The system Σ_0 (see Eq. 2.1) is defined by

$$A = \begin{bmatrix} 0.1 & -0.1 \\ 0.1 & 0.3 \end{bmatrix}, B = \begin{bmatrix} 25 & 0 \\ 0 & 2 \end{bmatrix},$$

$$C = \begin{bmatrix} 1 & 0 \\ 0 & 1 \end{bmatrix}, E = \begin{bmatrix} 1 \\ 1 \end{bmatrix}, \omega(x,t) = sin(t)$$

Then for Assumption 2.2, $\omega_0 = 1$. For simplicity, the tracking point is set as

$$r = \begin{bmatrix} 0 \\ 0 \end{bmatrix}$$

The possible faults set Φ are considered $\Phi = \{\bar{\Gamma}_{fj}\}, j = 1, 2, 3$, where

$$\bar{\Gamma}_{f1} = \begin{bmatrix} 1 & 0 \\ 0 & 1 \end{bmatrix}, \bar{\Gamma}_{f2} = \begin{bmatrix} 0.8 & 0 \\ 0 & 0.8 \end{bmatrix}, \bar{\Gamma}_{f3} = \begin{bmatrix} 0.2 & 0 \\ 0 & 0.5 \end{bmatrix}$$

Based on Theorem 3.1, by solving Eq. 3.16, we can get

$$P = \begin{bmatrix} 0.0501 & -0.0024 \\ -0.0024 & 0.0305 \end{bmatrix}, K = \begin{bmatrix} 1.028 & -0.0519 \\ -0.3563 & 5.2709 \end{bmatrix}, Kr = \begin{bmatrix} 1.0240 & -0.0479 \\ -0.4063 & 5.1209 \end{bmatrix}$$

$$\mu = 0.0123$$

Then based on the given above matrices, $\varrho = 0.044$ and $m = 0.02$ can be obtained based on Eq. 3.18. Since $\varrho > m$, Eq. 3.19 is satisfied.

Also $s = 0.033$ can be obtained based on Eq. 3.18.

The trajectory is shown in Fig. 3.5 with taking $x_0 = [-0.53; 0.95]^T$ near the boundary of $\Omega(P, \varrho)$ as the initial state. Here no fault is injected. It is obvious that the trajectory starting from x_0 in $\Omega(P, \varrho)$ enters $\Omega(P, s)$ and remains inside it.

If the fault $\bar{\Gamma}_{f3}$ happens at $t_f = 0.2s$, then the trajectory is shown in Fig. 3.6.

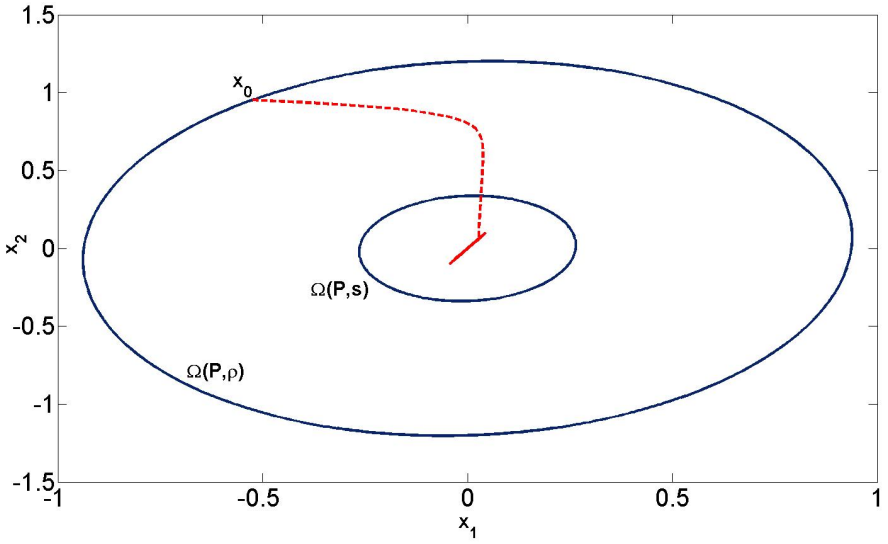

FIGURE 3.5: Invariant Ellipsoids and State Response without Fault

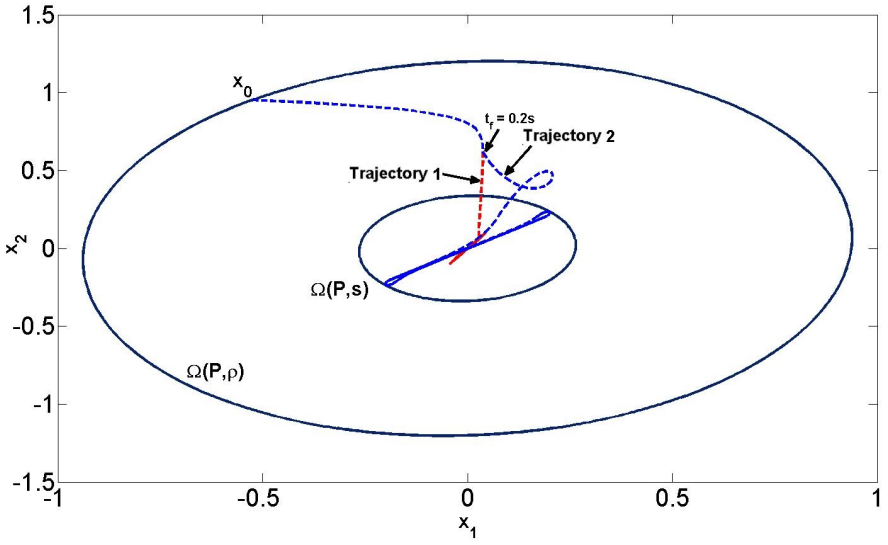

FIGURE 3.6: Trajectory 1: without Fault; Trajectory 2: with Fault $\bar{\Gamma}_{f3}$

Another trajectory with initial state $x_{01} = [0.53; -0.95]^T$ is shown in in Fig. 3.7. The fault $\bar{\Gamma}_{f2}$ happens at $t_{f1} = 0.1s$ and $\bar{\Gamma}_{f3}$ happens at $t_{f2} = 0.2s$. The trajectory without fault is also given as Trajectory 1.

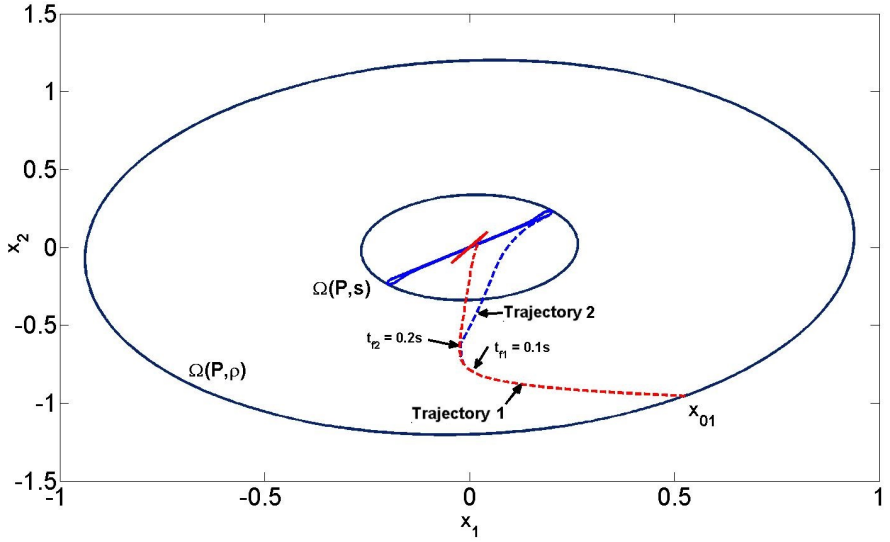

FIGURE 3.7: Trajectory 1: without Fault; Trajectory 2: with Fault

Based on the simulation results, we can see that with respect to disturbances and faults, the LMI based passive FTC approach proposed here can ensure the system's stability and tracking performance. However, PFTC actually sacrifices the size of the region of stability to achieve the fault tolerant capability. In comparison with the controller in section 3.2, the estimated region $\Omega(P, \varrho)$ is reduced, but the tracking mission can be guaranteed even if faults happen.

3.3.2 Active fault-tolerant control method

Passive FTC method refers to the design of controllers that is robust to potential faults without modification. It is relatively simple but it is impractical. As mentioned above in section 3.3.1.2, PFTC method will reduce the size of the stability region and also enlarge the estimated performance region. In contrast, AFTC method automatically modifies the control law in response to the faults. It can avoid the performance degradation comparing to PFTC method.

Eq. 3.2 can be rewritten as

$$\begin{aligned} \dot{x} &= Ax + B\sigma(u(t)) + B(\bar{\Gamma}_f - I)\sigma(u(t)) + E\omega(x,t) \\ &= Ax + B\sigma(u(t)) + Bf + E\omega(x,t) \end{aligned} \tag{3.22}$$

where f represents the vitual fault $(\bar{\Gamma}_f - I)\sigma(u(t))$.

Active FTC requires a fault detection and diagnosis (FDD) mechanism to detect and identify faults in real time, then a mechanism is used to reconfigure the controllers according to the online faults information obtained from FDD. Observer based FDD methods are often used to obtain faults information. In the following section, we will study this subject, and deal with the design of the observer for active fault-tolerant controllers.

3.3.2.1 Observer design

Based on Eq. 3.4 and Eq. 3.22 with $e = x - x_d$, the tracking error equation can be written as

$$\dot{e} = Ae + B\sigma(u(t)) + Bf - Bu_d(x_d) + E\omega(x,t) \tag{3.23}$$

In order estimate the virtual fault f for the controller design after, the following observer is constructed for Eq. 3.23 as in [58]:

$$\dot{\hat{e}} = A\hat{e} + B\sigma(u(t)) + B\hat{f} - Bu_d(x_d) - L(\hat{e} - e) \tag{3.24}$$

where $\hat{f}$ is the estimation of the virtual fault f in Eq. 3.23 with

$$\dot{\hat{f}} = -\Psi e_x \tag{3.25}$$

In Eq. 3.25, $e_x = \hat{e} - e$ and Ψ is a parameter that needs to be designed.

Let us define $e_f = \hat{f} - f$, then the following equation can be obtained as

$$\dot{e}_x = (A - L)e_x + Be_f - E\omega \tag{3.26}$$

$$\dot{e}_f = \dot{\hat{f}} - \dot{f} = -\Psi e_x - \dot{f} \tag{3.27}$$

Here, since the input is constrained, the derivative $\dot{f}$ of the fault f is bounded, thus the following error equation is constructed by combining Eq. 3.26 and Eq. 3.27,

$$\dot{\bar{e}} = (\bar{A} - \bar{L}\bar{C})\bar{e} - \bar{D}\vartheta \tag{3.28}$$

where

$$\bar{e} = \begin{bmatrix} e_x \\ e_f \end{bmatrix}, \vartheta = \begin{bmatrix} \omega \\ \dot{f} \end{bmatrix}, \bar{A} = \begin{bmatrix} A & B \\ 0 & 0 \end{bmatrix}$$

$$\bar{L} = \begin{bmatrix} L \\ \Psi \end{bmatrix}, \bar{C} = \begin{bmatrix} I & 0_{2\times 2} \end{bmatrix} \bar{D} = \begin{bmatrix} E & 0 \\ 0 & I_{2\times 2} \end{bmatrix}$$

Theorem 3.2. *[58] For a given $\epsilon, \tau > 0$, if there exists a positive symmetric matrix $\bar{P}$ that satisfies*

$$\begin{bmatrix} \varphi_1 & -\bar{P}\bar{D} & I \\ * & -\epsilon I & 0 \\ * & * & -\epsilon I \end{bmatrix} < 0 \tag{3.29}$$

$$\bar{P}\bar{A} + \bar{A}^T\bar{P}^T - \bar{P}\bar{L}\bar{C} - \bar{C}^T\bar{L}^T\bar{P}^T + 2\tau\bar{P} < 0$$

the designed observer can make sure that e_x, e_f will converge exponentially at the rate τ, with $\|\bar{e}\|_2 < \epsilon\|\vartheta\|_2$, where $\varphi_1 = \bar{P}\bar{A} + \bar{A}^T\bar{P}^T - \bar{P}\bar{L}\bar{C} - \bar{C}^T\bar{L}^T\bar{P}^T$.

Proof: Considering the derivative of $V(\bar{e})$ for system 3.28 with $V(\bar{e}) = \bar{e}'\bar{P}\bar{e}$, it is obtained that

$$\dot{V} = 2\bar{e}'\bar{P}(\bar{A} - \bar{L}\bar{C})\bar{e} - 2\bar{e}'\bar{P}\bar{D}\vartheta \tag{3.30}$$

Define

$$J = \int_0^T \frac{1}{\epsilon}\bar{e}^T\bar{e} - \epsilon\vartheta^T\vartheta dt \tag{3.31}$$

Under zero initial condition, we have

$$J \leq \int_0^T \zeta^T \Pi \zeta dt \tag{3.32}$$

where

$$\zeta = \begin{bmatrix} \bar{e} \\ \vartheta \end{bmatrix}, \Pi = \begin{bmatrix} \varphi_1 + \frac{1}{\epsilon}I & -\bar{P}\bar{D} \\ * & -\epsilon I \end{bmatrix}$$

With condition 3.29 in Theorem 3.2, based on Schur complement lemma, one gets $\Pi < 0$. Therefore, based on LaSalle's invariant principle, the error of the state estimation and the error of the fault estimation are stable and they satisfy $\|\bar{e}\|_2 < \epsilon\|\vartheta\|_2$. This ends the proof. □

3.3.2.2 Active fault-tolerant controller design

When considering the faults, we have Eq. 3.23

$$\dot{e} = Ae + B\sigma(u(t)) + Bf - Bu_d(x_d) + E\omega(x,t)$$

where f represents the virtual fault.

When no element of the input $u(t)$ saturates, it is easy to have the feedback fault tolerant controller based on observer as

$$u(t) = -Ke(t) + (K_r - K)x_d - \hat{f} \tag{3.33}$$

Therefore, Eq. 3.23 can be rewritten as

$$\begin{aligned} \dot{e} &= Ae + B\sigma(-Ke(t) + (K_r - K)x_d - \hat{f}) + Bf - Bu_d(x_d) + \omega(x,t) \\ &= (A - BK)e - Be_f + \omega(x,t) \\ &= (A - BK)e + [-B \ \ I]\eta(t) \end{aligned} \tag{3.34}$$

where $\eta(t) = [e_f \ \ \omega]^T$.

Lemma 3.1. *For a given $\varepsilon > 0$, if there exists a positive symmetric matrix P that satisfies*

$$\begin{bmatrix} \varphi_2 & -BP & P \\ * & -\varepsilon I & 0 \\ * & * & -\varepsilon I \end{bmatrix} < 0 \tag{3.35}$$

the designed controller can make sure that e will be robustly stable with $\|e\|_2 < \varepsilon\|\eta(t)\|_2$, where $\varphi_2 = (A - BK)P + P(A - BK)^T$.

Proof: the proof of Lemma 3.1 is similar to Theorem 3.2, the detail is omitted here.

Considering the input constraints, the feedback controller should also satisfies

$$|u(t)| = | - Ke(t) + (K_r - K)x_d - \hat{f}| \leq 1 \tag{3.36}$$

By defining

$$z = \begin{bmatrix} e \\ \hat{f} \\ x_d \end{bmatrix}, \bar{K} = \begin{bmatrix} -K & -I_{2\times 2} & (K_r - K) \end{bmatrix},$$

Based on Eq. 3.36, one has

$$|u(t)| = |\bar{K}z| = |\bar{K}P^{-1/2}P^{1/2}z| \leq 1 \tag{3.37}$$

Define $\Omega(P, 1)$ as the invariant set that

$$\Omega(P, z) = \{z \mid z'Pz \leq 1\} \tag{3.38}$$

then

$$|\bar{K}P^{-1/2}P^{1/2}z| \leq \|\bar{K}P^{-1/2}\|\|P^{1/2}z\| \leq \|\bar{K}P^{-1/2}\| \tag{3.39}$$

Consider Eq. 3.37 and Eq. 3.39, the following condition should be satisfied

$$\|\bar{K}P^{-1/2}\| \leq 1 \iff \begin{bmatrix} P & \bar{K}^T \\ \bar{K} & 1 \end{bmatrix} \geq 0 \tag{3.40}$$

Eq. 3.40 is a sufficient and essential condition to ensure that the designed $u(t)$ is feasible in $\Omega(P, 1)$.

Remark 3.6. *Although without violating the input limits, the designed AFTC can compensate the fault and reduce the performance degradation comparing with PFTC, the analysis of the stability and its fault tolerant capability are quite difficult. In Eq. 3.38, $\hat{f}$ is a unknown constrained matrix that is changed with the happened faults, thus there is no fixed stability region for the analyzed system. This is also the reason why few results consider this method when researching FTC method for systems with input constraints.*

Remark 3.7. *Considering the design process as a whole process, the observer design and the fault tolerant controller design are separated, therefore it is easy to find the parameters. However, because Eq. 3.34 is obtained with the assumption that $u(t)$ does not saturate, the input constraint is a hard constraint which must not be exceeded by the control law. Additionally, active FTC needs significantly more computations to be implemented and time-delay between the fault detection and the controller reconfiguration also implies that this mechanism can not be used on an unstable system, therefore, more difficulties arise in the design of observer-based AFTC for saturated systems.*

3.3.2.3 Illustrative example for AFTC

In this subsection, the following example is presented to illustrate the above proposed theories.

The system Σ_0 (see Eq. 2.1) is defined by

$$A = \begin{bmatrix} 0.1 & -0.1 \\ 0.1 & 0.3 \end{bmatrix}, B = \begin{bmatrix} 25 & 0 \\ 0 & 2 \end{bmatrix},$$

$$C = \begin{bmatrix} 1 & 0 \\ 0 & 1 \end{bmatrix}, E = \begin{bmatrix} 1 \\ 1 \end{bmatrix},$$

For simplicity, $\omega(x, t)$ is set as 0.

The tracking point x_d is set as

$$r = \begin{bmatrix} 15 \\ 0 \end{bmatrix}$$

Based on Theorem 3.2, the parameters $\bar{P}$, L, Ψ, ϵ and τ for observer are calculated as

$$\bar{P} = \begin{bmatrix} 10.3628 & 0.4235 & 5.5671 & -1.1356 \\ 0.4235 & 0.5187 & 0.1825 & 0.2334 \\ 5.5671 & 0.1825 & 3.8104 & -0.8328 \\ -1.1356 & 0.2334 & -0.8328 & 3.8005 \end{bmatrix}, L = \begin{bmatrix} 15.1400 & -4.3733 \\ -1.2933 & 30.2600 \end{bmatrix},$$

$$\Psi = \begin{bmatrix} 1.2467 & -0.0519 \\ -0.3563 & 1.8518 \end{bmatrix}, \epsilon = 17.3, \tau = 0.05$$

Based on Lemma 3.1, the parameters P, K, K_r, ε for controller are calculated as

$$P = \begin{bmatrix} 0.0125 & 0.0010 \\ 0.0010 & 0.0452 \end{bmatrix}, K = \begin{bmatrix} 1.2467 & -0.0519 \\ -0.3563 & 5.8518 \end{bmatrix},$$

$$K_r = \begin{bmatrix} 1.2427 & -0.0479 \\ -0.4063 & 5.7018 \end{bmatrix}, \varepsilon = 1$$

The initial state is $x_0 = [10; 1]^T$, the initial observer state $e = (x - x_d)$ is chosen as $\hat{e}_0 = [-5; 1]^T$. The estimation results of the designed observer are shown in Fig. 3.8 - Fig. 3.11, here no fault is injected.

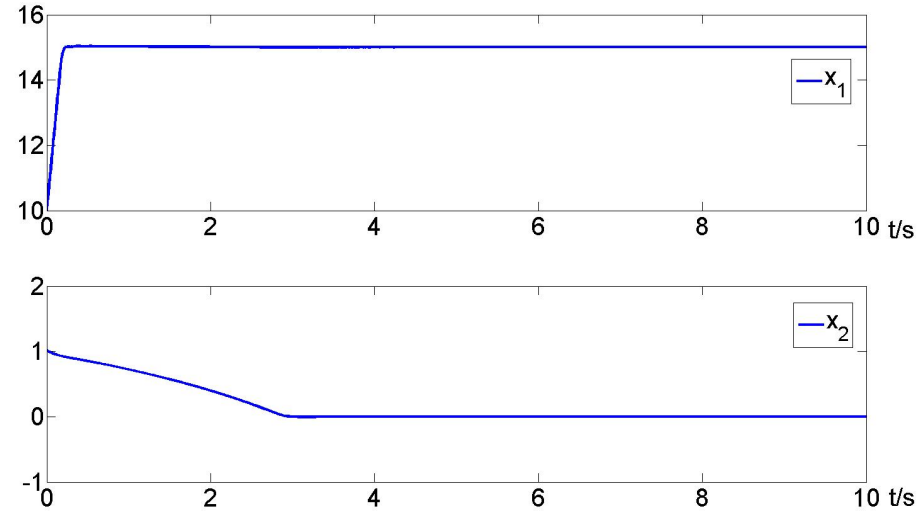

FIGURE 3.8: Response of State x: without Fault

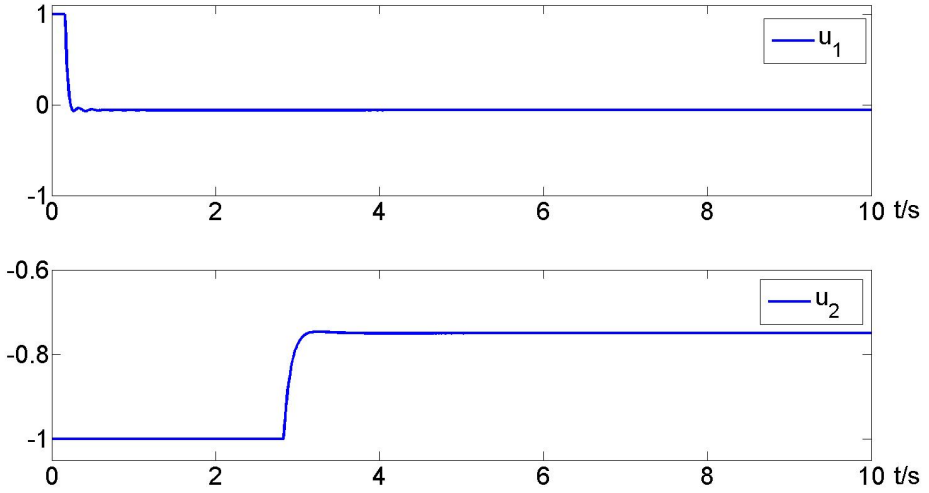

FIGURE 3.9: Control Signals: without Faults

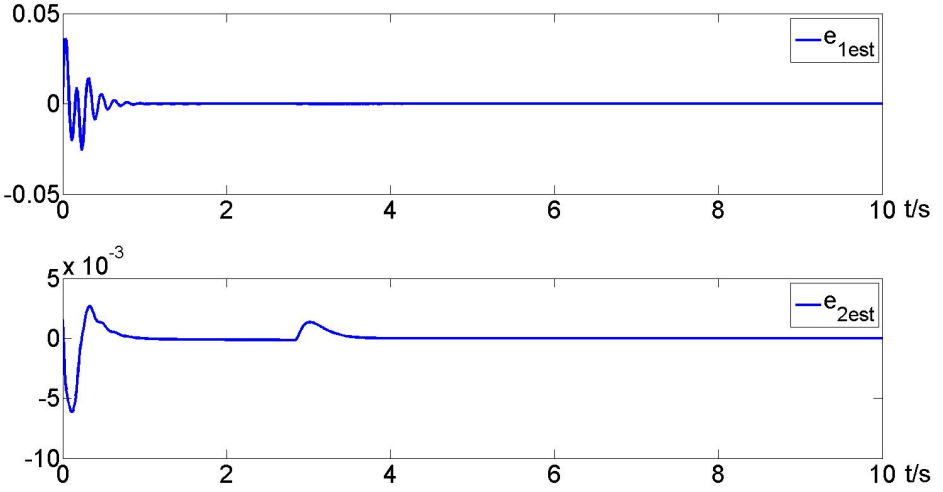

FIGURE 3.10: Estimation $\hat{e}$ of $e = x - x_d$: without Faults

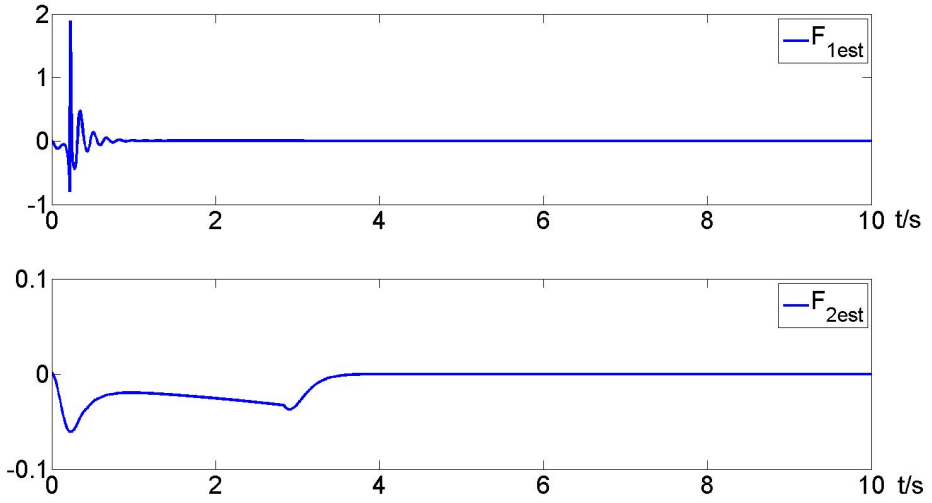

FIGURE 3.11: Estimation $F_{est} = \hat{f}/\sigma(u(t))$ of $(\bar{\Gamma}_f - I)$: without Faults

Through the above figures, we can see that the designed observer and controller can achieve the control requirements. The state reaches the tracking point in Fig. 3.8, estimated fault is 0 when no fault is injected, see Fig. 3.11.

The possible fault sets Φ are considered $\Phi = \{\bar{\Gamma}_{fj}\}, j = 1, 2$, where

$$\bar{\Gamma}_{f1} = \begin{bmatrix} 1 & 0 \\ 0 & 0.8 \end{bmatrix}, \bar{\Gamma}_{f2} = \begin{bmatrix} 1 & 0 \\ 0 & 0.5 \end{bmatrix}$$

The simulation results with faults are shown in Fig. 3.12 - Fig. 3.19, here the two faults are injected separately at $t = 5s$.

Fig. 3.12 - Fig. 3.15 are simulation results with $\bar{\Gamma}_{f1}$ happening.

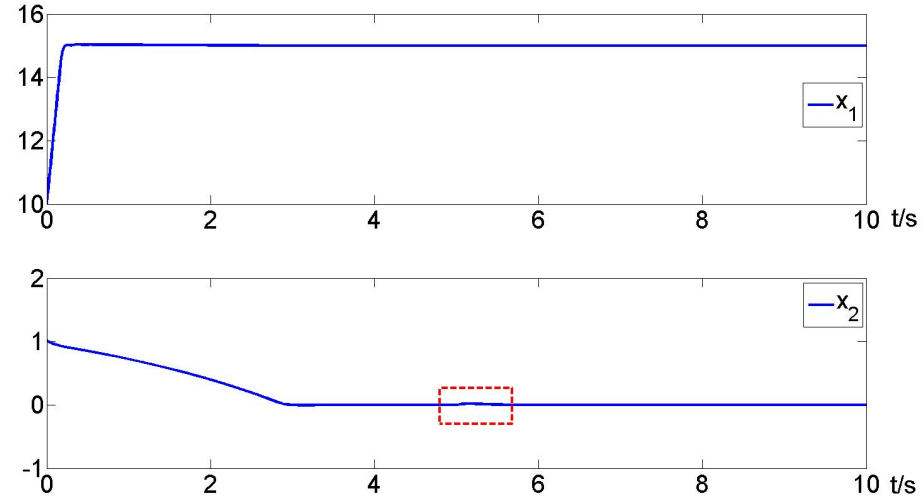

FIGURE 3.12: Response of State x: with Fault $\bar{\Gamma}_{f1}$

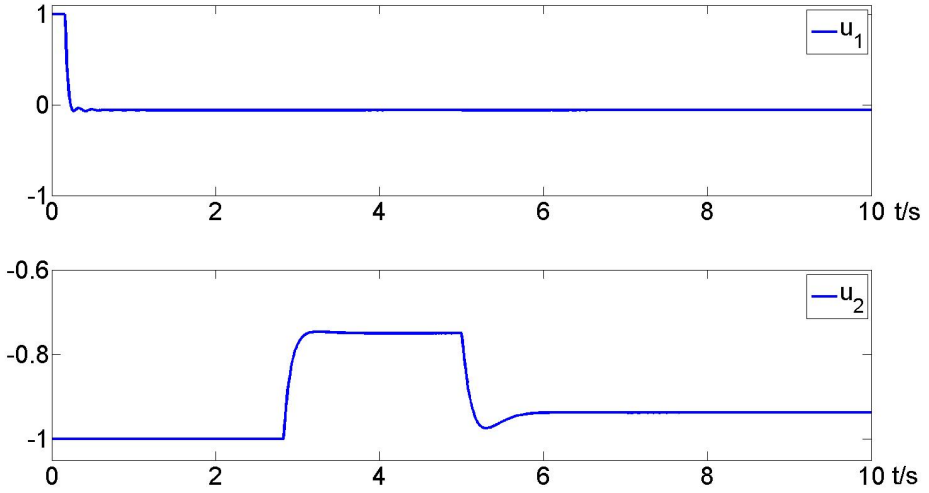

FIGURE 3.13: Control Signals: with Fault $\bar{\Gamma}_{f1}$

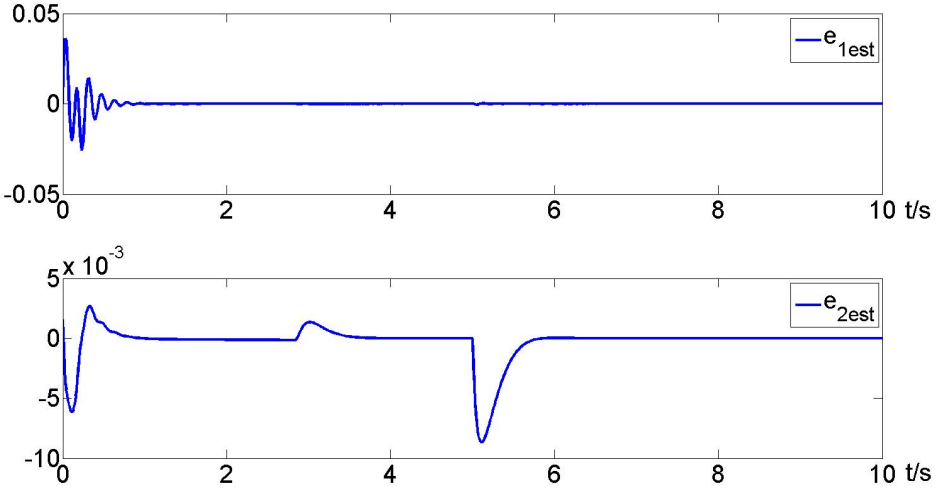

FIGURE 3.14: Estimation $\hat{e}$ of $e = x - x_d$: with Fault $\bar{\Gamma}_{f1}$

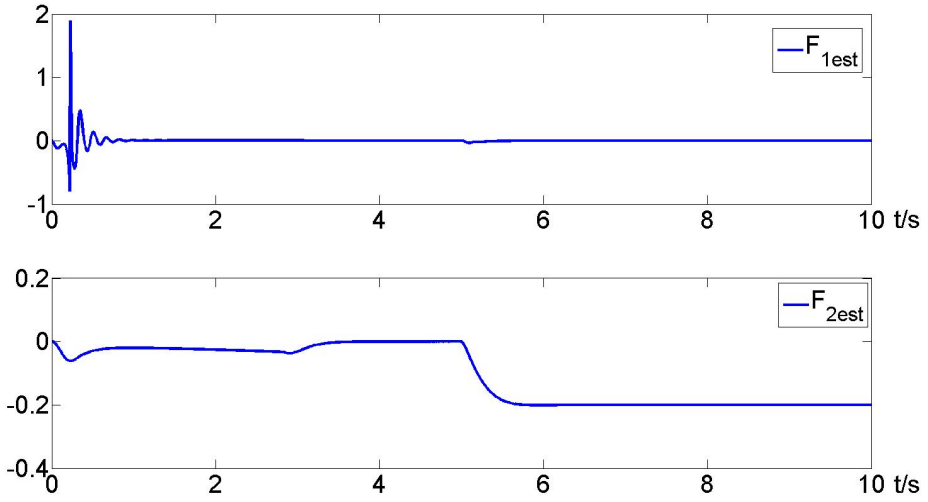

FIGURE 3.15: Estimation $F_{est} = \hat{f}/\sigma(u(t))$ of $(\bar{\Gamma}_f - I)$: with Fault $\bar{\Gamma}_{f1}$

we can see that the happened fault $\bar{\Gamma}_{f1}$ is not sufficiently high to make the control signal saturate in Fig. 3.13, thus the designed controller that uses the estimated fault from the observer can guarantee the state x track x_d, see Fig. 3.12. The influence of the fault can be seen in the red rectangle in Fig. 3.12, the change of state is very small when fault happens. The designed controller can compensate the fault influence.

The estimation result of fault can be seen in Fig. 3.15, by defining $F_{est} = \hat{f}/\sigma(u(t))$. The result shows $F_{est1} = 0, F_{est2} = -0.2$, thus the happened fault that $\hat{\bar{\Gamma}}_{f1} = diag\{1, 0.8\}$ can be estimated.

Fig. 3.16 - Fig. 3.19 are the simulation results when $\bar{\Gamma}_{f2}$ happens. We can see that the fault $\bar{\Gamma}_{f2}$ makes the control signal saturating in Fig. 3.17, that is, the fault is out of the stability region in Eq. 3.38. Therefore, the control objective and the estimation can not be guaranteed by the designed controller and observer, see Fig. 3.16 and Fig. 3.19.

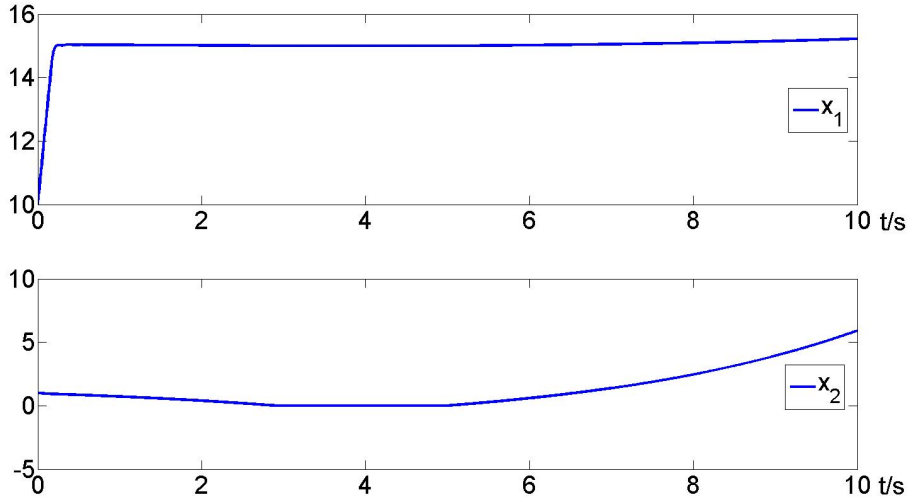

FIGURE 3.16: Response of State x: with Fault $\bar{\Gamma}_{f2}$

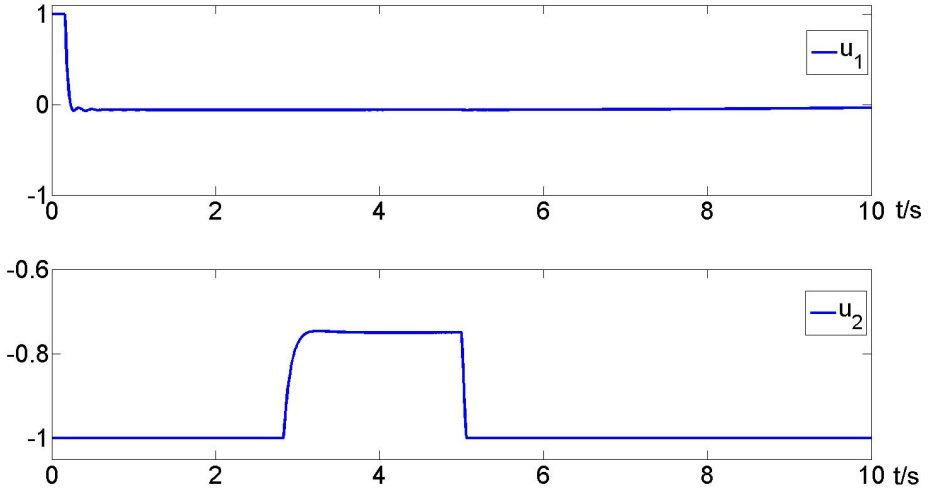

FIGURE 3.17: Control Signals: with Fault $\bar{\Gamma}_{f2}$

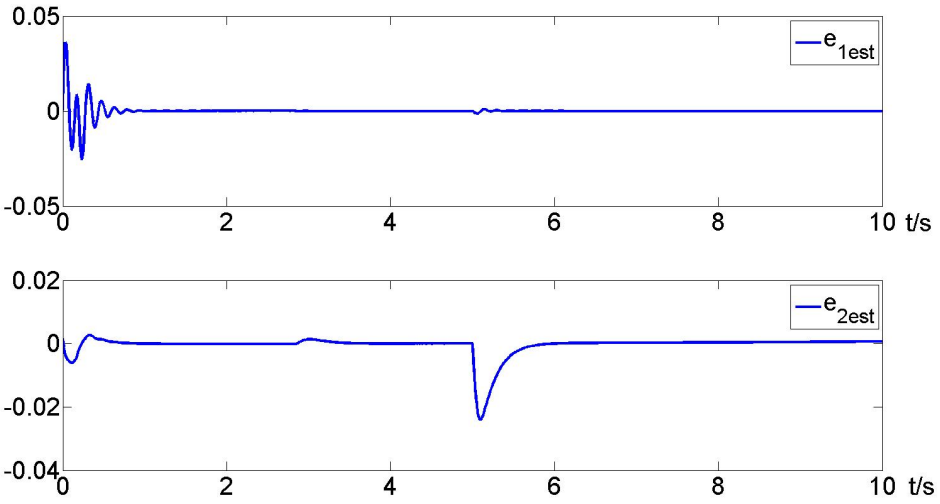

FIGURE 3.18: Estimation $\hat{e}$ of $e = x - x_d$: with Fault $\bar{\Gamma}_{f2}$

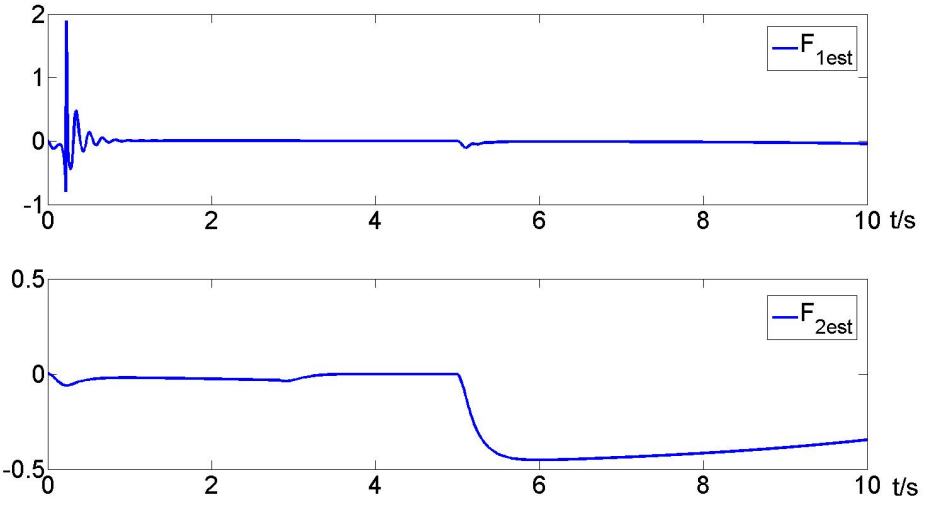

FIGURE 3.19: Estimation $F_{est} = \hat{f}/\sigma(u(t))$ of $(\bar{\Gamma}_f - I)$: with Fault $\bar{\Gamma}_{f2}$

From the simulation results of fault $\bar{\Gamma}_{f2}$, we can see that AFTC for saturating system is more restrictive. Although it can recover the system performance for some small faults, in this example, the faults that it can tolerate are smaller comparing to the PFTC method. Because of the unknown faults and their happening time, it is more difficult to analyze the stability region for a system with AFTC method. As we said in Remark 3.6, the restriction of the faults that AFTC can deal with and the complexity of the analysis are the main reasons that AFTC methods are seldomly used when input saturation is considered.

3.4 Fault-tolerant Control Scheme based on Reference Adjustment Technique

Usually, when designing a FTC, the objective is that the system recovers the unexpected performances when faults are present. These performances are expressed in different terms. Based on PFTC and AFTC methods in section 3.3, the performances that we discuss here are related to system stability, control preciseness (the error between the reference and the output) and fault tolerance capability.

The PFTC method and AFTC method we proposed in section 3.3.1 and 3.3.2 are formally proved by guaranteeing the stability properties. For the PFTC method, it is considered that the system can operate under degraded performance within its stability region; for the AFTC method, within the system's actuator capability, the degraded performance will be recovered, however, the available actuator capability will be significantly reduced due to the fault, and it is harder to analysis the system's stability region by using AFTC method.

The proposed PFTC and AFTC methods have both their restrictions when dealing with the input saturation problem. There are other constructive design algorithms that have been proved to induce suitable stability properties different from the above two methods. These algorithms consist of modifying the reference input so that the constraints will not be violated, which results in many other advantages especially in enlarging the set of feasible evolutions for the system, and on ensuring the feasibility of the designed controller.

Since these algorithms cope with input situation problems by adjusting the reference input, the considered performance of the system is mainly the error between the new reference and the original one. Before adopting the reference adjustment technique (RAT), the relative performance analysis principle should first be introduced.

3.4.1 Performance analysis principle

The performance analysis principle was introduced in [101]. Comparing to the traditional classification for control systems as stable ones and unstable ones, systems can also be classified as nominal, degraded and unaccepted systems based on the considered performance, see Fig. 3.20.

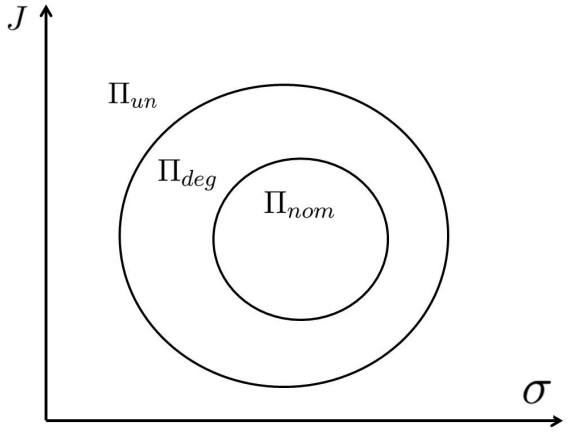

FIGURE 3.20: Classification of Systems based on Performance (Π_{nom}: Region of nominal performance; Π_{deg}: Region of degraded performance; Π_{un}: Region of unacceptable performance)

Here, defining a set Π that includes all possible performances in Fig. 3.20 as

$$\Pi = \Pi_{nom} \bigcup \Pi_{deg} \bigcup \Pi_{un} \tag{3.41}$$

The set Π is defined as

$$\Pi = \{J : \sigma = (u, o) \in R^m \times R^n\} \tag{3.42}$$

where J represents the performance index of the system, u, o are respectively the control vector and objective vector.

Let us define D_c the domain of performance coverage for a controlled and stable system as

$$D_c := \{J \in \Pi : (u, o) \in (U, O)\} \tag{3.43}$$

Let us consider the following two sets for the nominal case and the faulty case:

$$D_c^{nom} := \{J \in \Pi_{nom} : (u, o) \in (U_{nom}, O_{nom})\} \tag{3.44}$$

$$D_c^f := \{J \in \Pi : (u, o) \in (U_f, O_f)\} \tag{3.45}$$

For the nominal system with a perfect designed controller, D_c^{nom} should be completely included in Π_{nom}. For the faulty case, there will be three different domains defined as D_c^{nom} ,D_c^{deg} and D_c^{un}, see Fig. 3.21.

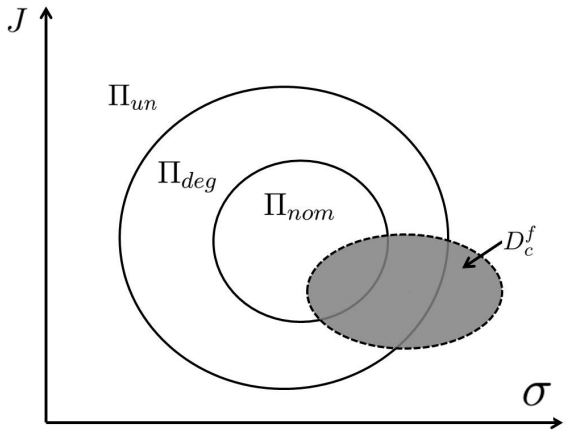

FIGURE 3.21: Domain of Performance Coverage in Faulty Case

where the three defined domains are expressed as

$$\begin{cases} D_c^{nom} = D_c^f \bigcap \Pi_{nom} \\ D_c^{deg} = D_c^f \bigcap \Pi_{deg} \\ D_c^{un} = D_c^f \bigcap \Pi_{un} \end{cases} \tag{3.46}$$

Based on the defined sets,the following cases arise:

Case 1: $D_c^{nom} \neq \varnothing$. The system is completely reconfigurable and the nominal objectives are achieved.

Case 2: $D_c^{nom} = \varnothing$ and $D_c^{deg} \neq \varnothing$. The nominal objectives cannot be achieved, and only degraded objectives are met.

Case 3: $D_c^{nom} = \varnothing$,$D_c^{deg} = \varnothing$ and $D_c^{un} \neq \varnothing$. The fault is severe and the system should be stopped.

3.4.2 Fault-tolerant control scheme design

For the sake of simplicity, in the following study we consider faults that happen after the nominal objective is reached.

As mentioned before in section 2.1.2, for the nominal system with control objective x_d, any trajectory which starts from $\Omega(P, \varrho_d)$ will enter $\Omega(P, s_d)$ and remain inside it with the nominal controller, see Fig. 3.22. Based on the stability region of the nominal system, define the performance sets Π_{nom} and Π_{deg} for the tracking system with faults. In order to define the references, the set of the domain of performance coverage D_c^f is also constructed.

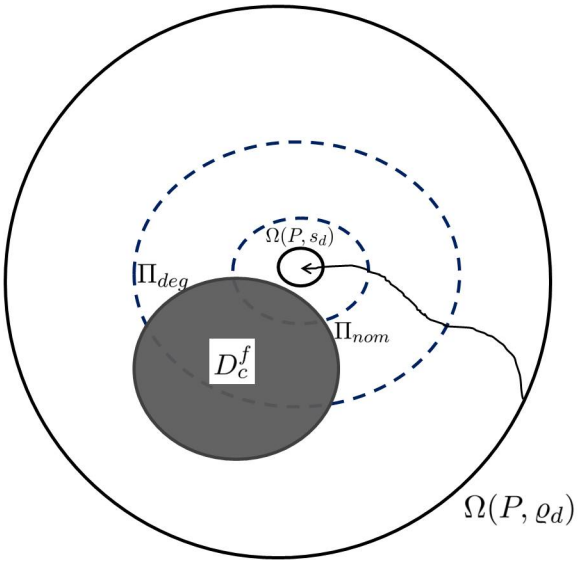

FIGURE 3.22: Description of Stability and Performance

Let us consider the nominal and faulty error equations for the tracking system described by the following representations as Eq. 2.6 in section 2.1 and Eq. 3.23 in section 3.3.2:

$$\Sigma_{e_{nom}} : \dot{e} = Ae + B\sigma(u(t)) - Bu_d(x_d) + E\omega(x,t) \tag{3.47}$$

$$\Sigma_{e_f} : \dot{e} = Ae + B\sigma(u(t)) + Bf - Bu_d(x_d) + E\omega(x,t) \tag{3.48}$$

where $e = x - x_d$, A, B, C, E are the matrices with appropriate dimensions, $\sigma(u)$ is the saturation function with the control input $u \in R^m$, $u_d(x_d)$ is the constant solution for the system with constant reference x_d, $\omega \in R^n$ represents the uncertainty and the disturbance, and f represents the virtual fault as in Eq. 3.22.

The faults will induce a shift of the performance coverage region, without obtaining the detail information of faults, the main idea here is to determine a degraded trajectory reference by the Reference Adjustment Technique (RAT),

it allows the system operate with degraded performance under faulty conditions without saturation. The degraded trajectory reference x_d^f should be included in D_c^{deg} ($x_d^f : x_d^f \in D_c^{deg}$). The original controller will ensure that the trajectory which starts from $\Omega(P, \varrho_f)$ will enter $\Omega(P, s_f)$ even under the worst fault case, see Fig. 3.23.

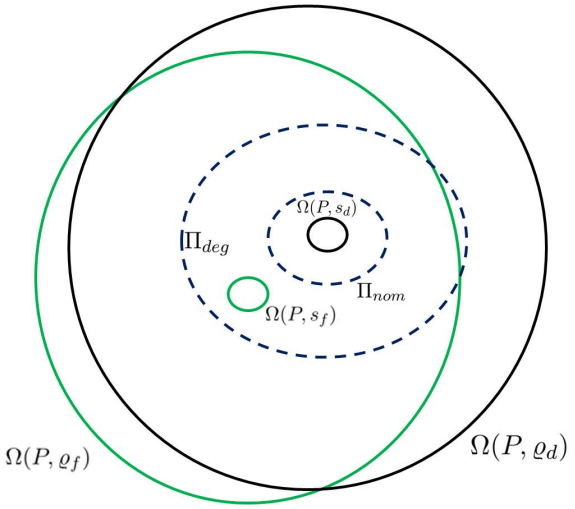

FIGURE 3.23: Description of Stability and Performance for x_d^f

Based on the above settings, the fault tolerant control mechanism based on RAT is proposed as in Fig. 3.24.

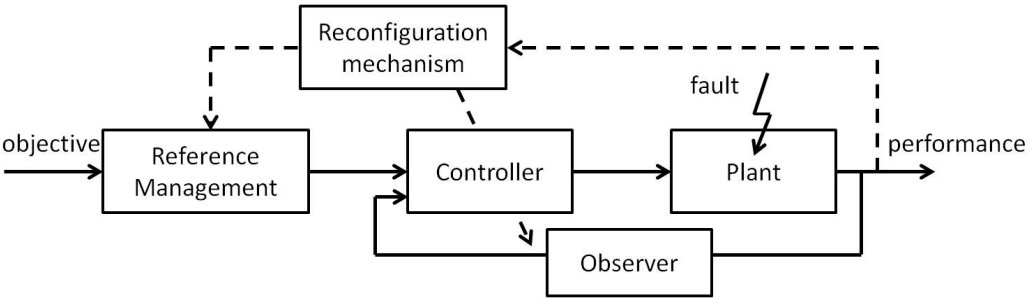

FIGURE 3.24: The Fault-tolerant Control Mechanism with RAT

The details of the proposed fault tolerant control mechanism will be explained as follows:

1. Controller Part:

For the nominal system $\Sigma_{e_{nom}}$ (see Eq. 3.47), the controller $u = -Ke + (K_r - K)x_d$ is designed based on Theorem 2.1 in section 2.1:

$$\begin{cases} K = (1+\rho)B'P \\ K_r = ((BK - A)^{-1}B)^+ \end{cases}$$

where P is a positive semi-definite and symmetric solution for

$$A'P + PA - PBB'P + \frac{1}{\mu}PEE'P + \frac{\mu}{\varrho_d}\omega_0^2 P < 0$$

ρ can be chosen to get the required control objective region s_d,

$$s_d = \frac{\mu\omega_0^2\varrho_d}{(2\rho+1)\lambda_{min}(M)\varrho_d + \mu\omega_0^2}$$

where $M = PBB'PP^{-1}$.

Under the given control law u, all the trajectory which starts from $\Omega(P, \varrho_d)$ will enter $\Omega(P, s_d)$ and stay within it.

2. Reference Adjustment Part:

   Let choose a suitable degraded reference $x_d^f \in D_c^{deg}$.

   Generally speaking, given a suitable degraded reference is not a simple task, not mention for the system with various possible faults. A satisfactory reference should be able to capture most of the control requirements but without violating the physical constraints. The choice of the degraded reference x_d^f is related to the designed controller u, the considered worst fault case and the performance set Π_{deg}.

   Similar to Eq. 3.8 in section 3.2, for the degraded reference x_d^f and the given controller $u(\rho, P)$, the worst fault case $\bar{\Gamma}_{f_w}$ can be obtained by

$$A'P + PA - PB\bar{\Gamma}_{f_w}B'P + \frac{1}{\mu}PEE'P + \frac{\mu}{\varrho_f}\omega_0^2 P \leq 0 \tag{3.49}$$

   where $\varrho_f = \min_i \frac{4(1-|u_{df_i}|)^2}{B_i'PB_i}$, u_{df} is the constant solution for $(Ax_d^f + B\bar{\Gamma}_{f_w}u_{df})$.

The performance region for system with the worst fault $\bar{\Gamma}_{f_w}$ can be also obtained as Eq. 3.12 in section 3.2

$$s_f = \frac{\mu\omega_0^2\varrho_f}{(2\rho+1)\lambda_{min}(M_f)\varrho + \mu\omega_0^2}$$

where $M_f = PB\bar{\Gamma}_{f_w}B'PP^{-1}$.

Therefore under the given control law u, even if the fault $\bar{\Gamma}_{f_w}$ happens, all the trajectory which starts from $\Omega(P,\varrho_d)$ will still enter $\Omega(P,s_d)$.

The chosen x_d^f should satisfy that

$$\begin{cases} \Omega(P,s_d) \subset \Pi_{deg} \\ \Pi_{nom} \subset \Omega(P,\varrho_d) \\ \Omega(P,s_d) \bigcap \Pi_{nom} = \varnothing \end{cases} \tag{3.50}$$

3. Observer Part:

   When the fault $\bar{\Gamma}_{f_j}$ happens, the nominal system $\Sigma_{e_{nom}}$ (see Eq. 3.47) is changed to Σ_{e_f} (see Eq. 3.48).

   In order to obtain the fault information, the observer which is adopted in AFTC method in section 3.3.2 is used to detect the fault and to estimate its value

   $$\dot{\hat{e}} = A\hat{e} + B\sigma(u(t)) + B\hat{f} - Bu_d(x_d) - L(\hat{e}-e) \tag{3.51}$$

   where $e_x = \hat{e} - e$, $\hat{f}$ is the estimation of the virtual fault $B(\bar{\Gamma}_{f_j} - I)$ with the following fault estimation algorithm

   $$\dot{\hat{f}} = -\Psi e_x$$

   where the parameters L, Ψ are chosen based on Theorem 3.2.

   Note that when x_d^f is adopted, $u_d(x_d^f)$ has to be changed correspondingly in Eq. 3.51.

4. Reconfiguration Mechanism Part :

   The whole process works as follows:

When there is no fault, the tracking system will reach x_d under the designed nominal controller u, the observer will give $\hat{f} = 0$.

For small faults, if the system still operates within Π_{nom}, no action will be implemented.

If the fault forces the system to enter Π_{deg}, the degraded reference x_d^f will be adopted. There are two cases to be discussed in this situation:

(1) Under the nominal controller u, if the tracking system can not reach x_d^f (i.e, can not entre $\Omega(P, s_d)$), the system should be stopped, because the fault is more severe than $\bar{\Gamma}_{f_w}$;

(2) Under the nominal controller u, if the tracking system can reach x_d^f (i.e, entre $\Omega(P, s_d)$), the estimated fault $\hat{f}$ will be obtained by the observer after that the faulty system enters $\Omega(P, s_d)$. Based on the estimated $\hat{f}$, a new controller u_n and a new reference x_{dn} (x_{dn} should be chosen as near as possible to x_d) will be adopted to make sure the faulty system can recover the performance as best as possible.

For example, for the original reference x_d, let us construct a new controller $u_n = K_n e + (K_{rn} - K_n)x_d$ with

$$\begin{cases} K_n = (1+\rho)B_f' P_n \\ K_{rn} = ((B_f K_n - A)^{-1} B_f)^+ \end{cases} \tag{3.52}$$

where $B_f = B + \hat{f}$, P is a symmetric positive semi-definite for

$$A'P_n + P_n A - P_n B_f B_f' P_n + \frac{1}{\mu} P_n E E' P_n + \frac{\mu}{\varrho_n} \omega_0^2 P_n < 0 \tag{3.53}$$

If $\Omega(P_n, s_f) \subset \Omega(P_n, \varrho_n)$, then the new controller u_n can recover the degraded performance and make the faulty system reach x_d.

Remark 3.8. *The proposed fault-tolerant control mechanism can not handle all possible faults, similar to PFTC, the worst fault case should be considered. However, thanks to RAT, it can tolerate more severe faults than PFTC. Different from PFTC, the observer is adopted here to obtain the fault information. After a new controller is reconstructed to recover the degraded performance as best as possible.*

Remark 3.9. *Compared with AFTC, since the estimated fault is not included in the control law, the proposed fault-tolerant control mechanism can tolerate more severe faults. Also thanks to RAT, the input saturation problem will be avoided, it guarantees the feasibility of the designed observer.*

Remark 3.10. *After obtaining the fault information from the designed observer, the choices of the new controller u_n and of the new reference x_{dn} are briefly discussed here. The giving example Eq. 3.52 with $x_{dn} = x_d$ just illustrate one simple design method. With different control design methods, the new reference x_{dn} should be chosen as near as possible to the original reference x_d.*

3.4.3 Illustrative example for RAT

In this section, the same example as in section 3.3.2 is taken to illustrate the above proposed reference adjustment technique for fault-tolerant control mechanism.

The system Σ_0 (see Eq. 2.1) is defined as

$$A = \begin{bmatrix} 0.1 & -0.1 \\ 0.1 & 0.3 \end{bmatrix}, B = \begin{bmatrix} 25 & 0 \\ 0 & 2 \end{bmatrix},$$

$$C = \begin{bmatrix} 1 & 0 \\ 0 & 1 \end{bmatrix}, E = \begin{bmatrix} 1 \\ 1 \end{bmatrix},$$

ω_0 is chosen as 0.05.

The tracking point $r = x_d$ is set as

$$x_d = \begin{bmatrix} 5 \\ 0 \end{bmatrix}$$

Based on theorem 2.1, one can obtain

$$P = \begin{bmatrix} 0.0101 & 0.014 \\ 0.014 & 0.058 \end{bmatrix}, \mu = 0.9, \varrho_d = 0.6086$$

that satisfy the following LMI

$$A'P + PA - PBB'P + \frac{1}{\mu}PEE'P + \frac{\mu}{\varrho_d}\omega_0^2 P < 0$$

By taking $\rho = 15$, based on Eq. 2.29, we can also get $s_d = 4.7557e-004$. The invariant sets $\Omega(P, \varrho_d)$ and $\Omega(P, s_d)$ are both obtained, see Fig. 3.25.

Finally the parameters of the designed controller are obtained

$$K = \begin{bmatrix} 4.04 & 5.6 \\ 0.448 & 1.856 \end{bmatrix}, K_r = \begin{bmatrix} 4.036 & 5.604 \\ 0.398 & 1.706 \end{bmatrix},$$

Around the tracking point $x_d = [5; 0]^T$, the nominal performance Π_{nom} and the degraded performance Π_{deg} are also chosen as

$$\Pi_{nom} : \{(x_1, x_2) | (x_1 - 5)^2 + (x_2)^2 - 1 = 0\}$$

$$\Pi_{deg} : \{(x_1, x_2) | (x_1 - 5)^2 + (x_2)^2 - 3.2^2 = 0\}$$

The degraded reference x_d^f is chosen as $x_d^f = [3; 0]^T$.

Suppose that the fault is

$$\bar{\Gamma}_{f_w} = \begin{bmatrix} 0.27 & 0 \\ 0 & 0.27 \end{bmatrix}$$

The inequality

$$A'P + PA - PB\bar{\Gamma}_{f_w}B'P + \frac{1}{\mu}PEE'P + \frac{\mu}{\varrho_f}\omega_0^2 P < 0$$

and inequality 3.49 is verified with $\varrho_f = 0.5786$, and we can obtain $s_f = 0.0018$. The sets $\Omega(P, \varrho_f)$ and $\Omega(P, s_f)$ are both obtained, see Fig. 3.25.

A selected point $x_0 = [10; -4]^T$ near the boundary of $\Omega(P, \varrho_d)$ is taken as the initial state, as shown in Fig. 3.26. Then by running the closed-loop system with the designed controller, the phase trajectory can be obtained as shown in Fig. 3.26. It is obvious that the trajectory starting from x_0 in $\Omega(P, \varrho_d)$ enters $\Omega(P, s_d)$ and remains inside it. The actuator control signals are shown in Fig. 3.27.

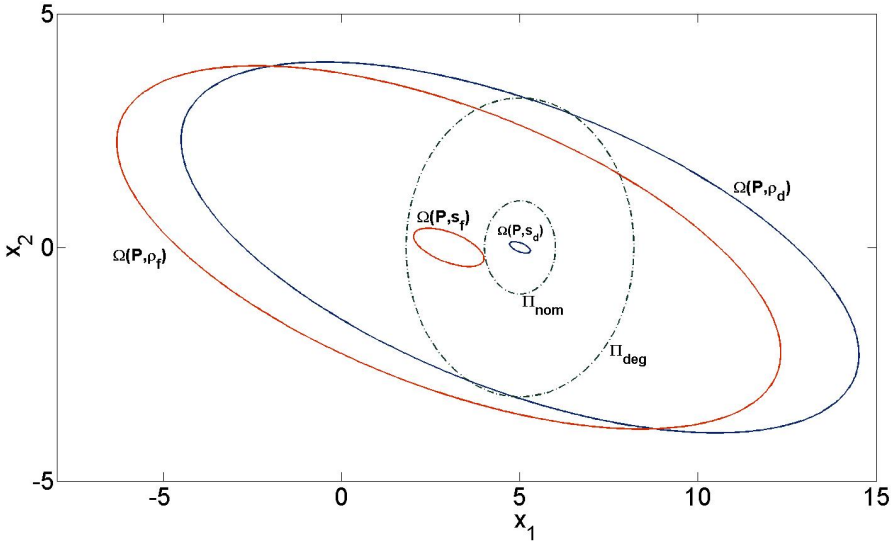

FIGURE 3.25: Invariant Ellipsoids and Performance Sets

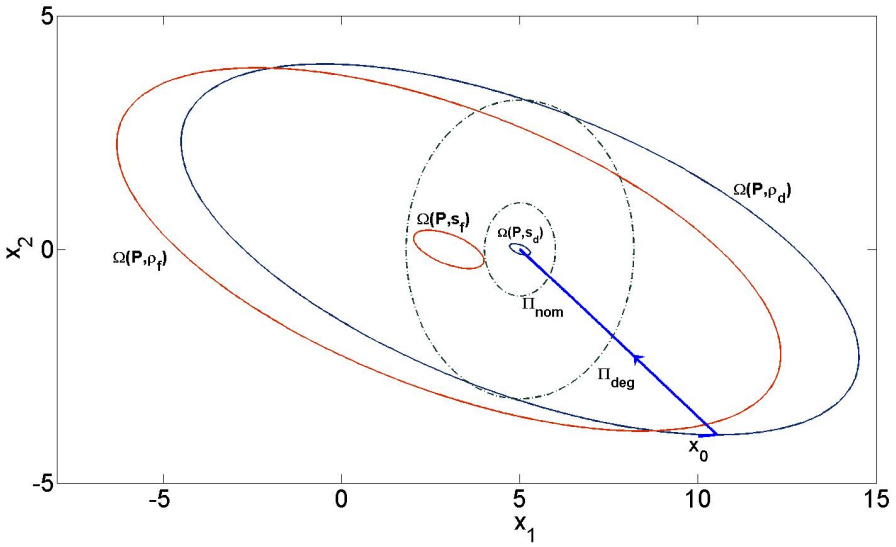

FIGURE 3.26: State Response with x_0

Based on Theorem 3.2, the parameters L, Ψ for observer are calculated as

$$L = \begin{bmatrix} 15.14 & -4.3733 \\ -1.2933 & 30.26 \end{bmatrix}, \Psi = \begin{bmatrix} 1.2467 & -0.0519 \\ -0.3563 & 1.8518 \end{bmatrix}$$

In no fault case, the estimated fault equals 0, see Fig. 3.28. It should be noted that the peak value of F_{2est} near $t = 2s$ is caused by $u_2(t_2) = 0$.

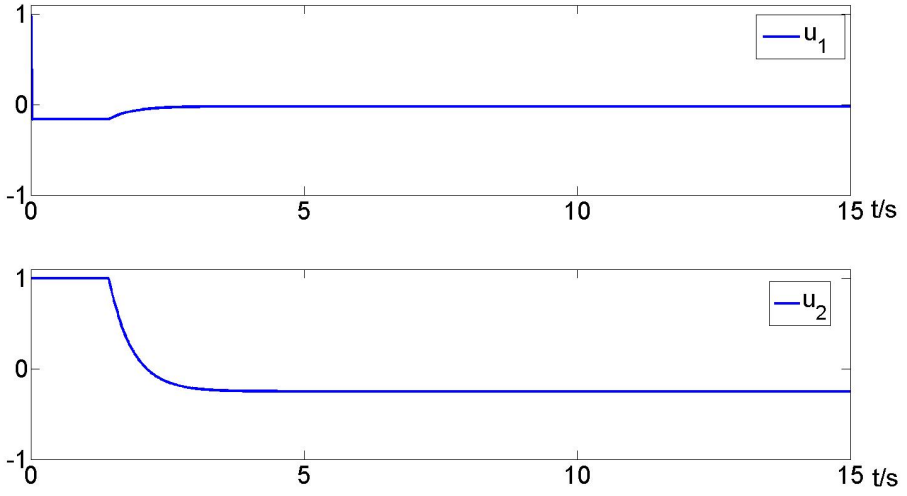

FIGURE 3.27: Actuator Control Signals

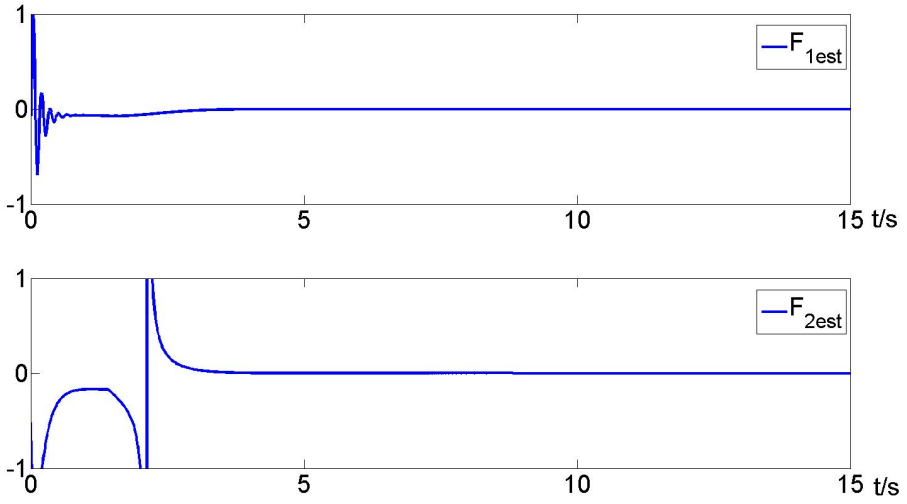

FIGURE 3.28: Estimation $F_{est} = \hat{f}/\sigma(u(t))$ of $(\bar{\Gamma}_f - I)$: without Fault

Three faults $\bar{\Gamma}_{fj}, j = 1, 2, 3$ are considered here

$$\bar{\Gamma}_{f1} = \begin{bmatrix} 1 & 0 \\ 0 & 0.5 \end{bmatrix}, \bar{\Gamma}_{f2} = \begin{bmatrix} 0.27 & 0 \\ 0 & 0.27 \end{bmatrix}, \bar{\Gamma}_{f3} = \begin{bmatrix} 0.2 & 0 \\ 0 & 0.2 \end{bmatrix}$$

For the sake of simplicity, we assume that the fault happens after x_d is reached. The fault occurs at $t_f = 15s$.

For the fault $\bar{\Gamma}_{f1}$, since the tracking performance is still within Π_{nom}, see Fig. 3.29 and Fig. 3.30, based on the proposed fault-tolerant control scheme, no action will

be implemented. The control input does not saturate, therefore the estimated fault can be obtained correctly, see 3.31.

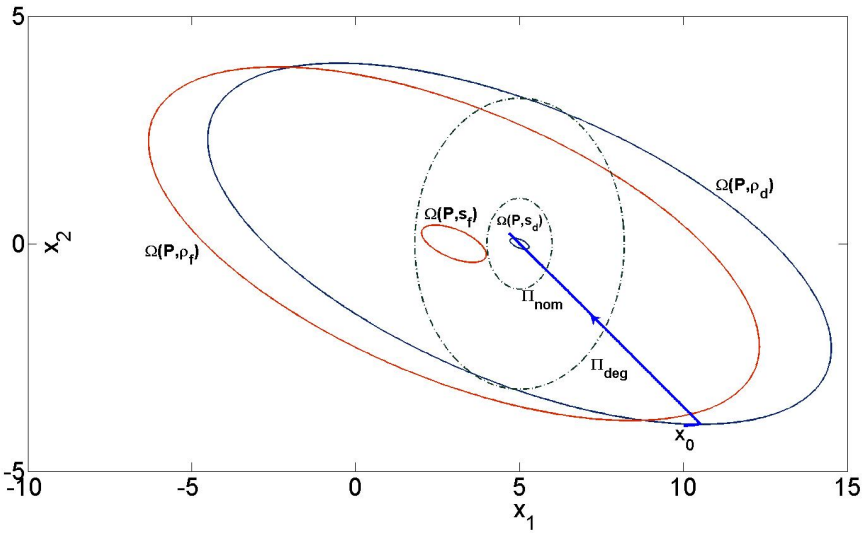

FIGURE 3.29: State Trajectory with Fault $\bar{\Gamma}_{f1}$ happens at $t_f = 15s$

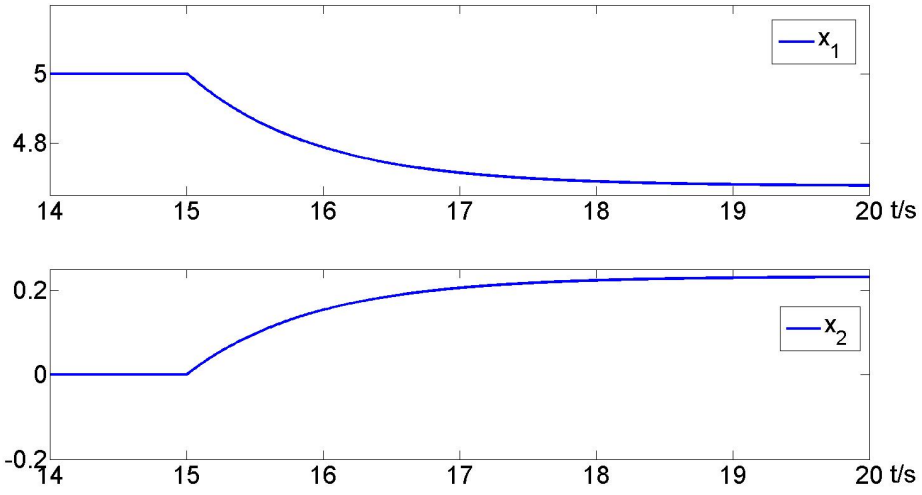

FIGURE 3.30: Response of State x with Fault $\bar{\Gamma}_{f1}$ happens at $t_f = 15s$

For the fault $\bar{\Gamma}_{f2}$, since the tracking performance will be out of Π_{nom} and Π_{deg} , see Trajectory 1 in Fig. 3.32, when the performance degrades to the boundary of Π_{nom}, at $t_d = 20s$, $x_d^f = [3; 0]^T$ is adopted. The faulty tracking system enters into $\Omega(P, s_f)$, see Trajectory 2 in Fig. 3.32, which means that the happened fault is not at least more severe than $\bar{\Gamma}_{f_w}$. The estimated fault can be obtained correctly by the designed observer thanks to using x_d^f, see the solid lines (with RAT) in Fig. 3.33.

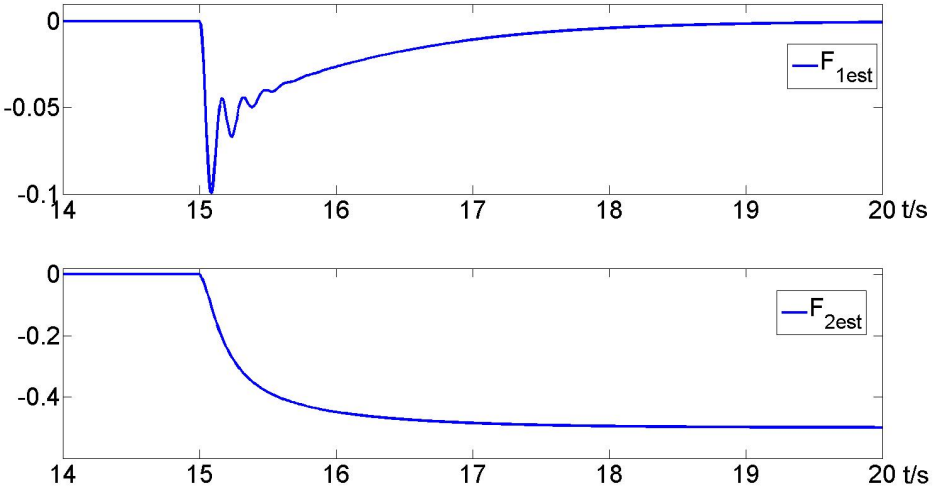

FIGURE 3.31: Estimation $F_{est} = \hat{f}/\sigma(u(t))$ of $(\bar{\Gamma}_f - I)$: with Fault $\bar{\Gamma}_{f1}$ happens at $t_f = 15s$

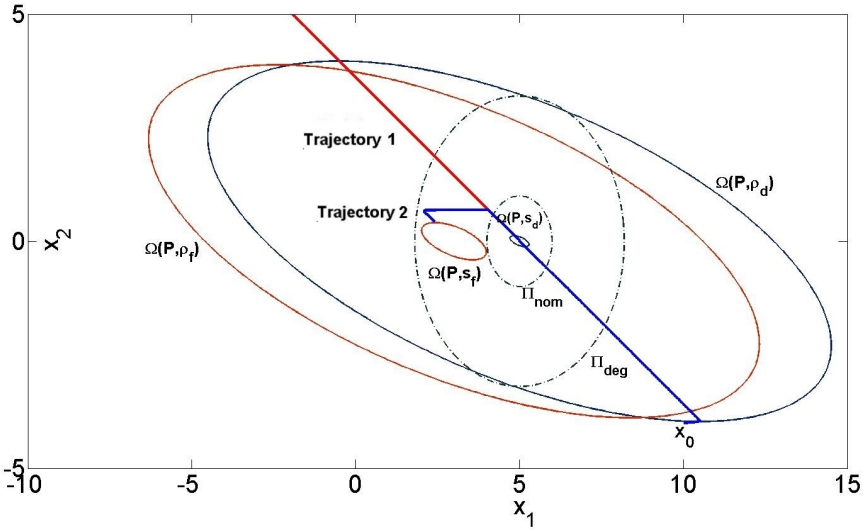

FIGURE 3.32: State Trajectories with Fault $\bar{\Gamma}_{f2}$ (Trajectory 1: without RAT; Trajectory 2: with RAT)

From Fig. 3.34, we can see that the proposed fault-tolerant control scheme can tolerate more severe faults than PFTC. Without adjusting the reference x_d to x_d^f, the tracking system will become unstable. After changing to x_d^f, the system can keep the stability and enter into $\Omega(P, s_f)$.

From Fig. 3.33 and Fig. 3.35, we can also see that without adjusting the reference, since the control input is saturated because of the fault, the estimated fault $\hat{f}$ is not correct. However, thanks to RAT by avoiding the input saturation situation,

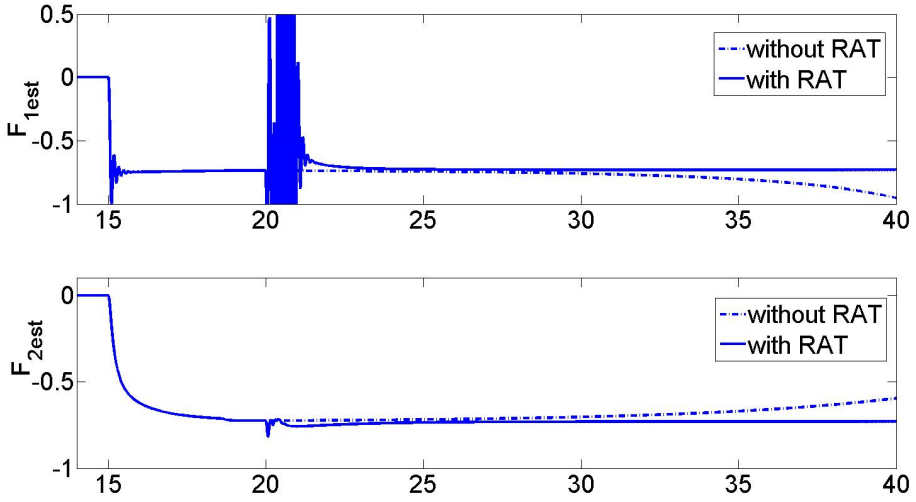

FIGURE 3.33: Estimation $F_{est} = \hat{f}/\sigma(u(t))$ of $(\bar{\Gamma}_f - I)$: with Fault $\bar{\Gamma}_{f2}$

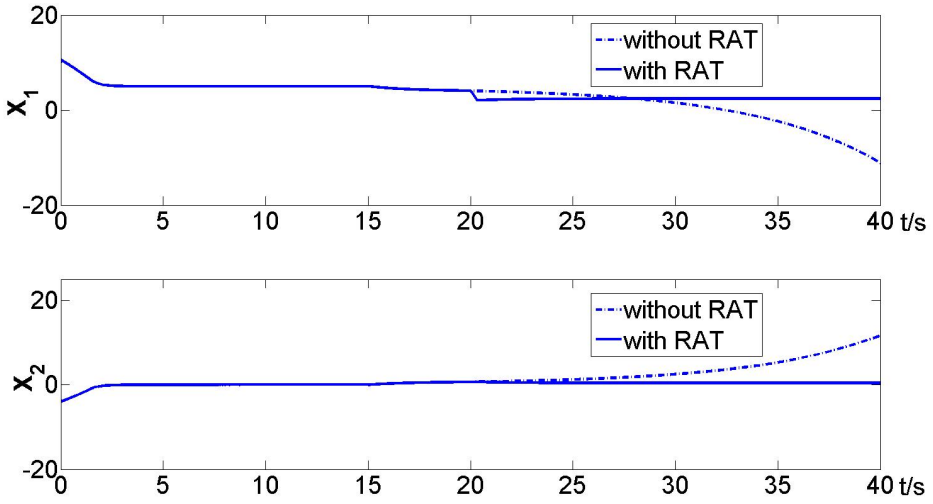

FIGURE 3.34: Response of State x with Fault $\bar{\Gamma}_{f2}$

the correct estimation of fault will be obtained .

After getting the fault information, based on Eq. 3.52 and Eq. 3.53, a new controller u_n is constructed with

$$P_n = \begin{bmatrix} 0.0601 & 0.035 \\ 0.035 & 0.078 \end{bmatrix}, K_n = \begin{bmatrix} 6.0851 & 3.5438 \\ 0.2835 & 0.6318 \end{bmatrix}, K_{rn} = \begin{bmatrix} 6.0703 & 3.5586 \\ 0.0983 & 0.0762 \end{bmatrix},$$

Based on Eq. 3.53, we can get $\varrho_n = 0.965$, $s_n = 0.043$. Since $\Omega(P_n, \varrho_n)$ satisfies $\Omega(P, s_f) \subset \Omega(P_n, \varrho_n)$, the original reference $x_d = [5; 0]^T$ will be adopted at $t_n =$

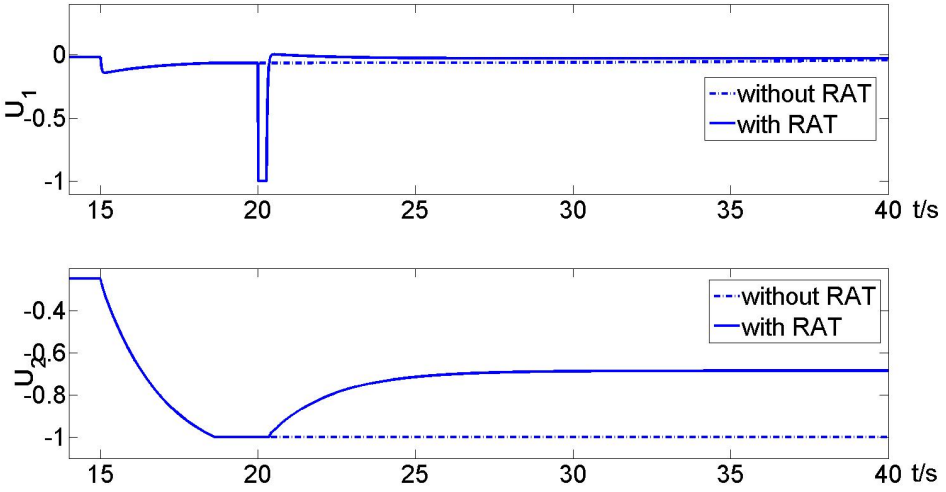

FIGURE 3.35: Actuator Control Signals with Fault $\bar{\Gamma}_{f2}$

$40s$. The new controller will recover the degraded performance and will make the system reach $\Omega(P_n, s_n)$, see Fig. 3.36.

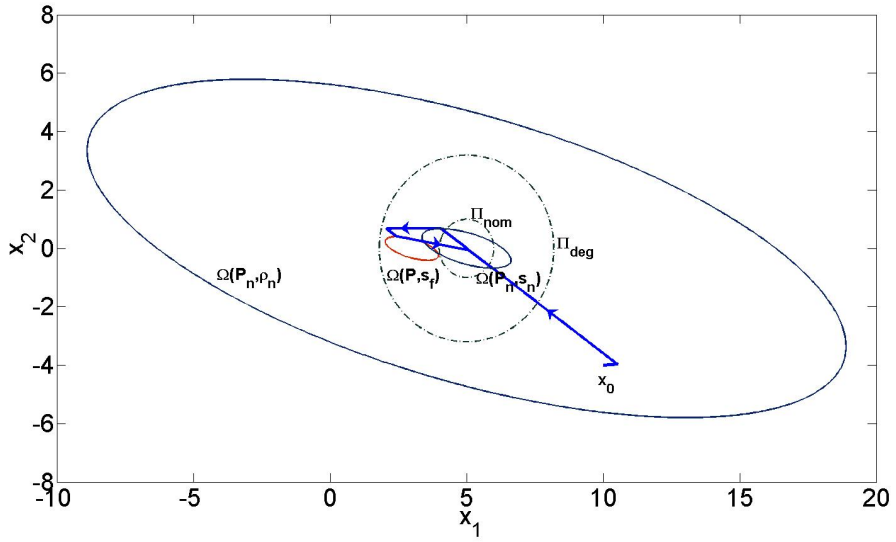

FIGURE 3.36: State Trajectories with New Controller

For the fault $\bar{\Gamma}_{f3}$, the tracking performance will be out of Π_{nom}. When the performance degrades to the boundary of Π_{nom}, at $t_d = 17s$, we fix $x_d^f = [3; 0]^T$. However the faulty tracking system will not enter into $\Omega(P, s_f)$, it means that the fault is more severe than $\bar{\Gamma}_{f_w}$. Therefore, when the performance degrades to the boundary of Π_{deg}, the system is stopped at $t_s = 28s$, see Fig. 3.37.

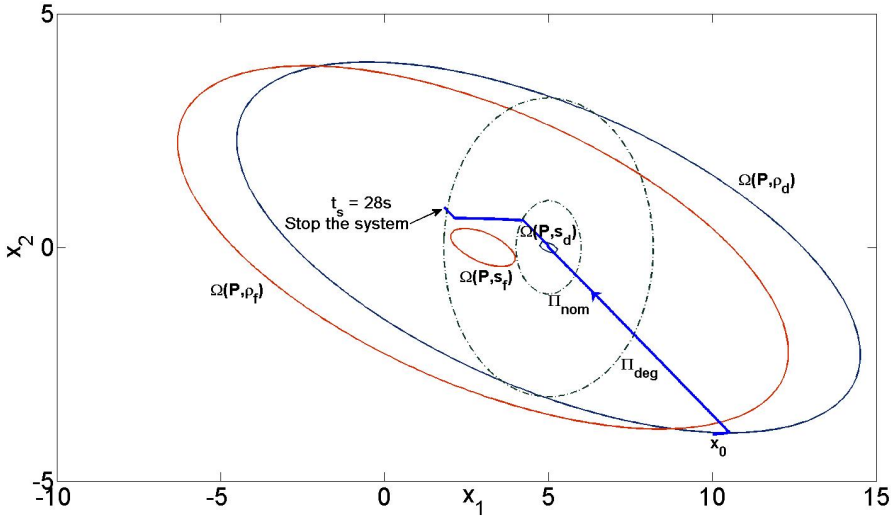

FIGURE 3.37: State Trajectory with Fault $\bar{\Gamma}_{f3}$ with RAT

3.5 Conclusion

In Chapter 3, fault-tolerant control methods for the linear tracking system with actuator saturation and certain actuator faults are considered. First, specific actuator faults are modelled in section 3.1; then for the tracking system with the nominal controller which was designed in chapter 2, the influence of the fault is discussed in section 3.2. The size of the happened faults will influence the system's stability region and the performance region. In order to guarantee the stability of the faulty system, and its performance, it is necessary to design a fault-tolerant controller to handle the possible faults.

Two main methods (PFTC and AFTC) in FTC design are studied in sections 3.3.1 and 3.3.2.

In section 3.3.1, considering a set of possible faults, a LMI based passive fault-tolerant controller is designed based on Theorem 3.1. The system's stability region and performance region are also estimated in section 3.3.1. Although the simulation results in section 3.3.1.2 show the effectiveness of the designed passive

fault-tolerant controller, there are several drawbacks: (1) the faults that PFTC can handle with are restricted in the given faults set; (2) PFTC reduces the size of the stability region to achieve the fault tolerant capability. The stability region and the performance region are actually decided by the worst fault in the given set. (3) Since there is no extra action for PFTC when the faults happen, the system may works with degraded performance.

In section 3.3.2, an observer based active fault-tolerant controller is proposed. The observer is used to estimate the fault. The parameters of the designed observer can be obtained by solving LMIs in Theorem 3.2. Then a feedback fault-tolerant controller (see Eq. 3.33) can be adjusted with the estimated fault information to counteract the influence of the fault and also recover the degraded performance. The stability of the observer should also be guaranteed, however, the observer can estimate the fault correctly only if the controller is not saturated, see Eq. 3.37. Although without violating the input limits, the designed AFTC can compensate the fault and reduce the performance degradation comparing to PFTC, the analysis of the stability and its fault-tolerant capability is quite difficult since $\hat{f}$ is used in the control law Eq. 3.2.

The proposed PFTC and AFTC methods have both their restrictions and drawbacks when dealing with the input saturation problem. Therefore, combining the PFTC method with the AFTC method, a fault-tolerant control scheme based on reference adjustment technique is proposed. The main idea of this control scheme is to change the reference when a fault happens in order to avoid saturation. Before adopting the referred reference adjustment technique (RAT), the relative performance analysis principle is introduced in section 3.4.1, the nominal performance set Π_{nom} and the degraded performance set Π_{deg} are important sets to be defined in the following proposed fault-tolerant control scheme in section 3.4.2.

In the proposed fault-tolerant control scheme, the controller is designed as in Chapter 2 based on Theorem 2.1. For the tracking system with the designed nominal controller, we can get the stability region $\Omega(P, \varrho_d)$ and the performance region $\Omega(P, s_d)$ under no fault condition. The fault tolerant capability is decided upon the nominal control law. The degraded reference x_d^f and the worst fault case

$\bar{\Gamma}_{fw}$ can be determined by Eq. 3.49, and also the stability region $\Omega(P, \varrho_f)$ and the performance region $\Omega(P, s_f)$ for the system with x_d^f and $\bar{\Gamma}_{fw}$. The observer that is used in AFTC method in section 3.3.2 is also introduced in this scheme. The condition to guarantee the stability of the observer is that the constraint must not be exceeded by the control law, this condition can be guaranteed by choosing x_d^f as the new reference when some severe faults happen. If a small fault occurs, the nominal controller will still be used. If the tracking performance degrades to the boundary of Π_{nom} because of a severe fault, the degraded reference x_d^f is chosen immediately to avoid input saturation. If the tracking system can enter into $\Omega(P, s_f)$, that means the happened fault is less severe than $\bar{\Gamma}_{fw}$, then the fault information can be estimated by the observer. With the estimated fault, for the faulty tracking system, the new control law and the new reference x_{dn} (which should be chosen as near as possible to x_d) can be designed in order to recover the degraded performance. In the other case, if the tracking system can not enter into $\Omega(P, s_f)$ even if x_d^f is chosen, the system will be stopped when the performance degrades to the boundary of Π_{deg}. In this case, the happened fault is more severe than $\bar{\Gamma}_{fw}$.

Thanks to choosing a degraded reference x_d^f, the proposed fault-tolerant control scheme can tolerate more severe faults comparing to the PFTC and AFTC methods. It also guarantees the feasibility of the designed observer which is used to estimate the fault. One example is simulated with MATLAB, the simulation results in section 3.4.3 show the effectiveness of the proposed FTC scheme based on reference adjustment technique. However, the part of designing the new controller and choosing the new reference after detecting and estimating the happened fault is just described briefly in section 3.4.2. No matter under which fault case, the new reference should be chosen as near as possible to the original reference with different possible control design methods.

Chapter 4

FAULT-TOLERANT CONTROL SCHEME FOR PATH TRACKING OF A 4WD ELECTRIC VEHICLE

Contents

Abstract This chapter investigates the path tracking problem for an electric vehicle (EV) which has four electromechanical wheel systems under normal and faulty conditions. With considering wheel slip constraints and certain faults, a passive fault-tolerant controller based on a low-high gain control is developed to maintain the system's stability and guarantee the acceptable tracking performance. Then, based on the designed controller, a simple active fault diagnosis approach is introduced for this typical over-actuated system to isolate and evaluate faults more precisely. With the diagnosed information, an accommodated fault-tolerant controller is finally designed to maintain the tracking performance.

4.1 Introduction

The four-wheels driving (4WD) electric vehicle (EV) reveals high potentials for the path tracking performance in critical situations. Many researches have been conducted on the control design of this typical overactuated system [132][133][134]. Among these researches, actuator saturation and input constraints are practical issues that should be considered. Due to the vehicle's physical characteristics, when the magnitude of the wheel slip reaches its limit, any further increase may lead to skipping which can cause system unstability. In [133] and [134], the authors use a controller based on a low-and-high gain technique (which has been introduced in section 2.1.1) to solve the control saturation problem for the 4WD EV path tracking problem with wheel slip constraints.

The number of actuators in such vehicles increases the probability of fault occurrence, such as loss of steering, loss of traction of wheels, etc. Fault Tolerant Control (FTC) methods have been proposed for the overactuated EV system [135][136], but few considers FTC with input saturation. This problem has been investigated in many other application fields, such as the spacecraft attitude system in aeronautics [137][138].

In practical situation, with considering faults and input constraints, the FTC methods may not be able to recover the system's original performance. In order to maintain the maximal performance, necessary accommodations for the controller are needed. In [136], an adaptive actuator allocation method based on an online parameter estimator and a control system reconfiguration strategy was proposed. Obviously, for an overactuated system, the most used method is control reallocation. In [139], control reallocation was applied for an Unmanned Aerial Vehicle (UAV): a quadrotor helicopter, which was equipped with two actuators. With considering control effector (actuator) failures or control surface damages in flight control systems, control reallocation was applied to a realistic and nonlinear aircraft model in [140]. The key problem of control reallocation is to design a fault diagnosis and isolation (FDI) module to isolate and estimate the fault. However, for the four-wheel independently-driven EV, the traditional FDI methods can not be used directly, because the wheels on the same side have the same effect on the vehicle's motion, and consequently it is hard to distinguish which one is faulty with the limited measurable states [141]. In [141], with the objective to isolate the faulty component for the 4WD EV system, an active fault diagnosis approach was proposed. It consists in actively changing the motor control gain by multiplying it by a positive value. This approach should be based on a controller that guarantees the system's stability all the time. For this reason, a passive fault-tolerant control (PFTC) method is considered. Such PFTC has the advantage to tolerate certain faulty situations without needing a precise fault information. However, the authors did not study its practical using and its feasibility under input saturation case.

Different from a typical control system design, for the FTC system, one should also consider the system performance under faults [142]-[143]. Fully compensating the performance degradation caused by faults may be not achievable due to actuator saturation. Rather than risking further damage or loss of stability of the vehicle, accepting an allowable performance degradation is also a practical way to handle the FTC problem with input saturation. In [143], the authors used a reference input adjustment technique to prevent actuator saturating and also to achieve acceptable performance.

In this chapter, one aims to design a FTC scheme for the 4WD EV path tracking control with input saturation. The key methods including the controller design, the reference adjustment technique and fault diagnosis method were all introduced in the previous chapters. One controller is first developed to maintain the system stability and to guarantee the allowable tracking performance under no fault condition. If the performance degrades under a given level because of faults, the active fault diagnosis (AFD) approach in [141] is used to isolate and evaluate the faults more precisely. During this period, the designed controller and the reference input adjustment technique are used to guarantee the safe implementation of AFD. As soon as the diagnosis information are available, an accommodated controller is reconstructed to recover the degraded tracking performance under faulty conditions.

The remainder of this chapter is organized as follows. For the 4WD EV system, section 4.2 and section 4.3 describe its nonlinear model and its linearization. Section 4.4 introduces the control scheme and the fault model. Section 4.5 presents the whole fault tolerant control scheme, including the passive fault tolerant controller design, the implementation of the reference adjustment technique and the active fault diagnosis approach. Then, based on the active fault diagnosis method, the new controller is implemented. Finally in section 4.6, the effectiveness of the proposed method is shown through simulations of traction engine faults.

4.2 System Modeling

The electric vehicle has four actuated wheels and two actuated steering systems, see Fig. 4.1. The 4DC traction motors deliver a relative important mass torque. Front and rear steering motions are obtained through 2DC actuators [144].

Fig. 4.2 describes the three features of the considered system, namely, vehicle body, four wheels and the reference path for tracking [145]. The measurable states are: the center of gravity (CG) speed $\nu = \|V\|$, the sideslip angle β, the yaw rate γ, the perpendicular distance y_c, the angle ϕ between the vehicle velocity and the tangent to the path curve.

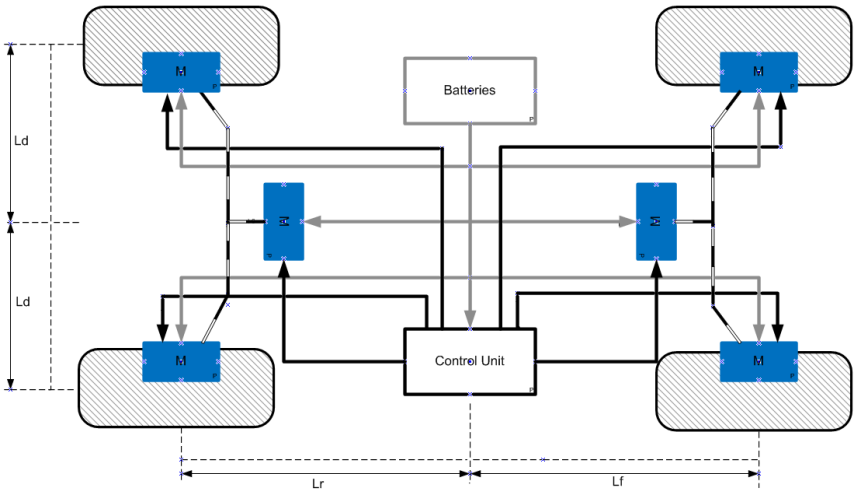

FIGURE 4.1: The Schematic Diagram of the 4WD4WS EV

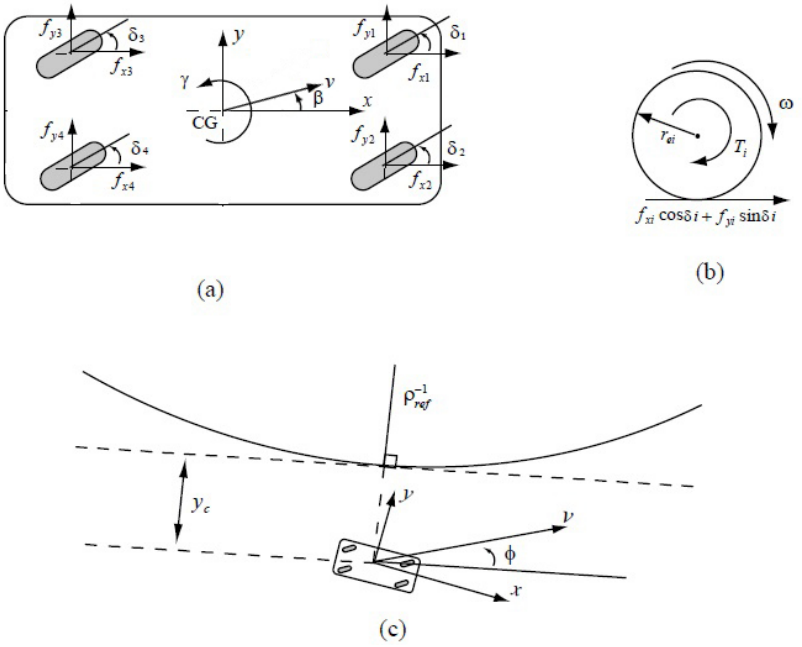

FIGURE 4.2: (a)Vehicle Body (b)Wheel Model (c)Path-tracking Kinematics

The dynamical equations of the three subsystems can be expressed as follows (see [133],[134],[146]):

A. Vehicle Body

$$\begin{bmatrix} m & 0 & 0 \\ 0 & m\nu & 0 \\ 0 & 0 & J_z \end{bmatrix} \frac{d}{dt} \begin{bmatrix} \nu \\ \beta \\ \gamma \end{bmatrix} = \begin{bmatrix} \cos\beta & \sin\beta & 0 \\ -\sin\beta & \cos\beta & 0 \\ 0 & 0 & 1 \end{bmatrix} \sum_{i=1}^{4} \begin{bmatrix} f_{xi} \\ f_{yi} \\ M_{zi} \end{bmatrix} + \begin{bmatrix} -\sigma_{aero}\nu^2\cos\beta \\ \sigma_{aero}\nu^2\sin\beta - m\nu\gamma \\ 0 \end{bmatrix} \tag{4.1}$$

where m is the mass of the vehicle, f_{xi} and f_{yi} are traction forces which mainly result from the tire-road frictions, σ_{aero} stands for the aerodynamical coefficient, M_{zi} is the yaw moment and it has the following form

$$\sum_{i=1}^{4} M_{zi} = \begin{bmatrix} -L_d & L_f \end{bmatrix} \begin{bmatrix} f_{x1} \\ f_{y1} \end{bmatrix} + \begin{bmatrix} L_d & L_f \end{bmatrix} \begin{bmatrix} f_{x2} \\ f_{y2} \end{bmatrix} + \begin{bmatrix} -L_d & -L_r \end{bmatrix} \begin{bmatrix} f_{x3} \\ f_{y3} \end{bmatrix} + \begin{bmatrix} L_d & -L_r \end{bmatrix} \begin{bmatrix} f_{x4} \\ f_{y4} \end{bmatrix} \tag{4.2}$$

where L_d is one half of the distance of the tread and L_f (resp. L_r) are the distances between the center of gravity and the front axle (resp. the rear axle), see Fig. 4.1.

B. Wheel Model

$$I_{wi}\frac{d}{dt}\omega_i = T_i - r_{ei}\begin{bmatrix} \cos\delta_i & \sin\delta_i \end{bmatrix} \begin{bmatrix} f_{xi} \\ f_{yi} \end{bmatrix} \tag{4.3}$$

where ω_i $(i = 1, 2, 3, 4)$ are the wheel angular speeds, I_{wi} is the inertia of the wheel, r_{ei} is the wheel's radius, δ_i is the steering angle and T_i is the wheel torque.

C. Path-tracking Kinematics

$$\begin{cases} \dot{y_c} = -\nu\sin\phi \\ \dot{\phi} = -\frac{\nu}{1/\rho_{ref}+y_c}\cos\phi + \dot{\beta} + \gamma \end{cases} \tag{4.4}$$

where ρ_{ref} is the tangent to the path curvature.

The friction forces (f_{xi}, f_{yi}) in Eq. 4.1 and Eq. 4.3 can be defined by the combined wheel slip S_i [134]:

$$\begin{bmatrix} f_{xi} \\ f_{yi} \end{bmatrix} = f_{zi} \underbrace{\begin{bmatrix} \cos\beta_i & -\sin\beta_i \\ \sin\beta_i & \cos\beta_i \end{bmatrix} \begin{bmatrix} 1 & 0 \\ 0 & k_{si} \end{bmatrix} \frac{\mu_{Res}(\|S_i\|_2, \chi)}{\|S_i\|_2} S_i}_{[\mu_{xi} \ \ \mu_{yi}]'} \tag{4.5}$$

where $[\mu_{xi} \ \ \mu_{yi}]'$ is the friction coefficient, k_{si} the tire-tread-profile attenuation factor of each wheel and $\mu_{Res}(\|S_i\|_2, \chi)$ the tire-road friction coefficient, using the model as in [147]

$$\mu_{Res}(\|S_i\|_2, \chi) = \mu_0 \|S_i\|_2 / (a\|S_i\|_2^2 + b\|S_i\|_2 + 1) \tag{4.6}$$

Here a,b are the corresponding parameters. Defining k_i as the initial slop depends mainly on road conditions as

$$\left.\frac{\partial \mu_{Res}(\|S_i\|_2, \chi)}{\partial \|S_i\|_2}\right|_{\|S_i\|_2=0} \triangleq k_i = \mu_0 \tag{4.7}$$

The combined wheel slip S_i consists of the longitudinal slip S_{Li} and the lateral slip S_{Si}, see Fig. 4.3.

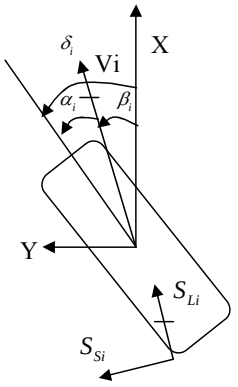

FIGURE 4.3: Angles and Slips for the i-th Wheel

It is characterized by

$$\begin{bmatrix} S_{Li} \\ S_{Si} \end{bmatrix} = \frac{1}{max(r_{ei}\omega_i \cos\alpha_i, \|V_i\|)} \begin{bmatrix} r_{ei}\omega_i \cos\alpha_i - \|V_i\| \\ r_{ei}\omega_i \sin\alpha_i \end{bmatrix} \tag{4.8}$$

where V_i presents the velocity of each wheel center, it can be calculated by $V_i = \sqrt{v_{xi}^2 + v_{yi}^2}$ with

$$V_1 = \begin{bmatrix} v_{x1} \\ v_{y1} \end{bmatrix} = \begin{bmatrix} \nu\cos\beta - L_d\gamma \\ \nu\sin\beta + L_f\gamma \end{bmatrix}, V_2 = \begin{bmatrix} v_{x2} \\ v_{y2} \end{bmatrix} = \begin{bmatrix} \nu\cos\beta + L_d\gamma \\ \nu\sin\beta + L_f\gamma \end{bmatrix}$$

$$V_3 = \begin{bmatrix} v_{x3} \\ v_{y3} \end{bmatrix} = \begin{bmatrix} \nu\cos\beta - L_d\gamma \\ \nu\sin\beta - L_r\gamma \end{bmatrix}, V_4 = \begin{bmatrix} v_{x4} \\ v_{y4} \end{bmatrix} = \begin{bmatrix} \nu\cos\beta + L_d\gamma \\ \nu\sin\beta - L_r\gamma \end{bmatrix}$$

The part $r_{ei}\omega_i$ in Eq. 4.8 can be replaced by $\|V_{iref}\|$ which can also be calculated by $V_{iref} = \sqrt{v_{xiref}^2 + v_{yiref}^2}$.

The slip angle α_i, the sideslip angle β_i and the steering angle δ_i, see Fig. 4.3, can be expressed with V_i and V_{iref} as

$$\alpha_i = \delta_i - \beta_i, \delta_i = \tan^{-1}(v_{yi}/v_{xi}), \beta_i = \tan^{-1}(v_{yiref}/v_{xiref})$$

Based on the assumption of zero slip, Eq. 4.5 can be rewritten as

$$\begin{bmatrix} f_{xi} \\ f_{yi} \end{bmatrix} = f_{zi} \begin{bmatrix} \frac{v_{xi}}{\sqrt{v_{xi}^2+v_{yi}^2}} & \frac{-k_{si}v_{yi}}{\sqrt{v_{xi}^2+v_{yi}^2}} \\ \frac{v_{yi}}{\sqrt{v_{xi}^2+v_{yi}^2}} & \frac{k_{si}v_{xi}}{\sqrt{v_{xi}^2+v_{yi}^2}} \end{bmatrix} \frac{\mu_{Res}(\|S_i\|_2)}{\|S_i\|_2} S_i \tag{4.9}$$

where

$$S_i = \frac{1}{K_m} \begin{bmatrix} \frac{v_{xiref}v_{xi}+v_{yiref}v_{xi}}{\sqrt{v_{xi}^2+v_{yi}^2}} - \sqrt{v_{xi}^2 + v_{yi}^2} \\ \frac{v_{yiref}v_{xi}-v_{xiref}v_{yi}}{\sqrt{v_{xi}^2+v_{yi}^2}} \end{bmatrix} \tag{4.10}$$

Define K_m satisfying

$$K_m \triangleq max(r_{ei}\omega_i\cos\alpha_i, \|V_i\|) \tag{4.11}$$

We can verify that

$$\|S_i\|_2 = \frac{1}{K_m}\sqrt{(v_{xiref} - v_{xi})^2 + (v_{yiref} - v_{yi})^2} \tag{4.12}$$

Let us define

$$E_i = \begin{bmatrix} E_{xi} \\ E_{yi} \end{bmatrix} = \begin{bmatrix} v_{xiref} - v_{xi} \\ v_{yiref} - v_{yi} \end{bmatrix} \tag{4.13}$$

In [148] and [149], the Input-to-State Stability (ISS) of the the error dynamics equation is studied, and the following condition is derivated

$$\|S_i\|_2 = \frac{\|E_i\|_2}{K_m} \leq \frac{\sqrt{2}}{c} ln(\frac{1}{1 - \frac{1}{\theta g \mu_{Res}^{sat} \sup_{t_0 \leq \tau \leq t} \|\dot{V}_{iref(\tau)}\|}}) \tag{4.14}$$

where $\mu_{Res}^{sat} = \mu_{Res}(\|S_i\| = 1)$, c, θ are the suitable parameters which are related to the friction coefficient $\mu_{Res}(\|S_i\|_2, \chi)$, their specific values in this chapter are given in Section 4.6.

The dynamical normal loads $F_z = [f_{z1} \ f_{z2} \ f_{z3} \ f_{z4}]'$ appearing in Eq. 4.5 can be calculated by (see [133])

$$F_z = (I_{4\times4} + GN)^{-1} F_{zs} \tag{4.15}$$

with

$$G = \frac{h}{2L_d} \begin{bmatrix} \frac{L_d}{L_f+L_r} & \frac{L_d}{L_f+L_r} & \frac{-L_d}{L_f+L_r} & \frac{-L_d}{L_f+L_r} \\ \frac{K_{fr}}{K_{fr}+K_{rr}} & \frac{-K_{fr}}{K_{fr}+K_{rr}} & \frac{K_{fr}}{K_{rr}+K_{rr}} & \frac{-K_{rr}}{K_{fr}+K_{rr}} \end{bmatrix}'$$

$$N = \begin{bmatrix} \mu_{x1} & \mu_{x2} & \mu_{x3} & \mu_{x4} \\ \mu_{y1} & \mu_{y2} & \mu_{y3} & \mu_{y4} \end{bmatrix}$$

where K_{fr} and K_{rr} are respectively the front and rear roll stiffness.

The static normal load F_{zs} with elements f_{zsi} has the following form

$$F_{zs} = \frac{mg}{2} [\frac{L_r}{L_f + L_r} \ \frac{L_r}{L_f + L_r} \ \frac{L_f}{L_f + L_r} \ \frac{L_f}{L_f + L_r}]^T \tag{4.16}$$

In theory, if the magnitude of $\|S_i\|_2$ exceeds the threshold related to road condition, so does the friction force in Eq. 4.5. Conversely, if $\|S_i\|_2$ is limited, the saturation of friction force can be avoided.

4.3 Simplified Model

The friction forces and the vehicle system are modeled by the nonlinear and coupled models given by Eq. 4.1 - Eq. 4.5. To simplified the control design, the model

equations are linearized around a free rolling condition. The objective of the control system is to maintain this equilibrium point, which makes the linearized model valid.

Around the specific point: $\|V_0\| = \nu_0$, $\omega_{i0} = \nu_0/r_{ei}$, $\delta_i = 0$, the following linearized wheel subsystem is obtained:

$$\begin{aligned} I_{wi}\frac{d}{dt}\omega_i &= I_{wi}\frac{d}{dt}(\omega_{i0} + \partial\omega_i) \\ &= T_i - r_{ei}f_{zsi}k_i\frac{r_{ei}\omega_i - \nu - (-1)^i L_d\gamma}{\nu_0} \\ &= T_i - \frac{r_{ei}f_{zsi}k_i}{\nu_0}(r_{ei}\omega_i - r_{ei}\omega_{i0} + \nu_0 - \nu - (-1)^i L_d\gamma) \\ &= T_i - \frac{r_{ei}^2 f_{zsi}k_i}{\nu_0}\partial\omega_i - \frac{r_{ei}f_{zsi}k_i}{\nu_0}(-\partial\nu - (-1)^i L_d\gamma) \end{aligned}$$

that is,

$$(\frac{I_{wi}\nu_0}{r_{ei}^2 f_{zsi}k_i})\frac{d}{dt}\partial\omega_i = \frac{\nu_0}{r_{ei}^2 f_{zsi}k_i}T_i - \partial\omega_i + \frac{1}{r_{ei}}(\partial\nu + (-1)^i L_d\gamma) \tag{4.17}$$

where $\partial\omega_i = \omega_i - \omega_{i0}$, $\partial\nu = \nu - \nu_0$. Through Eq. 4.17, one can see that the wheel subsystem is much faster and ISS, therefore based on the singular perturbation theory, it can be simplified by its quasi-steady state [133]

$$\partial\omega_i = \frac{\nu_0}{r_{ei}^2 f_{zsi}k_i}T_i + \frac{1}{r_{ei}}(\partial\nu + (-1)^i L_d\gamma) \tag{4.18}$$

Around the equilibrium point: $\|V_0\| = \nu_0$, $\beta_0 = 0$, $\gamma_0 = 0$, $y_{c0} = 0$, $\phi_0 = 0$, the following linearized system for Eq. 4.1 - Eq. 4.5 is obtained:

$$\dot{x} = \begin{bmatrix} -2\sigma_{aero}\nu_0/m & 0 & 0 & 0 & 0 \\ 0 & \sigma_{aero}\nu_0/m & -1 & 0 & 0 \\ 0 & 0 & 0 & 0 & 0 \\ 0 & 0 & 0 & 0 & -\nu_0 \\ 0 & \sigma_{aero}\nu_0/m & 0 & 0 & 0 \end{bmatrix} x$$

$$+ \begin{bmatrix} 1/m & 0 & 0 \\ 0 & 1/m\nu_0 & 0 \\ 0 & 0 & 1/J_z \\ 0 & 0 & 0 \\ 0 & 1/m\nu_0 & 0 \end{bmatrix} \sum_{i=1}^{4} \begin{bmatrix} f_{xi} \\ f_{yi} \\ M_{zi} \end{bmatrix} + \begin{bmatrix} -\sigma_{aero}\nu_0^2/m \\ 0 \\ 0 \\ 0 \\ -\nu_0\rho_{ref} \end{bmatrix} \tag{4.19}$$

where $x = [\partial\upsilon \ \beta \ \gamma \ y_c \ \phi]^T$ are the measurable states. The information of these states can be obtained by using the inertial measurement unit (IMU) which is installed on the vehicle.

With Eq. 4.18, the quasi-steady-state combined wheel slip is given in function of the control input (T_i, δ_i) (see [133])

$$\tilde{S}_i = \begin{bmatrix} \frac{T_i}{r_{ei} f_{zsi} k_i} \\ -\beta - \frac{l_i}{\nu_0}\gamma + \delta_i \end{bmatrix} \tag{4.20}$$

where $l_1 = l_2 = L_f$, $l_3 = l_4 = -L_r$.

The simplified friction forces and yaw moments can be expressed as

$$\begin{bmatrix} f_{xi} \\ f_{yi} \\ M_{zi} \end{bmatrix} = \begin{bmatrix} 1 & 0 \\ 0 & 1 \\ l_{1i} & l_{2i} \end{bmatrix} \begin{bmatrix} f_{zsi} k_i & 0 \\ 0 & k_{si} f_{zsi} k_i \end{bmatrix} \tilde{S}_i \tag{4.21}$$

where $l_{11} = l_{13} = -L_d$, $l_{12} = l_{14} = L_d$, $l_{21} = l_{22} = L_f$, $l_{23} = l_{24} = -L_r$.

Suppose that the linearized system Eq. 4.19 - Eq. 4.21 can be stabilized by the control input (T_i, δ_i) with state feedback and the magnitude of $\tilde{S}_i$ is ensured to stay below a prescribed constraint. Since Jocobian linearization and singular perturbation theory guarantee that the local stability of the original system can be

concluded from the stability of its reduced system, the original nonlinear vehicle system can be locally stabilized using the same control scheme.

Different working points are chosen to be linearized. Define k working points as $X_1, X_2..., X_k$, which are all in D_c^f (see Fig. 3.21).

$$D_c^f = \{X_d : X_1, X_2..., X_k\} \tag{4.22}$$

where $X_k = [\upsilon_k \ 0 \ \upsilon_k \rho_{ref} \ 0 \ 0]^T$.

Let us assume that among these k working points, m are within D_c^{nom}, p working points are within D_c^{deg} and $(k-m-p)$ working points are within D_c^{un} (the definitions of D_c^{nom},D_c^{deg} and D_c^{un} see Section 3.4.1 in Chapter 3), i.e.,

$$D_c^{nom} = \{X_d : X_1, X_2..., X_m\} \tag{4.23}$$

$$D_c^{deg} = \{X_d : X_{(m+1)}, X_{(m+2)}..., X_{(m+p)}\} \tag{4.24}$$

$$D_c^{un} = \{X_d : X_{(m+p+1)}, X_{(m+2)}..., X_k\} \tag{4.25}$$

Let us consider a performance index as

$$J_k = (X_k - X_0)^T P (X_k - X_0) \tag{4.26}$$

where X_0 is the original objective

$$X_0 = [\upsilon_0 \ 0 \ \upsilon_0 \rho_{ref} \ 0 \ 0]^T$$

and P as a positive symmetric matrix to be chosen.

As mentioned in previous chapters, the stability of the system with input constraints can be guaranteed if all states are within its attraction region. Let define $\Omega(P, \varrho_0)$ as the attraction region for the nominal tracking system.

The choosing working points should satisfy that

$$J_k > J_{(k-1)} > J_{(k-2)} > ... > J_0 \tag{4.27}$$

and

$$J_{(i)} - J_{(i-1)} \leq \varrho_0 \quad i = 1, 2, ..., k \tag{4.28}$$

Eq. 4.28 guarantees the stabilization of the nominal nonlinear vehicle system.

4.4 Control Scheme

Consider the vehicle tracking along a path of curvature ρ_{ref} with a constant speed v_0. The control objective for Eq. 4.19 is set as

$$x_d = [\partial v_d \ \ \beta_d \ \ \gamma_d \ \ y_{cd} \ \ \phi_d]^T = [0 \ \ 0 \ \ v_0\rho_{ref} \ \ 0 \ \ 0]^T$$

Before designing the controller, some features of the 4WD2WS EV may be stated.

Submitting Eq. 4.20 and Eq. 4.21 into Eq. 4.19, the system can be presented as

$$\dot{x} = A_c x + B_c u_c + d \tag{4.29}$$

where defining $u_c = [T_1, T_2, T_3, T_4, \delta_f, \delta_r]^T$, and A_c, B_c, d are as follows

$$A_c = \begin{bmatrix} 0 & 0 & 0 & 0 & 0 \\ 0 & -\frac{C_f+C_r}{m\nu_0} & -\frac{L_fC_f-L_rC_r}{m\nu_0^2} - 1 & 0 & 0 \\ 0 & -\frac{L_fC_f-L_rC_r}{J_z} & -\frac{L_f^2C_f+L_r^2C_r}{J_z\nu_0} & 0 & 0 \\ 0 & 0 & 0 & 0 & -\nu_0 \\ 0 & -\frac{C_f+C_r}{m\nu_0} & -\frac{L_fC_f-L_rC_r}{m\nu_0^2} & 0 & 0 \end{bmatrix}, d = \begin{bmatrix} -\sigma_{aero}\nu_0^2/m \\ 0 \\ 0 \\ 0 \\ -\nu_0\rho_{ref} \end{bmatrix}$$

$$B_c = \begin{bmatrix} \frac{1}{mr_{e1}} & \frac{1}{mr_{e2}} & \frac{1}{mr_{e3}} & \frac{1}{mr_{e4}} & 0 & 0 \\ 0 & 0 & 0 & 0 & \frac{C_f}{m\nu_0} & \frac{C_r}{m\nu_0} \\ \frac{-L_d}{J_zr_{e1}} & \frac{L_d}{J_zr_{e1}} & \frac{-L_d}{J_zr_{e3}} & \frac{L_d}{J_zr_{e4}} & \frac{L_fC_f}{J_z} & -\frac{L_fC_r}{J_z} \\ 0 & 0 & 0 & 0 & 0 & 0 \\ 0 & 0 & 0 & 0 & \frac{C_f}{m\nu_0} & \frac{C_r}{m\nu_0} \end{bmatrix}$$

Assume that $r_{ei} = \tilde{r}_e$ $(i = 1, ..., 4)$, $\tilde{r}_e$ is the estimated effective radius. With this assumption, obviously the control matrix B_c is not full column rank, one can see

that the front and rear wheels on the same side (T_1 and T_3, T_2 and T_4) have the same effect on the vehicle yaw and longitudinal motion [134][146].

The saturation problem which we stated previously should be considered. In order to avoid friction saturation, u_c should be limited. Considering the relationship between u_c and $\tilde{S}_i$ (see Eq. 4.20), $\tilde{S}_i$ should be limited. Choosing $\tilde{S}_i$ as the control signals, by combining Eq. 4.19 - Eq. 4.21, the path-tracking control for 4WD2WS EV is transferred into a state regulation problem subject to input constraints. Solving this control problem lies on designing a feedback controller which can stabilize the vehicle such that the outputs of the closed-loop system can track the reference signals.

Based on Eq. 4.20, choosing $\tilde{S}_i$ as the control signals,

$$\begin{bmatrix} u_i \\ u_{\delta i} \end{bmatrix} = \tilde{S}_i = \begin{bmatrix} \tilde{S}_{Li} \\ \tilde{S}_{Si} \end{bmatrix} \tag{4.30}$$

the wheel torque T_i and wheel steering δ_i are derived as

$$\begin{bmatrix} T_i \\ \delta_i \end{bmatrix} = \begin{bmatrix} \tilde{r}_e f_{zsi} \tilde{k} & 0 \\ 0 & 1 \end{bmatrix} \left(\begin{bmatrix} 0 \\ \beta + \frac{l_i \gamma}{\nu_0} \end{bmatrix} + \begin{bmatrix} u_i \\ u_{\delta i} \end{bmatrix} \right) \tag{4.31}$$

where $\tilde{r_e}$, $\tilde{k}$ are the estimated effective radius, slop of Eq. 4.21.

Assumption 4.1. *Let us assume that faults happen after the system has achieved its original tracking objective.*

Let us consider the same type of faults as in Chapter 3, a traction engine actuator fault with a fault gain $0 \leq f_i \leq 1$. Such fault can make the actual applied torques as

$$T_{fi} = f_i T_i \tag{4.32}$$

where $f_i = 1$ presents no fault situation, $f_i < 1$ the loss of effectiveness while $f_i = 0$ the complete failure. Therefore, combining Eq. 4.31 with Eq. 4.32, the

actual (T_i , δ_i) are derived as

$$\begin{bmatrix} T_i \\ \delta_i \end{bmatrix} = \begin{bmatrix} \tilde{r}_e f_{zsi} \tilde{k} f_i & 0 \\ 0 & 1 \end{bmatrix} \left(\begin{bmatrix} 0 \\ \beta + \frac{l_i \gamma}{\nu_0} \end{bmatrix} + \begin{bmatrix} u_i \\ u_{\delta i} \end{bmatrix} \right) \tag{4.33}$$

Fig. 4.4 shows the complete control scheme.

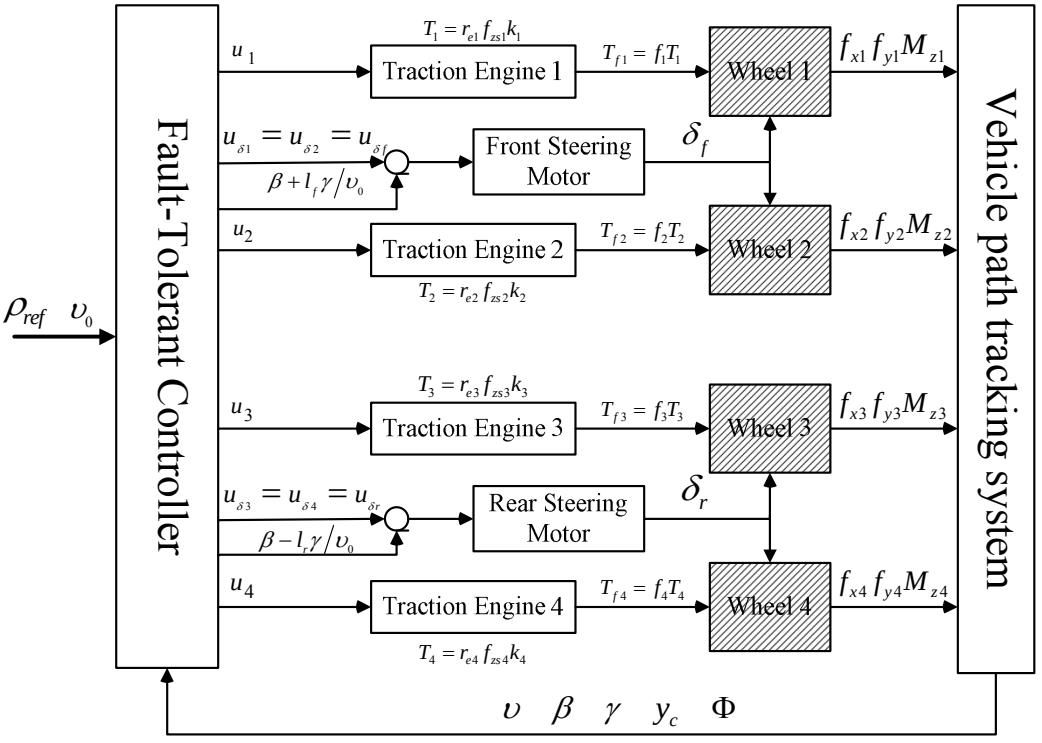

FIGURE 4.4: The Complete Control Scheme

Since the front and rear wheels on the same side have the same effect on vehicle's yaw and longitudinal motions, the torque mass can be distributed according to the vehicle's gravity center, or by a certain percentage based on optimal control. Here, we simply fix $u_1 = u_3 = u_l$, $u_2 = u_4 = u_r$. Based on the vehicle's structure, obviously we have $u_{\delta 1} = u_{\delta 2} = u_{\delta f}$, $u_{\delta 3} = u_{\delta 4} = u_{\delta r}$.

Let us substitute Eq. 4.33 into Eq. 4.29 with the assumption that all four wheels have the same radius, attenuation factor and initial slop, and let $\tilde{k}_s$ be the estimated attenuation factor, then the system can be represented as

$$\begin{aligned} \dot{x} &= Ax + B_f(I_4 + \Delta_b)u + d \\ &= Ax + BF(I_4 + \Delta_b)u + d \end{aligned} \tag{4.34}$$

where the matrices in Eq. 4.34 are defined as

$$A = \begin{bmatrix} -\frac{2\sigma_{aero}\nu_0}{m} & 0 & 0 & 0 & 0 \\ 0 & \frac{\sigma_{aero}\nu_0}{m} & -1 & 0 & 0 \\ 0 & 0 & 0 & 0 & 0 \\ 0 & 0 & 0 & 0 & -\nu_0 \\ 0 & \frac{\sigma_{aero}\nu_0}{m} & 0 & 0 & 0 \end{bmatrix} u = \begin{bmatrix} u_l \\ u_{\delta f} \\ u_r \\ u_{\delta r} \end{bmatrix}$$

$$d = \begin{bmatrix} -\frac{\sigma_{aero}\nu_0^2}{m} \\ 0 \\ 0 \\ 0 \\ -\nu_0\rho_{ref} \end{bmatrix} F = \begin{bmatrix} \frac{f_{zs1}f_1+f_{zs3}f_3}{f_{zs1}+f_{zs3}} & 0 & 0 & 0 \\ 0 & 1 & 0 & 0 \\ 0 & 0 & \frac{f_{zs2}f_2+f_{zs4}f_4}{f_{zs2}+f_{zs4}} & 0 \\ 0 & 0 & 0 & 1 \end{bmatrix}$$

$$B = \begin{bmatrix} \frac{(f_{zs1}+f_{zs3})\tilde{k}}{m} & 0 & \frac{(f_{zs2}+f_{zs4})\tilde{k}}{m} & 0 \\ 0 & \frac{\tilde{k_s}(f_{zs1}+f_{zs2})\tilde{k}}{m\nu_0} & 0 & \frac{\tilde{k_s}(f_{zs3}+f_{zs4})\tilde{k}}{m\nu_0} \\ \frac{-L_d(f_{zs1}+f_{zs3})\tilde{k}}{J_z} & \frac{L_f\tilde{k_s}(f_{zs1}+f_{zs2})\tilde{k}}{J_z} & \frac{L_d(f_{zs2}+f_{zs4})\tilde{k}}{J_z} & \frac{-L_r\tilde{k_s}(f_{zs3}+f_{zs4})\tilde{k}}{J_z} \\ 0 & 0 & 0 & 0 \\ 0 & \frac{\tilde{k_s}(f_{zs1}+f_{zs2})\tilde{k}}{m\nu_0} & 0 & \frac{\tilde{k_s}(f_{zs3}+f_{zs4})\tilde{k}}{m\nu_0} \end{bmatrix}$$

$$\Delta_b = diag\{\frac{(\tilde{r_e}-r_e)}{r_e}, \frac{(k_sk-\tilde{k_s}\tilde{k})}{\tilde{k_s}\tilde{k}}, \frac{(\tilde{r_e}-r_e)}{r_e}, \frac{(k_sk-\tilde{k_s}\tilde{k})}{\tilde{k_s}\tilde{k}}\}$$

and $(\tilde{r_e}, \tilde{k_s}, \tilde{k})$ are chosen to satisfy

$$\tilde{r_e}\tilde{k} \leq r_ek, \quad \tilde{k_s}\tilde{k} \leq k_sk, \quad \tilde{r_e} \geq r_e \tag{4.35}$$

to make Δ_b positive or semi-positive [134].

As mentioned before, the wheel slip should be limited to avoid friction saturation, therefore the following assumption is made.

Assumption 4.2. *Let us assume that the control signals of the motor's wheels are limited, that is,*

$$|u_i| \leq u_{max} \quad and \quad |u_{\delta i}| \leq u_{max} \quad i = 1, 2, 3, 4 \tag{4.36}$$

where u_{max} which is related to the physic of each tire is supposed to be known, the chosen criterion of u_{max} has been explained in Section 4.2 (see Eq. 4.14).

With the chosen k working points in Eq. 4.22, based on Eq. 4.34, the system model working at different points can be represented as

$$\dot{x} = A_k x + B_k F(I_4 + \Delta_b)u + d_k \tag{4.37}$$

where A_k, B_k, d_k are corresponding appropriate matrices with (υ_k, ρ_{ref}).

As mentioned above, the original nonlinear vehicle system can be locally stabilized by using the same control scheme with the reduced linear system since the control input (T_i, δ_i) can stabilize the linearized system and the magnitude of $\tilde{S}_i$ is ensured to stay below a prescribed constraint. In order to guarantee the linearization condition and to to achieve the path tracking mission, a fault-tolerant control scheme has to be designed for system 4.34.

4.5 Fault-tolerant Control Scheme Design

Fig. 4.5 presents the flow chart of the proposed FTC methodology. Without fault, the developed passive fault-tolerant controller (PFTC) can achieve the control requirements. After faults happen, if the system's performance degrades over a given threshold, the input reference will be adjusted and an active fault diagnosis (AFD) approach will be implemented to explicitly localize the faulty wheel and to estimate its control gain. The designed PFTC can guarantee the system's stability during the activation of AFD. Then after obtaining the fault information, an accommodated controller (a new PFTC) is applied to recover the degraded performance caused by faults. Each part of the proposed fault-tolerant control scheme will be described in the remainder of this section.

4.5.1 Passive fault-tolerant control design

The control objective is to track a path of curvature ρ_{ref} with a constant speed υ_0, i.e., $x_d = [\partial\upsilon_d \ \beta_d \ \gamma_d \ y_{cd} \ \phi_d]^T = [0 \ 0 \ \upsilon_0\rho_{ref} \ 0 \ 0]^T$. For the steady states above, when

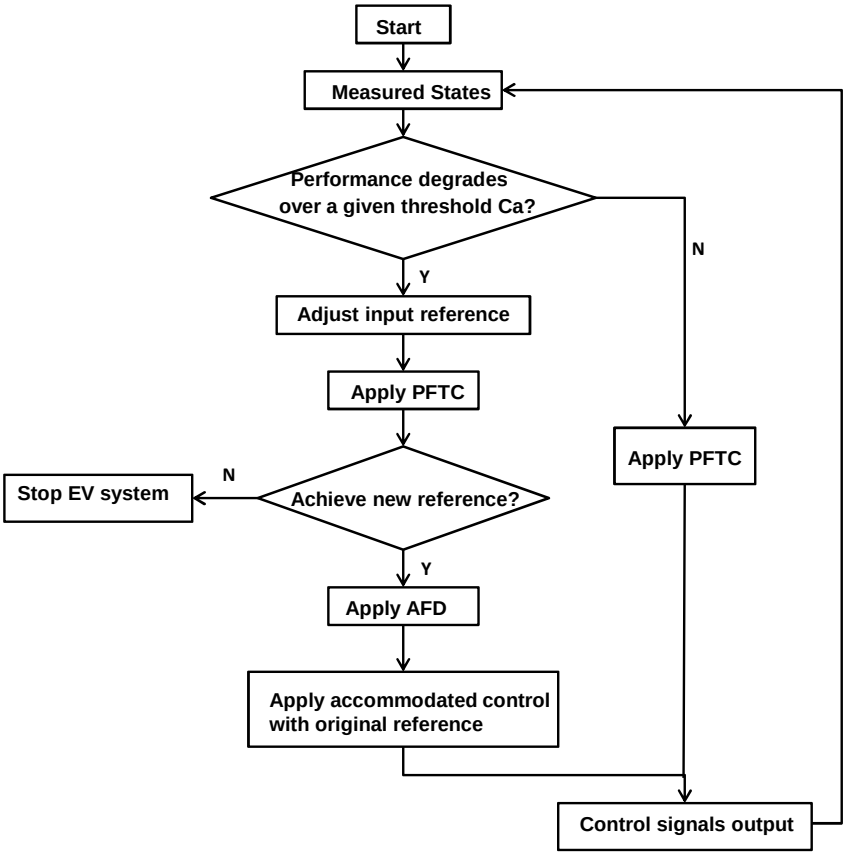

FIGURE 4.5: Flow Chart of the Proposed FTC Methodology

applying the control, we can have the constant solution Γ for $Ax_d + B\Gamma + d = 0$, it yields:

$$\begin{cases} \frac{(f_{zs1}+f_{zs3})\tilde{k}\Gamma_1}{m} + \frac{(f_{zs2}+f_{zs4})\tilde{k}\Gamma_3}{m} - \frac{\sigma_{aero}\nu_0^2}{m} = 0 \\ \frac{\tilde{k_s}(f_{zs1}+f_{zs2})\tilde{k}\Gamma_2}{m\nu_0} + \frac{\tilde{k_s}(f_{zs3}+f_{zs4})\tilde{k}\Gamma_4}{m\nu_0} - \nu_0\rho_{ref} = 0 \\ -\frac{l_d(f_{zs1}+f_{zs3})\tilde{k}\Gamma_1}{J_z} + \frac{l_f\tilde{k_s}(f_{zs1}+f_{zs2})\tilde{k}\Gamma_2}{J_z} \\ +\frac{l_d(f_{zs2}+f_{zs4})\tilde{k}\Gamma_3}{J_z} - \frac{l_r\tilde{k_s}(f_{zs3}+f_{zs4})\tilde{k}\Gamma_4}{J_z} = 0 \end{cases} \tag{4.38}$$

with

$$\begin{cases} 2\tilde{k}\Gamma_1(f_{zs1} + f_{zs3}) = \sigma_{aero}\nu_0^2 \\ 2\tilde{k}\Gamma_3(f_{zs2} + f_{zs4}) = \sigma_{aero}\nu_0^2 \\ \Gamma_2 = \Gamma_4 = m\nu_0^2\rho_{ref}/\sum_{i=1}^{4} f_{zsi}\tilde{k}\tilde{k_s} \end{cases} \tag{4.39}$$

With considering faults, the related part in Eq. 4.39 turns to

$$\begin{cases} 2\tilde{k}\Gamma_1(f_{zs1}f_1 + f_{zs3}f_3) = \sigma_{aero}\nu_0^2 \\ 2\tilde{k}\Gamma_3(f_{zs2}f_2 + f_{zs4}f_4) = \sigma_{aero}\nu_0^2 \end{cases} \tag{4.40}$$

It should be noted that to achieve a cornering motion in a constant speed v_0 with curvature ρ_{ref}, one should have as in [133] [134]

$$u_{max} > \sigma = \max\{\Gamma_1, \Gamma_3, \Gamma_2, \Gamma_4\} \tag{4.41}$$

Let define $e = x - x_d$, the dynamical error equation for system 4.34 can be obtained as

$$\dot{e} = Ae + B[(I_4 + \Delta_b)Fu - \Gamma] \tag{4.42}$$

Introducing the integral compensation $z = [z_1 \quad z_2 \quad z_3]^T$ with $\dot{z} = [\partial v \quad \beta \quad y_c]^T$ to eliminate steady-state error for healthy system [134], we can get the following augmented system

$$\dot{\eta} = \tilde{A}\eta + \tilde{B}[(I_4 + \Delta_b)Fu - \Gamma] \tag{4.43}$$

where

$$\eta = \begin{bmatrix} e \\ z \end{bmatrix} \quad \tilde{A} = \begin{bmatrix} A & 0_{5\times3} \\ C & 0_{3\times3} \end{bmatrix}, \tilde{B} = \begin{bmatrix} B \\ 0_{3\times4} \end{bmatrix} \quad C = \begin{bmatrix} 1 & 0 & 0 & 0 & 0 \\ 0 & 1 & 0 & 0 & 0 \\ 0 & 0 & 0 & 1 & 0 \end{bmatrix}$$

and $(\tilde{A}, \tilde{B})$ is controllable.

For Eq. 4.43, a passive fault-tolerant controller is designed similar to the low-high gain control in Chapter 2:

$$u = -u_{max} S_{ball}(u_{max}^{-1} \gamma_H \tilde{B}' P \eta) \tag{4.44}$$

where γ_H is a chosen parameter, $P = P' > 0_{8\times8}$, S_{ball} is a unit-ball saturation function as

$$S_{ball}(z) = \begin{cases} z & \|z\|_2 \leq 1 \\ z/(\|z\|_2) & \|z\|_2 > 1 \end{cases} \quad z \in \mathcal{R}^2$$

Theorem 4.1. *Let P be a positive symmetric matrix which is the solution of the following Riccati equation:*

$$P\tilde{A} + \tilde{A}^T P - P\tilde{B}\tilde{B}'P + \varepsilon I_8 = 0 \tag{4.45}$$

Define $\tilde{\sigma} = \sigma/u_{max}$ *(*σ *see Eq. 4.41). For a given* γ_H *in Eq. 4.44, the designed controller 4.44 can guarantee the local stabilization of the path tracking system with its states in* $L_v(\mu)$ *under condition that the happened fault satisfies*

$$\begin{cases} \frac{\tilde{\sigma}^2}{\hbar\sqrt{\lambda_{min}\gamma_H - 1}} P < \varepsilon I_8 + P\tilde{B}\tilde{B}'P \\ \frac{\hbar}{2\sqrt{\lambda_{min}\gamma_H - 1}} < \frac{(\lambda_{min} - \tilde{\sigma})^2}{\lambda_{max}(\tilde{B}'P\tilde{B})} \end{cases}$$

where λ_{min} *is the minimal eigenvalue related to the fault matrix* F *(see Eq. 4.34),* $\hbar$ *is an auxiliary parameter to adjust* γ_H *and* λ_{min}*, and*

$$L_v(\mu) = \{\eta : \mu_1 \leq \eta^T P \eta \leq \mu_2\} \tag{4.46}$$

with $\mu_1 = 2u_{max}^2\hbar/\sqrt{\lambda_{min}\gamma_H - 1}, \mu_2 = 4(\lambda_{min} - \tilde{\sigma})^2 u_{max}^2/\lambda_{max}(\tilde{B}'P\tilde{B})$.

Proof: Choose a Lyapunov function $V = \eta^T P \eta$. Computing its derivative with Eq. 4.43 - Eq. 4.45, one gets

$$\dot{V} = \eta^T(\tilde{A}^T P + P\tilde{A})\eta + 2\eta^T P\tilde{B}(I_4 + \Delta_b)Fu - 2\Gamma^T\tilde{B}^T P\eta$$

Define $\dot{V}_\Delta = 2\eta^T P\tilde{B}\Delta_b F u$, since Δ_b is chosen to be positive or semi-positive (see Eq. 4.35), it can be confirmed that $\dot{V}_\Delta \leq 0$.

Then by defining $u_L = \tilde{B}'P\eta$, one has

$$\dot{V} = \dot{V}_\Delta - \varepsilon\eta^T\eta - u_L'u_L + 2\sum_{j=1}^{4}(u_{Lj}^2 - u_{Lj}\Gamma_j - \lambda_{fj}u_{max}u_{Lj}S_{ball}(u_{max}^{-1}\gamma_H u_{Lj}))$$

In the unsaturated region $\Omega_{us} : \{|u_{Lj}| \leq u_{max}/\gamma_H\}$,

$$\begin{aligned} \dot{V} &\leq \dot{V}_\Delta - \varepsilon\eta^T\eta - u_L'u_L + 2\sum_{j=1}^{4}(u_{Lj}^2 - \lambda_{fj}\gamma_H u_{Lj}^2 - u_{Lj}\Gamma_j) \\ &\leq \dot{V}_\Delta - \varepsilon\eta^T\eta - u_L'u_L + 2\sum_{j=1}^{4}\Gamma_j^2/4(\lambda_{fj}\gamma_H - 1) \\ &\leq \dot{V}_\Delta - \frac{\tilde{\sigma}^2}{\hbar\sqrt{\lambda_{min}\gamma_H - 1}}(\eta^T P\eta - \frac{2u_{max}^2\hbar}{\sqrt{\lambda_{min}\gamma_H - 1}}) \end{aligned}$$

In the saturated region $\Omega_s : \{|u_{Lj}| \geq u_{max}/\gamma_H\}$,

$$\begin{aligned}\dot{V}_2 &\leq \dot{V}_\Delta - \varepsilon\eta^T\eta + \sum_{j=1}^{4}(u_{Lj}^2 - 2\lambda_{min}u_{max}|u_{Lj}| + 2|u_{Lj}|\Gamma_j) \\ &\leq \dot{V}_\Delta - \varepsilon\eta^T\eta + \sum_{j=1}^{4}|u_{Lj}|(|u_{Lj}| - 2\lambda_{fj}u_{max} + 2\Gamma_j)\end{aligned}$$

Here, only satisfying

$$|u_{Lj}| \leq 2(\lambda_{fj}u_{max} - \Gamma_j) \tag{4.47}$$

can guarantee the system's stability under inputs saturation.

Therefore, we can conclude that in the region $L_v(\mu)$, the designed controller can guarantee the stability of the faulty system under certain faults. □

To caculate the value of λ_{min}, the following inequalities based on Theorem 4.1 and its proof are given:

$$\begin{cases} \frac{\tilde{\sigma}^2}{\hbar\sqrt{\lambda_{min}\gamma_H - 1}}P < \varepsilon I_8 + P\tilde{B}\tilde{B}'P \\ \frac{\hbar}{2\sqrt{\lambda_{min}\gamma_H - 1}} < \frac{(\lambda_{min} - \tilde{\sigma})^2}{\lambda_{max}(\tilde{B}'P\tilde{B})} \\ \lambda_{min}\gamma_H - 1 > 0 \\ \lambda_{min}u_{max} - \sigma > 0 \end{cases}$$

The last inequality requires that the controller can generate enough control signals for the tracking objective even if the fault happens, as the Assumption 3.1 in Chapter 3.

The first, second and the third inequalities are used to calculate the attraction and performance regions for the tracking system. Let define $\Omega(P, \varrho_0)$ as the attraction region for the nominal system and $\Omega(P, s_0)$ the performance region; and $\Omega(P, \varrho_f)$ as the attraction region for the faulty system and $\Omega(P, s_f)$ the performance region.

For the nominal system, with an appropriate $\hbar_0$ and a given γ_H, we can get

$$\begin{cases} \varrho_0 = 4(1 - \tilde{\sigma})^2 u_{max}^2/\lambda_{max}(\tilde{B}'P\tilde{B}) \\ s_0 = 2u_{max}^2\hbar_0/\sqrt{\gamma_H - 1} \end{cases}$$

Based on Theorem. 4.1, we have $\varrho_f = \mu_2$ and $s_f = \mu_1$ with an appropriate $\hbar_f$ for the faulty system.

Then three cases are discussed:

(1). $\varrho_f \geq s_f > s_0$ under condition that $(\lambda_{min} u_{max} - \sigma > 0)$.

Based on the results in previous chapters, one has that all trajectories starting from $\Omega(P, \varrho_f)$ will enter $\Omega(P, s_f)$ and stay within it. With Assumption 4.1, If $\varrho_f > s_0$, i.e., $\Omega(P, s_0) \subset \Omega(P, \varrho_f)$, all trajectories starting from $\Omega(P, s_0)$ will enter $\Omega(P, s_f)$. Since $\Omega(P, s_0) \subset \Omega(P, s_f)$, the initial states which are already within $\Omega(P, s_0)$ will not change, i.e., the performance degradation caused by the happened fault will be fully compensated.

Denote λ_{min1} the eigenvalue of the fault matrix F in this case. When the fault which is less severe than λ_{min1} happens, the controller can fully recover the degraded performance.

(2). $s_f > \varrho_f \geq s_0$ under condition that $(\lambda_{min} u_{max} - \sigma > 0)$.

In this case, since $\Omega(P, s_0) \subset \Omega(P, \varrho_f)$, the stability of the tracking system can be guaranteed. However, $(s_f > \varrho_f)$ means that when the fault happens, the initial states which are within $\Omega(P, s_0)$ will degrade to $\Omega(P, s_f)$, i.e., the performance is degraded.

Denote λ_{min2} the eigenvalue of the fault matrix F in this case. The minimal value of λ_{min2} is $\lambda_{min2} = \tilde{\sigma} = \sigma / u_{max}$. When the fault which is more severe than λ_{min2} happens, the system's stability will not be guaranteed. If the fault is less severe than λ_{min2}, the faulty system will be stable but with degraded performance.

(3). $\varrho_f < s_0$ with $(\lambda_{min} u_{max} - \sigma < 0)$.

As what was stated in Lemma 2.2 in Chapter 2, the stability of the tracking system, which is not asymptotically null controllable with bounded controls (ANCBC), will not be guaranteed.

Remark 4.1. *The designed controller can only tolerate certain faults, however, faults are unpredictable and unkown. For small faults, the designed fault-tolerant controller can tolerate them and also guarantee the tracking performance. For non small faults, the controller can only guarantee a degraded performance or even*

can not ensure the system's stability. For such cases, as what we have stated in Chapter 3, the reference adjustment technique may be considered.

4.5.2 Reference adjustment technique

The reference adjustment technique (RAT) presented in Chapter 3 is used to avoid input saturation and to guarantee the design condition of the observer which can estimate the fault information. In this chapter, this technique is also used for the same purpose, but an active fault diagnosis method (AFD) is adopted here to replace the observer and to get the fault information. Unlike the observer which works with the system from the beginning, this active fault diagnosis method just works after detecting the faults. And as for its design condition, the input signals should also not to be saturated. Through the above analysis, we can see that two criteria are needed, one is to detect the fault (i.e., to active RAT) and the other is to activate AFD.

Criterion 1: Define P_{det} with four elements P_{detj}, $(j = 1, 2, 3, 4)$, s.t. $P_{detj} = |u_{Lj}|$. Based on Eq. 4.47, when there is no fault, $|u_{Lj}| \leq 2(u_{max} - \Gamma_j)$ can guarantee the system's stability under input constraints. The criterion C_a , the criterion to detect fault and to activate the reference adjustment technique (RAT), can be chosen as

$$C_a = \min_{j=1}^{4}\{|2(u_{max} - \Gamma_j)|\} \tag{4.48}$$

If $P_{detj} > C_a$, the system's stability is destroyed, then the AFD should be used to get the fault information. In order to ensure the implementation of AFD, RAT should be adopted first to avoid input saturation.

Criterion 2: Define P_{afd} with four elements P_{afdj}, $(j = 1, 2, 3, 4)$, s.t. $P_{afdj} = \frac{|u_{Lj}|\gamma_H}{u_{max}} = \frac{|u_j|}{u_{max}}$ (u_j is given by Eq. 4.44). Since k different working points are chosen within D_c^f in Section 4.4, the reference adjustment technique will choose a proper working point X_k to avoid input saturation. It should also make sure that after the AFD is activated, the controller can still compensate the degraded performance. The criterion C_f to activate AFD can be chosen as

$$C_f = K_f \tag{4.49}$$

where $K_f \in (0,1)$ is one chosen parameter.

The choosing process of the reference point is described in Fig. 4.6.

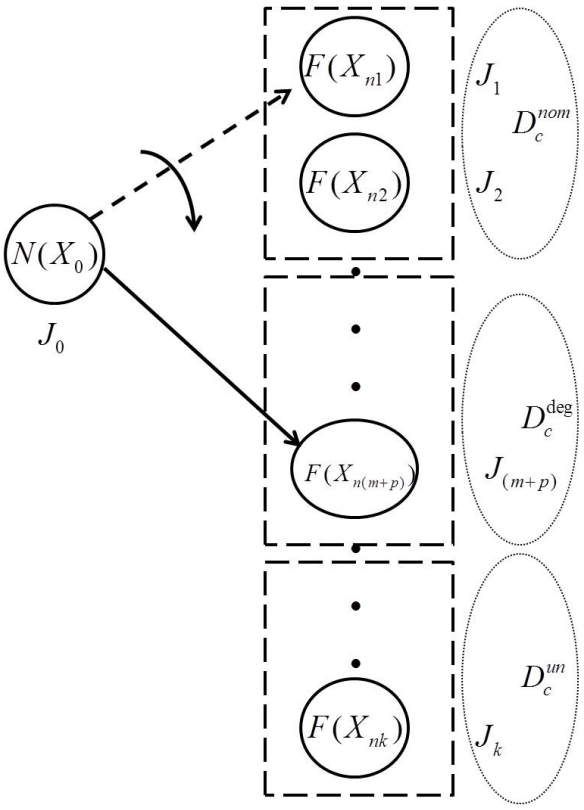

FIGURE 4.6: Reference Adjustment Methodology

The given working points are chosen according to the index J, until one working point X_i with υ_i is found and it satisfies both $P_{detj} < C_a$ and $P_{afdj} \leq C_f$. Then the active fault diagnosis (AFD) can be implemented after.

Until now, two criteria have been mentioned. C_a is chosen as the threshold for P_{det} to reference adjustment technique, C_f the threshold for P_{afd} to activate AFD method.

Remark 4.2. *When $P_{detj} < C_a$ (C_a see Eq. 4.48), the system's stability can be ensured, however the degraded performance may not be recovered. Rather than aiming at tolerating more faults, in order to ensure one specific performance, it is better to pre-select $C_{a\epsilon}$ as $\min_{j=1}^{4}\{|2(\epsilon u_{max} - \Gamma_j)|\}$ ($\epsilon \in [\Gamma_j/u_{max}, 1)$). When $P_{detj} > C_{a\epsilon}$, the reference adjustment technique is implemented.*

Remark 4.3. *Note that even if the last working point is chosen in D_c^{deg}, the system can not achieve this new reference, then the vehicle will be stopped because*

the happened fault is too severe; Another case is when the system can achieve this new reference but P_{afdj} can not satisfy the condition that $P_{afdj} \leq C_f$, then the system will work at this point, but without implementing the AFD.

4.5.3 Active fault diagnosis

The AFD method in [141] consists in actively changing the motor control gain by deliberately multiplying the motor control signal by a positive value to explicitly localize the faulty wheel and estimate its magnitude. Obviously, without obtaining the precise fault information, any change of the motor control gain may lead to actuator saturation and make the AFD method unfeasible. Therefore, in order to implement the AFD method without violating of actuator capability, it is straightforward to modify the reference input so that this problem can be avoided [143], as in Section 4.5.2:

Assume X_i is chosen as the new reference in the reference adjustment methodology with ν_i with ρ_{ref}. Let define $\Psi = diag\{\kappa_1, \kappa_2, \kappa_3, \kappa_4\}$ as the control gain that will multiply the control signals u (see Eq. 4.34) of the 4 traction engines.

Remark 4.4. *The choice of K_f is related to the control gain κ_i $(i = 1, 2, 3, 4)$ which will be injected into the system. Substituting Ψ into the matrix F (see Eq. 4.34), the minimal eigenvalue λ_{min}^{Ψ} of $F(\Psi)$ can be obtained. To make sure that even if κ_i is injected, the control signals are still not saturated, Ψ and K_f should satisfy $\lambda_{min}^{\Psi} > K_f$.*

Then the active fault diagnosis method is applied:

(1) The designed controller u in Eq. 4.44 can maintain the vehicle driving in the desired trajectory. Based on the designed controller and Eq. 4.39, for the healthy system, the following equation holds:

$$(f_{zs1} + f_{zs3})u_{lh} = (f_{zs2} + f_{zs4})u_{rh} = \frac{\sigma_{aero}\nu_0^2}{2\tilde{k}} \tag{4.50}$$

(2) After a fault occurs, if PFTC can maintain the system's stability with an acceptable performance degradation (i.e., $P_{detj} < C_a$), no extra action is needed.

Otherwise, the new input reference should be found and be adopted in order to avoid the control signals reach their limit. If $P_{afdj} \leq C_f$ when one working point X_j is chosen, then the following equation is obtained:

$$(f_{zs1}f_1 + f_{zs3}f_3)u_{lf} = (f_{zs2}f_2 + f_{zs4}f_4)u_{rf} = \frac{\sigma_{aero}\nu_i^2}{2\tilde{k}} \tag{4.51}$$

In these two above equations, the subscripts h, f represent respectively the healthy system and the faulty one.

(3) f_1, f_3, f_2, f_4 are all unknown in these above equations, so virtual faults should be added to obtain another equation to compute these unknown parameters. Let us apply two control gains κ_1, κ_3 such that $\kappa_1 \neq \kappa_3$, one has

$$(\kappa_1 f_{zs1}f_1 + \kappa_3 f_{zs3}f_3)u_{l_{f\kappa}} = (f_{zs2}f_2 + f_{zs4}f_4)u_{r_{f\kappa}} = \frac{\sigma_{aero}\nu_i^2}{2\tilde{k}} \tag{4.52}$$

From Eq. 4.50 - Eq. 4.52, we can get the estimated values $\hat{f}_1$, $\hat{f}_3$ of f_1 and f_3 separately. Based on the same principle, we can also get $\hat{f}_2$, $\hat{f}_4$ of f_2 and f_4 with injecting κ_2 and κ_4 ($\kappa_2 \neq \kappa_4$).

Remark 4.5. *The choice of K_f and κ_i can guarantee the tenability of Eq. 4.52 and the accuracy of the whole AFD. Although in AFD process we multiply the control signals by κ_i, for the designed PFTC, κ_i will be treated as a new actuator fault. Note that this proposed AFD works for multiple faults situations and not only for single fault.*

4.5.4 Control accommodation

When $\hat{f}_1, \hat{f}_2, \hat{f}_3, \hat{f}_4$, the estimation of the fault gains, are obtained, the controller will be accommodated to recover as best performance as possible. The actuator faults occur at t_f which is unknown, the control matrix $\tilde{B}$ is changed to $\tilde{B}_f$. Once $\hat{\tilde{B}}_f$ (the estimation of $\tilde{B}_f$) is identified at $t = t_{fdi} > t_f$ using the AFD method, the control law is accommodated to

$$u = -u_{max}S_{ball}(u_{max}^{-1}\gamma_H \hat{\tilde{B}}_f' P_f \eta) \tag{4.53}$$

and applied at $t = t_{ftc} > t_{fdi}$, where P_f is the solution of

$$P_f\tilde{A} + \tilde{A}^T P_f - P_f\hat{\tilde{B}}_f\hat{\tilde{B}}'_f P_f + \varepsilon I_8 = 0 \tag{4.54}$$

Note that the reference should also be checked to verify the condition Eq. 4.41. If the original objective could not be achieved by the new controller, one appropriate reference from D^f_{nom} and D^f_{deg} should be chosen as the new reference.

Four time periods have to be considered [145], see Fig. 4.7.

$[0, t_f)$: The EV system is controlled by PFTC;

$[t_f, t_{fdi}]$: After the faults happen, if the system performance is over the given threshold, RAT and AFD methods are implemented to get the fault information, the system is still controlled by controller Eq. 4.44;

$[t_{fdi}, t_{ftc})$: Obtaining the fault information, the Riccati equation Eq. 4.54 is solved to get a new controller and an appropriate reference;

$[t_{ftc}, \infty)$: The system is controlled with the accommodated controller Eq. 4.53.

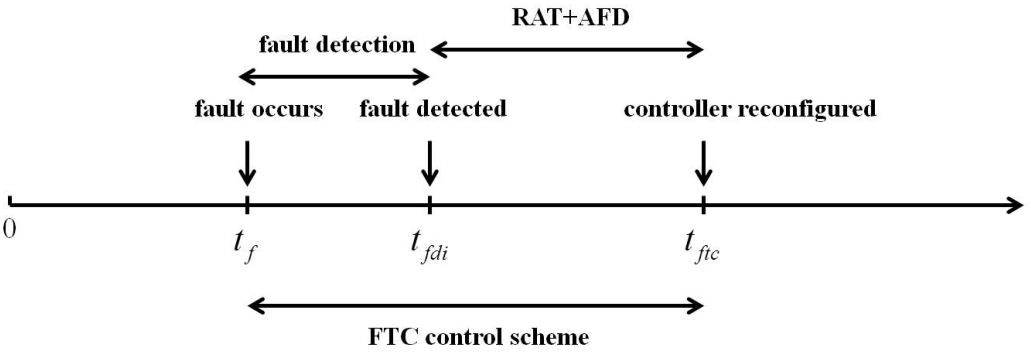

FIGURE 4.7: FTC Scheme in Time Map

Remark 4.6. *The accommodated controller Eq. 4.53 may not be able to fully compensate the degraded performance, that is to say, if some faults happen, only by simply changing* $\tilde{B}_f{}'$ *and* P_f *may be not enough. Here, we simply give one choice of designing the accommodated controller. For the 4WD EV system, a typical over-actuated system, a control allocation method could also be used as in [139] [140].*

4.6 Simulations

The proposed FTC scheme is applied by using MATLAB software and **simulating the original nonlinear EV system**.

The parameters in $\mu_{Res}(\|S_i\|_2, \chi)$ are chosen as: $\mu_0 = 28.6, a = 35, b = 1$. In Fig. 4.8, the black line is described by the following equation

$$\mu_{Res}(\|S_i\|) = \mu_{Res}^{sat}[1 - e^{-c\|S_i\|}]$$

where $c = 50$. From Fig. 4.8, we can get $\mu_{Res}^{sat} = 0.757$ (see the red dot line), choosing $\theta = 0.9999$ in Eq. 4.14, $\|S_i\|_2$ can be seen in Fig. 4.9.

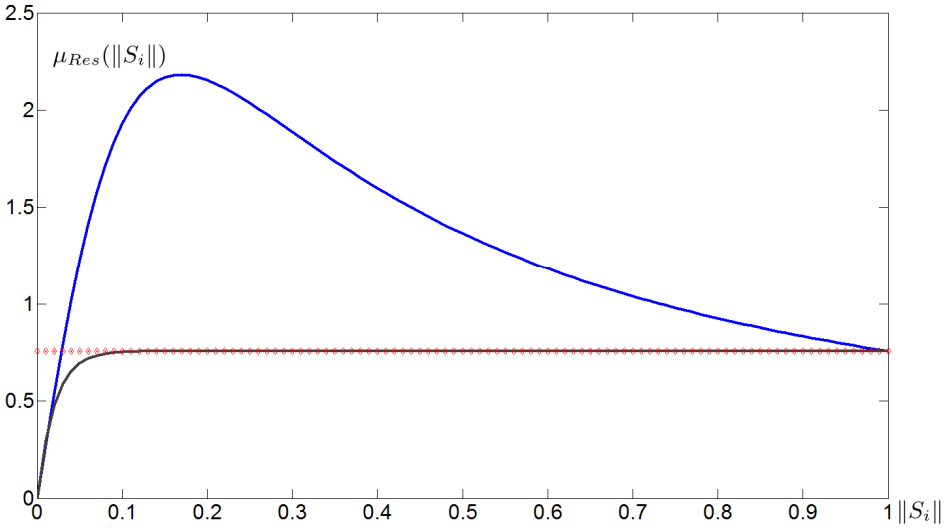

FIGURE 4.8: The Friction Coefficient

The parameters and the reference path of the studied EV are given in Table. 4.1. As $\|\dot{V}_{iref(\tau)}\|$ would be roughly equal to the acceleration of the vehicle $v_0^2\rho_{ref} = 0.5625$, from Fig. 4.9, the constraint of $\|S_i\|_2$ should be chosen as 0.01, i.e., $u_{max} = 0.01$.

The vehicle starts with the initial states: $\nu(0) = 14.8\, m/s, \beta(0) = 0\, rad, \gamma(0) = 0.0375\, rad/s, y_c(0) = 0\, m, \phi(0) = 0\, rad, \omega_i(0) = 40\, rad/s$. The aerodynamical coefficient σ_{aero} is $0.4\, kg/m$. In order to satisfy Eq. 4.35, we choose $\tilde{r_e} = 0.37, \tilde{k_s} =$

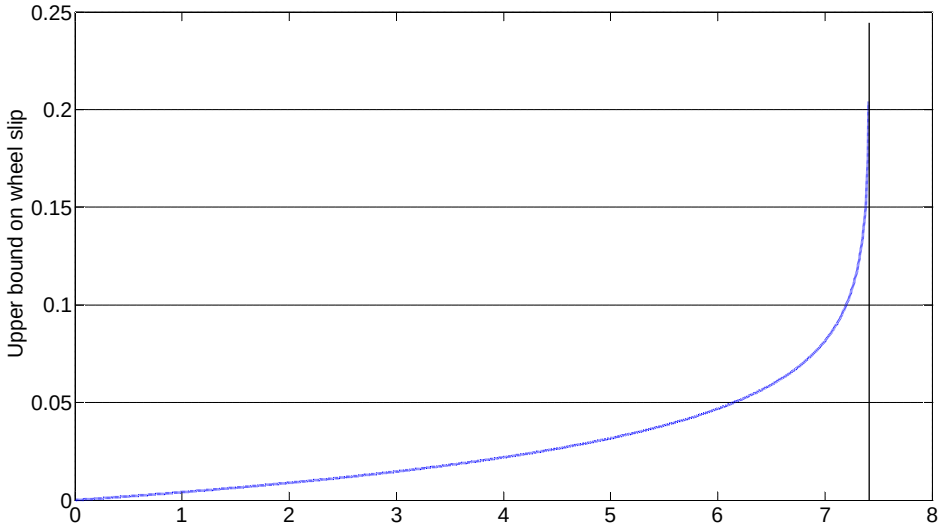

FIGURE 4.9: Upper Bound on Wheel Slip for One Given Road Condition

TABLE 4.1: Parameters of the EV and the reference path

Parameter	Value
$m(\mathrm{kg})$	350
$l_f(m)$	0.401
$l_r(m)$	0.802
$l_d(m)$	0.605
$r_{ei}(m)$	0.350
$I_{\omega i}(kg \cdot m^2)$	0.7
$J_z(kgm^2)$	82
$\upsilon_0(m/s)$	15
$\rho_{ref}(m^{-1})$	1/400
k_s	0.9
k	28.6
K_{fr}	1144.5
K_{rr}	2289

$0.87, \tilde{k} = 28.3$ to get

$$\Delta_b = diag\{0.0571, 0.0454, 0.0571, 0.0454\}$$

The other matrices in Eq. 4.43 can be obtained as

$$A = \begin{bmatrix} -0.0343 & 0 & 0 & 0 & 0 \\ 0 & 0.0171 & -1 & 0 & 0 \\ 0 & 0 & 0 & 0 & 0 \\ 0 & 0 & 0 & 0 & -15 \\ 0 & 0.0171 & 0 & 0 & 0 \end{bmatrix}, d = \begin{bmatrix} -0.2571 \\ 0 \\ 0 \\ 0 \\ -0.0375 \end{bmatrix}$$

$$B = \begin{bmatrix} 138.8115 & 0 & 138.8115 & 0 \\ 0 & 10.7348 & 0 & 5.3674 \\ -358.4553 & 275.6018 & 358.4553 & -275.6018 \\ 0 & 0 & 0 & 0 \\ 0 & 10.7348 & 0 & 5.3674 \end{bmatrix}$$

For the original reference X_0 with $\nu_0 = 15\, m/s$, choosing $\varepsilon = 4.26 \times 10^{-3}$ and $\gamma_H = 25$, P can be obtained from Eq. 4.12 by using MATLAB function *care*.

$$P = 10^{-3}\times$$

$$\begin{bmatrix} 0.3567 & 0 & 0 & 0 & 0 & 0.3325 & 0 & 0 \\ 0 & 7.6848 & -0.1810 & 0.4765 & -7,1706 & 0 & 4.4331 & 0.1932 \\ 0 & -0.1810 & 0.1068 & 0.0139 & 0.0389 & 0 & -0.1032 & 0.0129 \\ 0 & 0.4765 & 0.0139 & 2.7048 & -7.7840 & 0 & 0.3846 & 2.1638 \\ 0 & -7.1706 & 0.0389 & -7.7840 & 43.4064 & 0 & -4.0717 & -5.3533 \\ 0.3325 & 0 & 0 & 0 & 0 & 4.5804 & 0 & 0 \\ 0 & 4.4331 & -0.01032 & 0.3846 & -4.0717 & 0 & 7.4760 & 0.1820 \\ 0 & 0.1932 & 0.0129 & 2.1638 & -5.3533 & 0 & 0.1820 & 6.0456 \end{bmatrix}$$

Based on Theorem 4.1, one gets $\varrho_0 = 7.58 \times 10^{-6}$.

Based on Condition Eq. 4.28, 11 working points are chosen: the vehicle tracking along a path of curvature $\rho_{ref} = 1/400$ with different speeds $\upsilon_{(k)}$. By choosing $C_a = \min_{j=1}^{4}\{|2(u_{max} - \Gamma_j)|\}$ and $K_f = 0.7$ the following table 4.2 is given with the chosen working points and their corresponding criteria $C_{a(k)}$ and $C_{f(k)}$:

TABLE 4.2: Working points and the corresponding criterions

$*$	$v_{n(k)}\ (m/s)$	$C_{a(k)}$	$C_{f(k)}$
v_0	15	0.0181	0.7
v_1	14.64	0.0182	0.7
v_2	14.28	0.0183	0.7
v_3	13.92	0.0184	0.7
v_4	13.56	0.0185	0.7
v_5	13.2	0.0186	0.7
v_6	12.84	0.0186	0.7
v_7	12.48	0.0187	0.7
v_8	12.11	0.0188	0.7
v_9	11.74	0.0189	0.7
v_{10}	11.37	0.0189	0.7
v_{11}	11	0.0190	0.7

where X_i with v_i, $(i = 0, 1, ..., 8)$ belong to D_c^{nom} and X_j with v_j, $(j = 9, 10, 11)$ belong to D_c^{deg}. Considering the existence of a time-delay of FDD in real system, we choose $C_a = 0.02$ for all working points.

The faults considered here are traction engines' faults. Two cases will be simulated to illustrate the proposed fault-tolerant control scheme in Section 4.5.

1. Case 1: The nominal gain of each engine is set during 3 seconds, then faults are introduced: the gain of front-left is reduced to $f_1 = 0.1$, and rear-left to $f_3 = 0.4$; the gain of front-right is reduced to $f_2 = 0.5$, and rear-right to $f_4 = 0.5$. The simulations results are shown in Fig. 4.10 - Fig. 4.16.

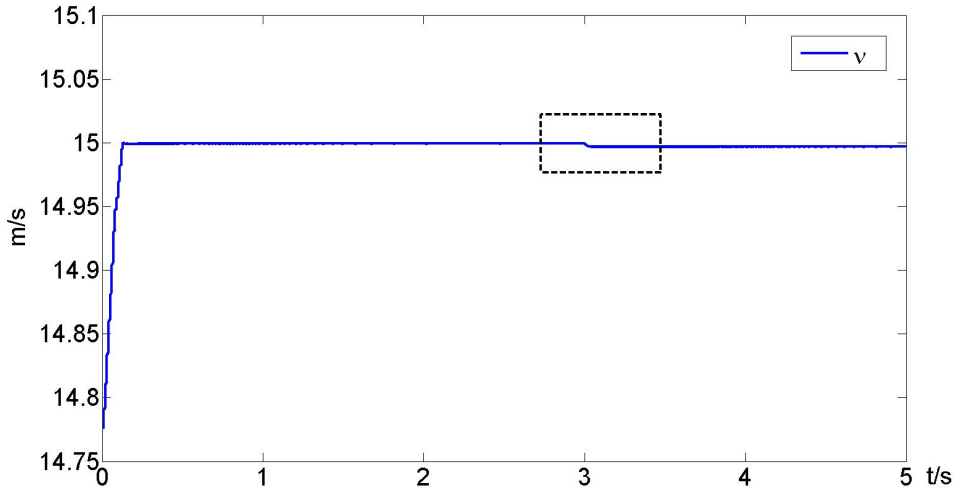

FIGURE 4.10: Speed of Vehicle Mass Centre ν : Case 1

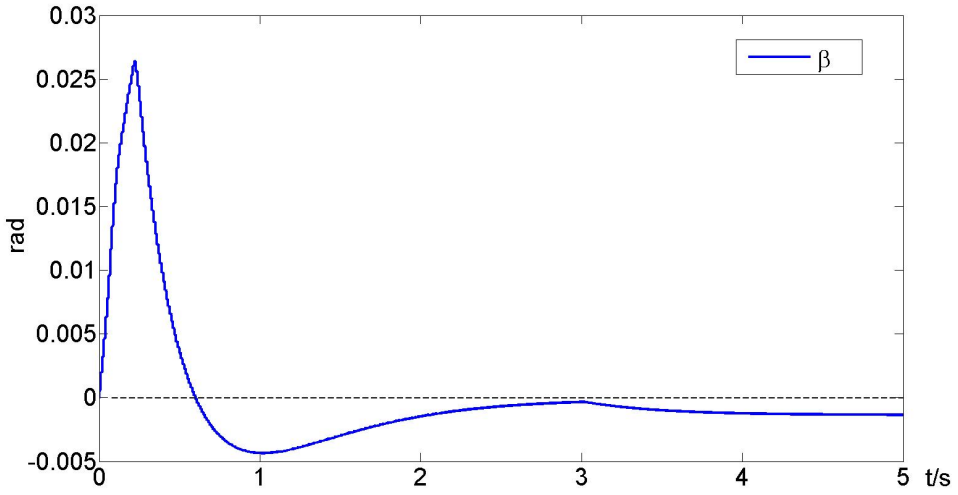

FIGURE 4.11: Side Slip Angle β : Case 1

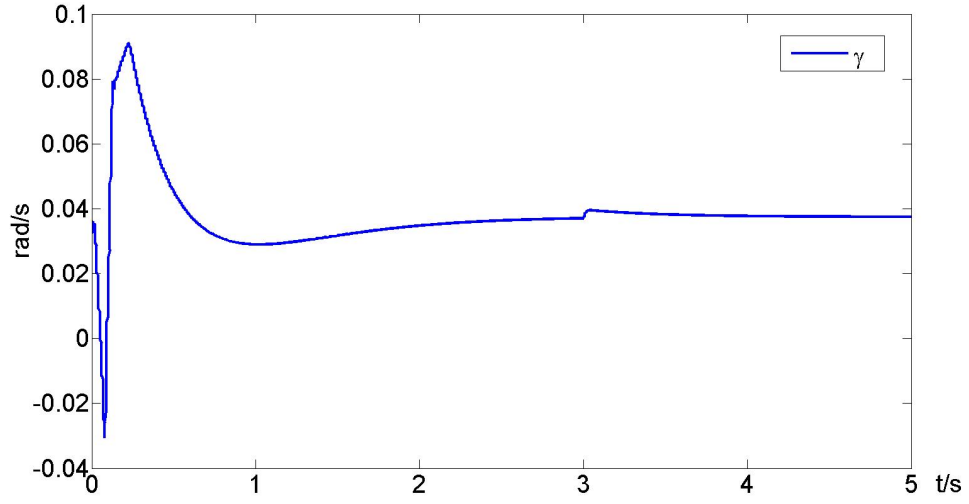

FIGURE 4.12: Yaw Rate γ : Case 1

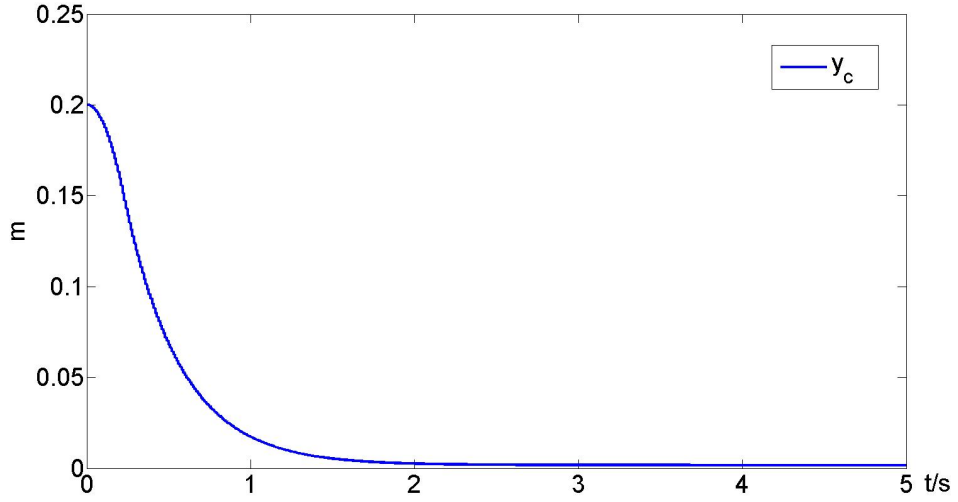

FIGURE 4.13: Distance y_c : Case 1

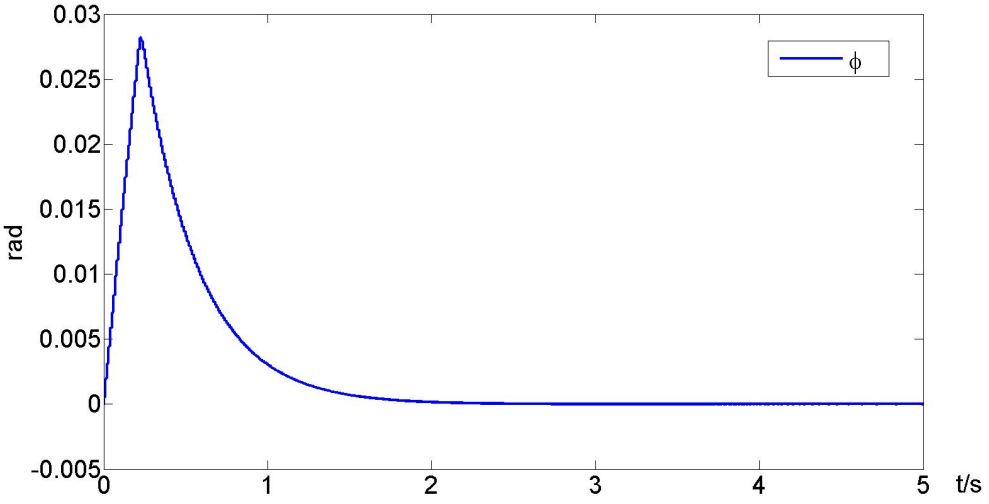

FIGURE 4.14: Angle ϕ : Case 1

From Fig. 4.10 - Fig. 4.14, we can see that although the performance of ν and β degrades because of the happened faults, the stability of the whole system can be guaranteed, each element of P_{detj} (see Fig. 4.15) does not exceed the set threshold C_a. RAT and AFD methods are not needed to be implemented. The control signals are shown in Fig. 4.16.

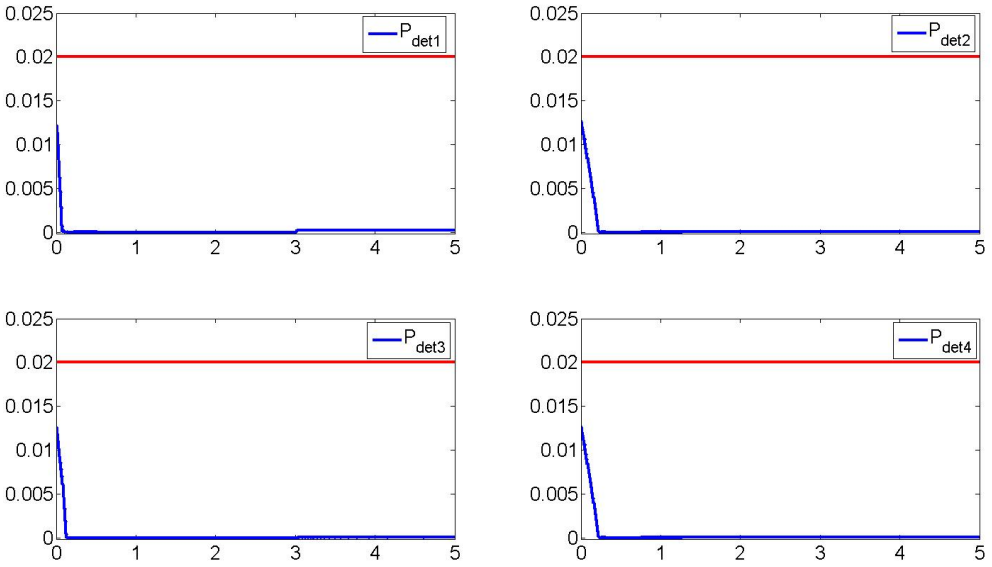

FIGURE 4.15: Criterion P_{detj} and C_a: Case 1

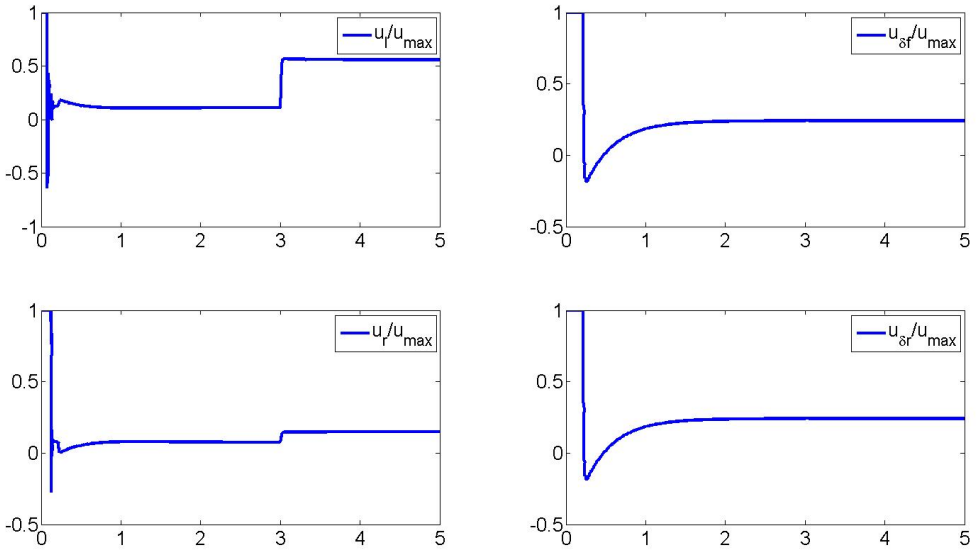

FIGURE 4.16: u/u_{max} : Case 1

2. Case 2: The nominal gain of each engine is set during 3 seconds, then faults are introduced: the gain of front-left is reduced to $f_1 = 0.1$, and rear-left to $f_3 = 0.1$; the gain of front-right is reduced to $f_2 = 0.5$, and rear-right to $f_3 = 0.5$.

From Fig. 4.17 - Fig. 4.21, we can see that before $3s$, the system with the proposed controller is stable and shows good performance. After faults happen, P_{det1} exceeds the threshold at $3.5s$, see Fig. 4.22. Then reference adjustment technique should be adopted to find a new reference from the given working points (see Table. 4.2).

Fig. 4.17 - Fig. 4.23 show the whole reference adjustment process. We extract P_{det1} and P_{afd1} from Fig. 4.22 and Fig. 4.23 to analyse the process of choosing different references. Since $P_{afd1} = \frac{|u_1|}{u_{max}}$, we will use $|u_1| = u_{max} P_{afdj}$ here to replace P_{afd1}. The details of the reference adjustment process are shown in Fig. 4.24.

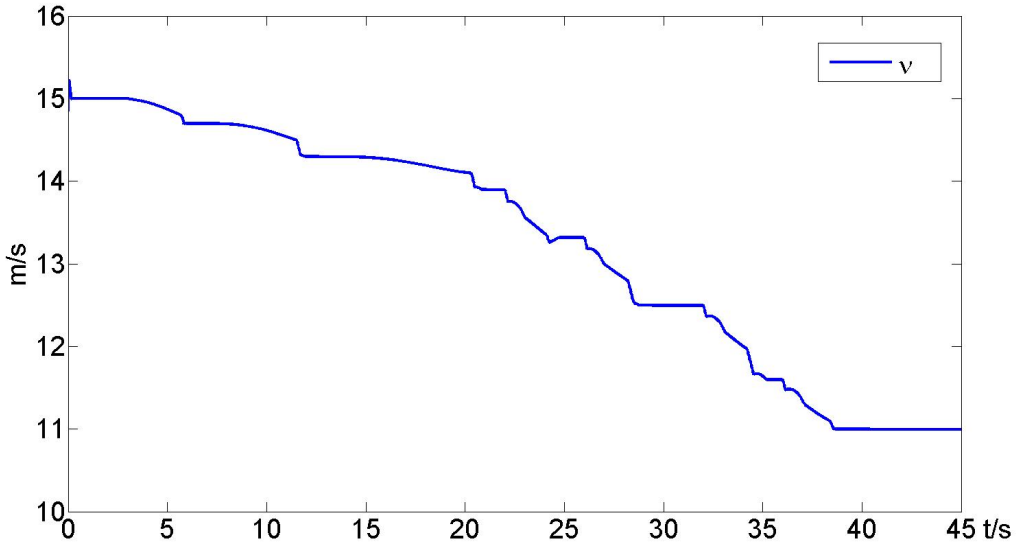

FIGURE 4.17: Speed of Vehicle Mass Centre ν : Case 2

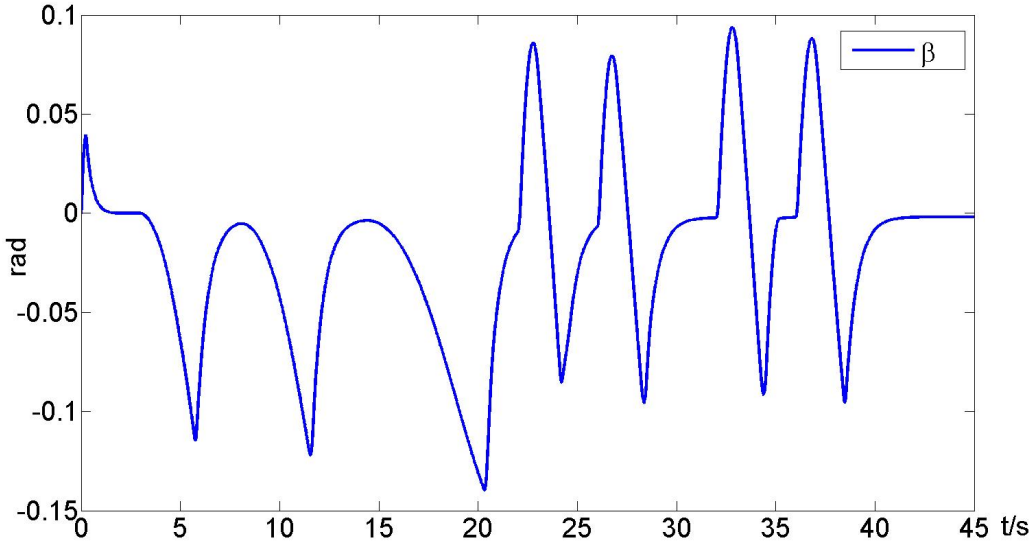

FIGURE 4.18: Side Slip Angle β : Case 2

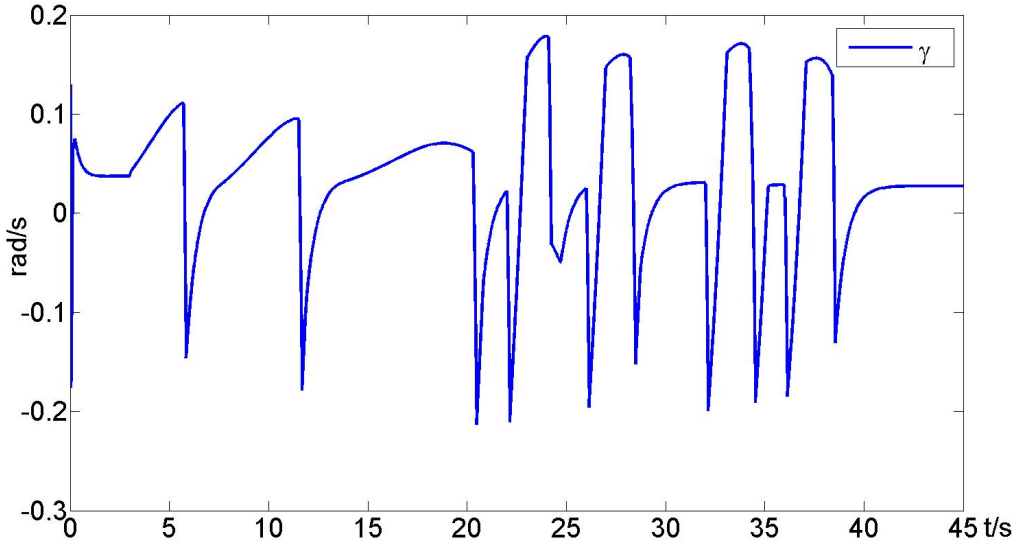

FIGURE 4.19: Yaw Rate γ : Case 2

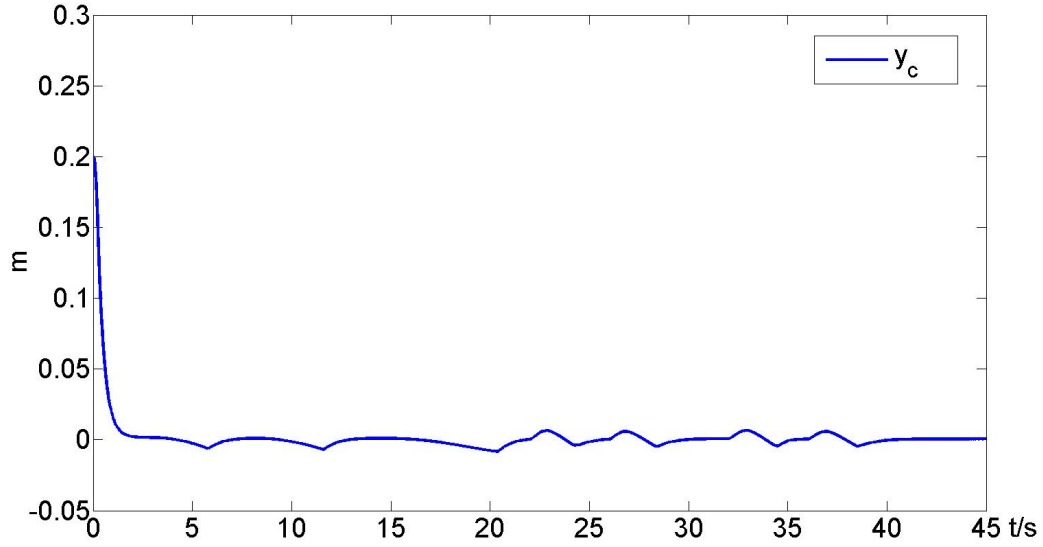

FIGURE 4.20: Distance y_c : Case 2

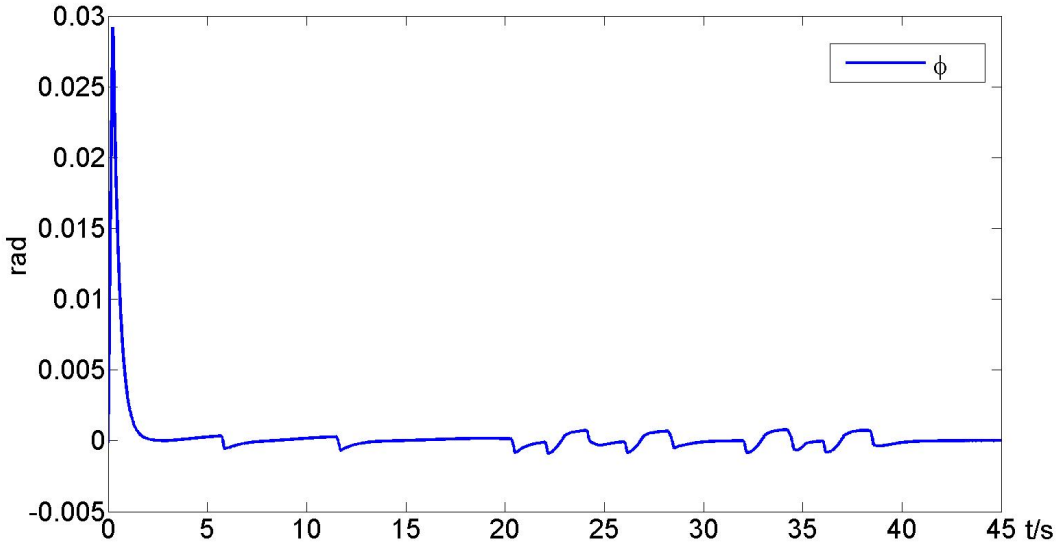

FIGURE 4.21: Angle ϕ : Case 2

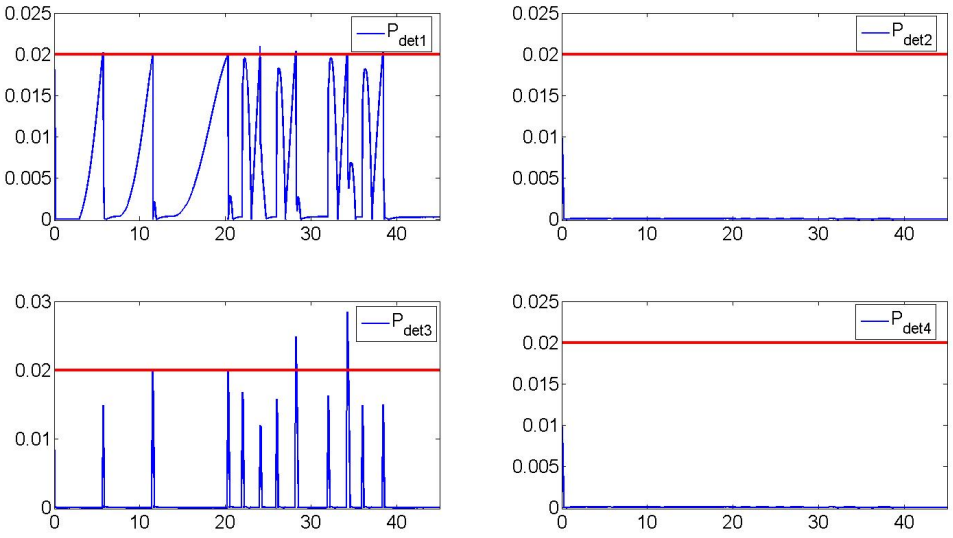

FIGURE 4.22: Criterion P_{detj} and C_a: Case 2

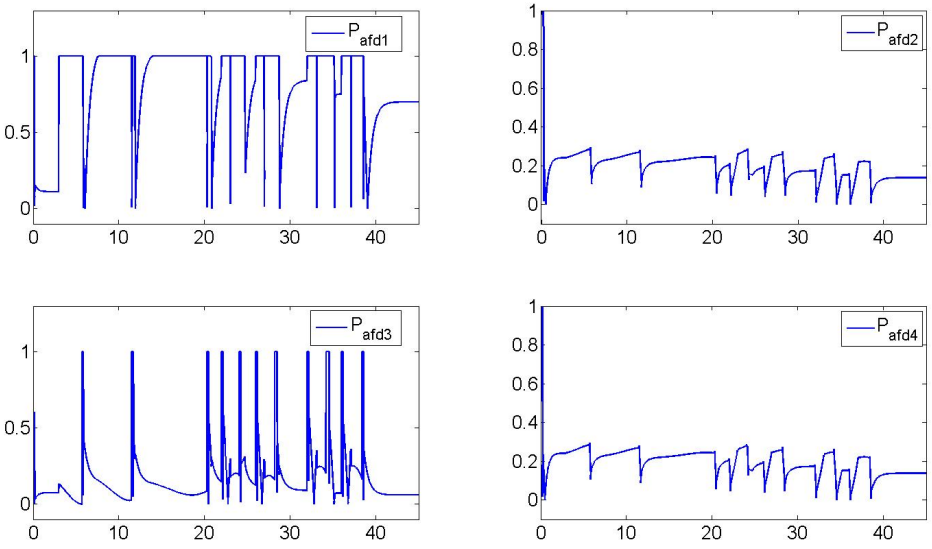

FIGURE 4.23: Criterion P_{afdj}: Case 2

At $t = 3.5\,s$, $P_{det1} > C_a$, the first working point X_1 with υ_1 (sees Table. 4.2) is chosen. However, because of the fault, the performance of the system continues reducing, $P_{det1} > C_a$ at $t = 11.5\,s$, then X_2 with υ_2 is chosen. Also, X_3 with υ_3 is chosen at $t = 20.3\,s$. Although X_3 can be achieved under faulty condition, $|u_1| = P_{afd1}u_{max}$ does not satisfy $|u_1| = K_f u_{max} = 0.7u_{max}$, then X_4 with υ_4 is selected at $t = 22\,s$. Since each working point is chosen such that Eq. 4.28 is satisfied, X_4 is within the attraction region of X_3 for the nominal system. However, this may not be guaranteed anymore for the faulty system, because of the fault, the attraction region of each working point is reduced. As what is shown in Fig. 4.24, X_4 can not be achieved, then at $t = 24.1\,s$, $P_{det1} > C_a$, X_5 with υ_5 is chosen. Until υ_{11} with υ_{11} which satisfies $P_{det1} > 0.02$ and $P_{afdj} < C_f = 0.7$ is chosen at $t = 38.4\,s$, see Fig. 4.24.

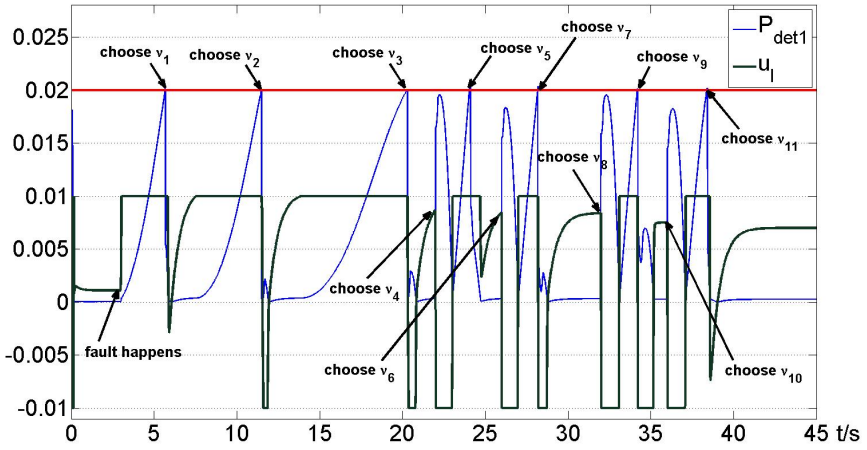

FIGURE 4.24: The Whole Reference Adjustment Process

Then the AFD can be applied after adjusting the reference, see Fig. 4.25. After the new reference is achieved, $\kappa_1 = 0.9, \kappa_3 = 0.7, \kappa_2 = 1, \kappa_4 = 1$ is injected at 45 s. After getting the stable control signals, $\kappa_2 = 0.9, \kappa_4 = 0.7, \kappa_1 = 1, \kappa_4 = 1$ is injected at 50s. All required data can be obtained, see Table. 4.3. With the control signal values we collect, based on Eq. 4.50 - Eq. 4.52, we can calculate $\hat{f}_1 = 0.07$, $\hat{f}_3 = 0.0633$, $\hat{f}_2 = 0.29$ and $\hat{f}_4 = 0.3086$.

TABLE 4.3: Data for AFD

$*$	achieving X_{11}	$inject\kappa_1, \kappa_3$	$inject\kappa_2, \kappa_4$
u_l/u_{max}	0.7	0.84	0.699
u_l/u_{max}	0.06	0.059	0.092

With the estimated fault, based on Eq. 4.53 , a new controller is designed. However, with the accommodated controller, the original reference that the EV system should track with $\nu_0 = 15m/s$ can not be achieved, since condition Eq. 4.41 is not satisfied. The new reference $\nu_6 = 12.8m/s$ $\rho_{ref} = 1/400$ within D_c^{nom} is chosen.

At $55s$, the virtual faults are canceled and the new controller with the new reference is applied. The new reference can be achieved, see Fig. 4.26 - Fig. 4.30. The control signals are shown in Fig. 4.25.

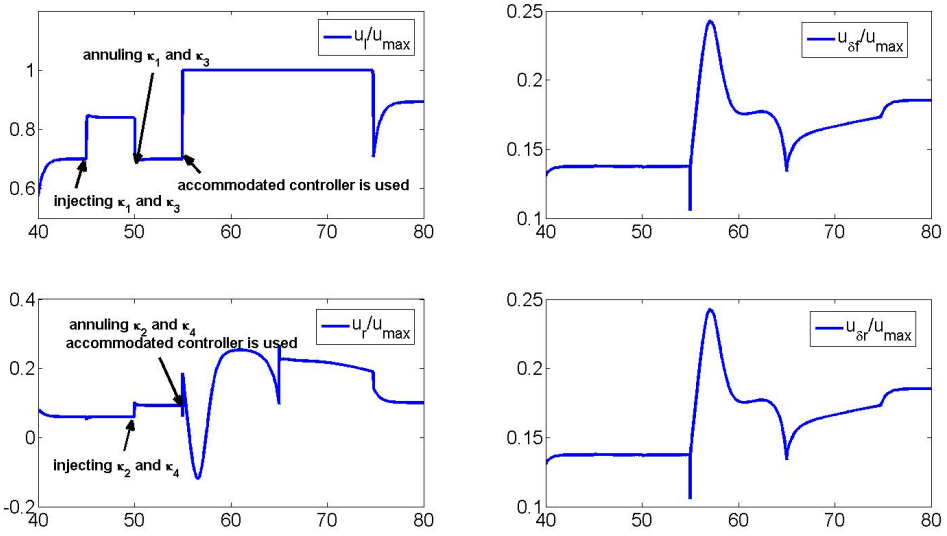

FIGURE 4.25: u/u_{max} : With AFD and Accommodated Controller

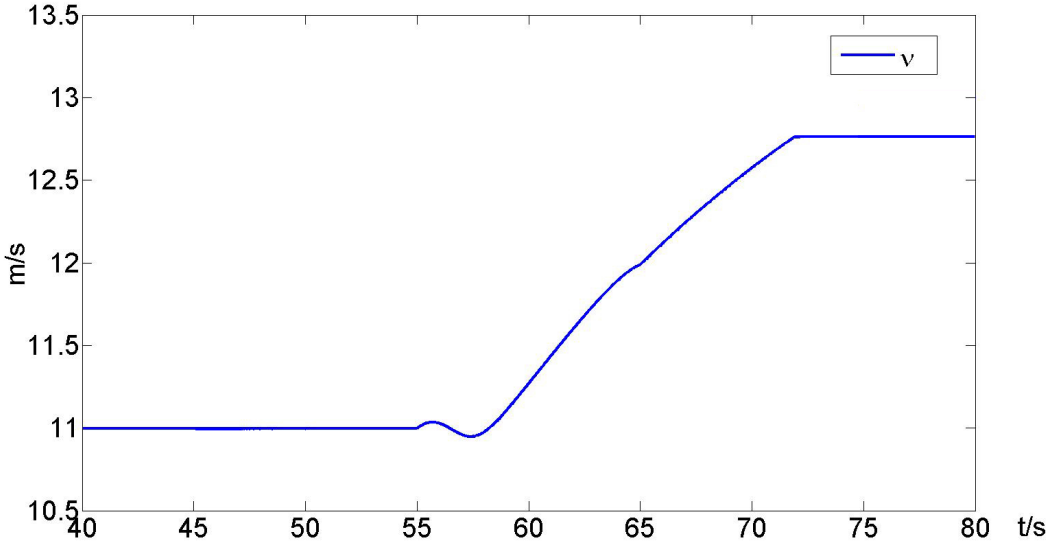

FIGURE 4.26: Speed of Vehicle Mass Centre ν : With AFD and Accommodated Controller

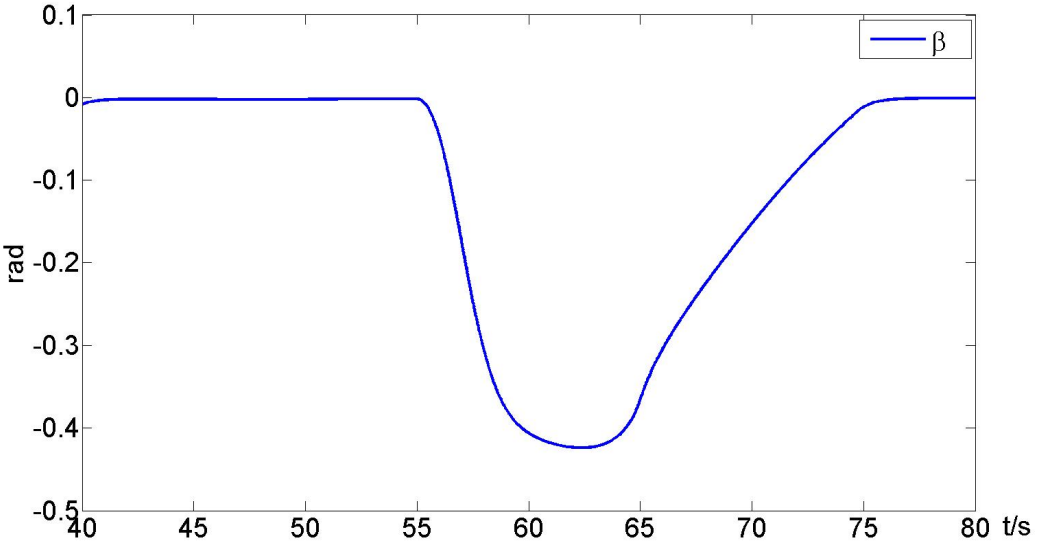

FIGURE 4.27: Side Slip Angle β : With AFD and Accommodated Controller

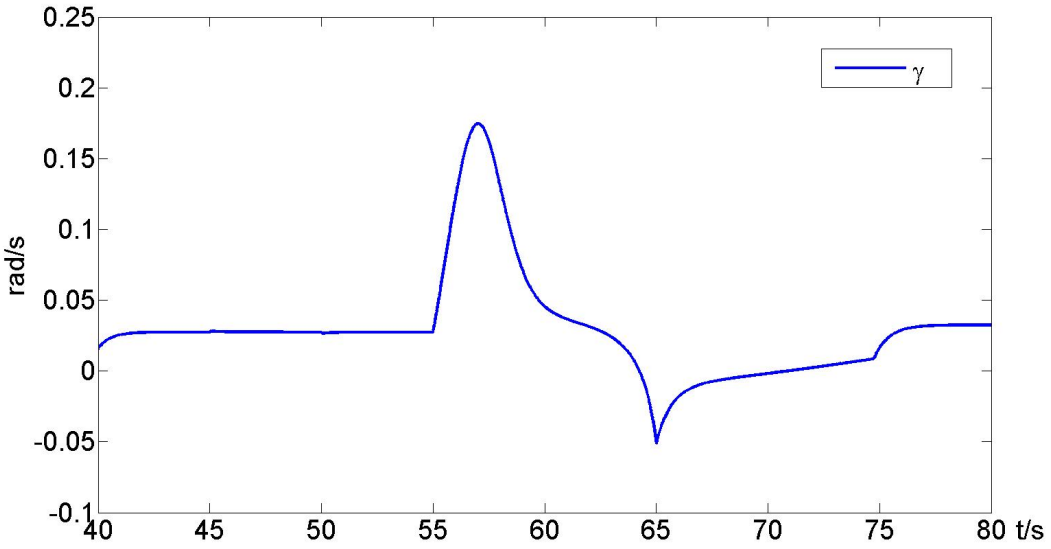

FIGURE 4.28: Yaw Rate γ : With AFD and Accommodated Controller

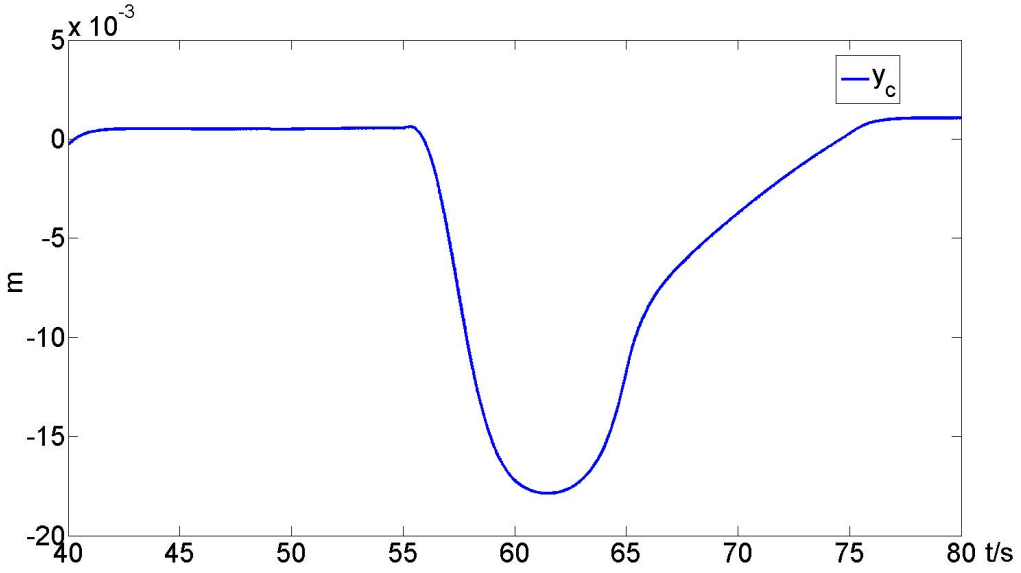

FIGURE 4.29: Distance y_c : With AFD and Accommodated Controller

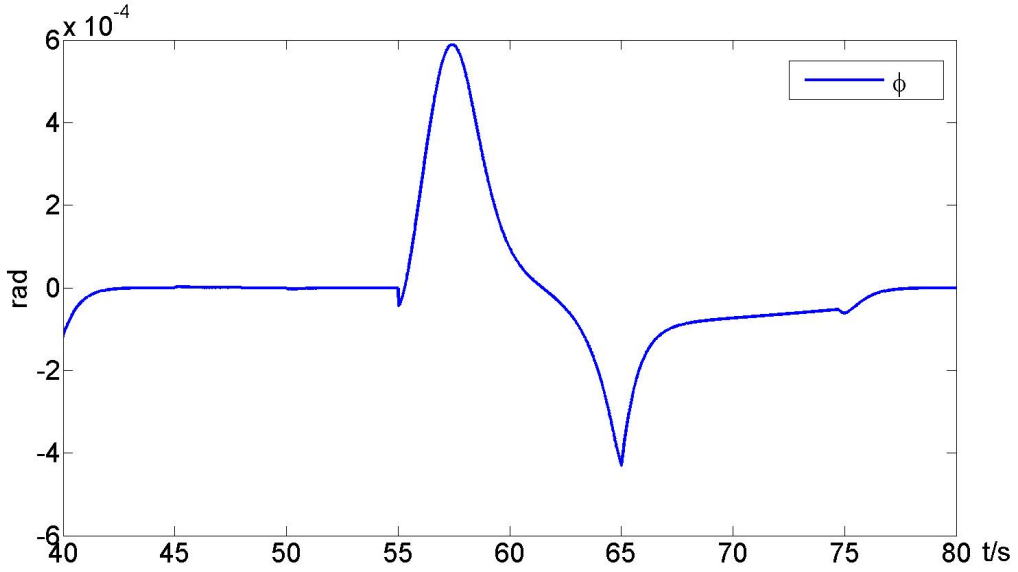

FIGURE 4.30: Angle ϕ : With AFD and Accommodated Controller

4.7 Conclusion

With considering wheel slip constraints and actuator faults, a fault-tolerant control scheme for the 4WD2WS EV path-tracking system has been proposed..

The nonlinear system is first linearized to obtain a simplified model for the control design. Several working points which satisfy condition Eq. 4.28 within D_c^f are also chosen.

For the healthy system, a controller (Eq. 4.44) based on the low-high gain control is designed. Then two criteria P_{detj} and P_{afdj}, see section 4.5.2, are introduced. P_{detj} is used to detect fault, if $P_{detj} > C_a$, the reference adjustment method is implemented, different working points are selected within D_c^f to avoid input saturation. Until the other criterion P_{afdj} satisfies condition $P_{afdj} > C_f$ (Eq. 4.49), active fault diagnosis (AFD) approach is implemented to explicitly localize the faulty wheels and to estimate the control gains. The AFD consists in actively changing the motor control gain by virtually multiplying the motor control signal by a positive value. Its implementation is possible thanks to the designed passive fault-tolerant controller and the reference input adjustment method, which guarantee that the system can stay stable and achieve one chosen working point.

With the fault information obtained from AFD, an accommodated controller is adopted to recover the degraded performance as best as possible. In section 4.5.4 , an accommodated controller is designed to illustrate one simple design method. If the original objective could not be achieved by the new controller, one appropriate reference from D_c^f should be chosen as the new reference.

Finally, the FTC scheme is applied to the original nonlinear EV system. The simulation results demonstrate the effectiveness of the proposed method.

Chapter 5

CONCLUSION AND FUTURE RESEARCH

This thesis develops new methodologies to deal with fault-tolerant control systems with input constraints. A linear control system with actuator saturation is taken as the research object, and the system under normal and faulty situations is studied.

For the nominal system, a low-high gain controller is designed based on Lyapunov stability theory and the resolution of LMI. An iterative Ricatti equation algorithm is given to find such controller. Based on the designed controller, with the analysis of the linear system subject to actuator saturation, the invariant ellipsoids of attraction and performance regions are calculated. For the case that the initial state is not within the attraction region, a novel methodology based on the reference adjustment technique is proposed in the thesis to achieve large-region stabilization.

Generally, in the existing literature on control systems with actuator saturation, two main objectives are achieved for saturated linear system with feedback control: one is to estimate the attraction region for the saturated system under a given feedback control law as in [89][120]; the other is to design the feedback control law to obtain an attraction region as large as possible, see [102][103]. In this thesis, we

adopted the invariant set theory with the Lyapunov function to design the controller and to estimate the stability region. The stability region estimated for the designed low-high-gain controller with the proposed method has less conservatism. Besides, the proposed method can not only be used to estimate the stability region but can also give the performance region. A lot of existing researches focus on maximising the domain of attraction to solve the large-region stabilization problem for systems with actuator saturation. Only few uses the reference adjustment technique. The former way actually has a lot of limitations comparing to the reference adjustment technique. Different from [101][113][114] which also adjusted the reference when encountering the saturation problem, a new algorithm is designed in the thesis to realize large-region stabilization, and the proposed algorithm and method can be systematically expressed by the invariant sets.

For the system with certain actuator faults, the fault's influence is analysed first, its size and the time when it happens will decide whether the tracking system is stable or not and will influence the system's tracking performance. Then two main FTC design methods (PFTC and AFTC) are used to cope with faults and actuator saturation together. The proposed PFTC and AFTC methods have both their restrictions when dealing with the input saturation problem : Since the passive fault-tolerant controller is designed for presumed faults, it can guarantee that the system operates with degraded performance in a small stability region which is decided by the worst fault case. For the AFTC method, the degraded performance caused by faults will be recovered by designing an observer to obtain the fault information. However, its control capability will be reduced due to the fault, and it is hard to analyse the system stability region. Based on the existing performance analysis principle and the implementation results of PFTC and AFTC, a novel fault-tolerant control scheme based on the reference adjustment technique is proposed to guarantee the tracking performance in an acceptable region.

In the existing literature of fault-tolerant systems with actuator saturation, FTC objective is achieved by either designing the controller based on the solution of LMI/BMI to obtain an attraction region as large as possible as in[102][103] and based on adopting the reference adjustment technique as in [113][114]. In the thesis, we treat the FTC design problem from a different view. The controller used

in the proposed scheme is still the nominal one and it decides the fault tolerant capability for the faulty system. Based on the performance analysis principle in [101], a nominal performance set Ω_{nom} and a degraded performance set Ω_{deg} are defined. Then for the worst fault case that the controller can handle, a degraded but acceptable reference is chosen off-line. When small faults happen that will not disturb the tracking performance (i.e., the tracking performance is still within Ω_{nom}), the nominal controller will still be used. If the tracking performance degrades to the boundary of Ω_{nom} because of some severe faults, the degraded reference is chosen immediately to avoid input saturation. During the whole control process, an observer used in AFTC method to obtain the fault information is adopted here. If the tracking system can reach the degraded reference, then with the estimated fault, a new control law and a new reference are designed to recover more degraded performance for the faulty system. If the performance continues degrading even adopting the degraded reference, then the system will be stopped.

The idea of the proposed fault-tolerant control scheme in the thesis is applied to the path tracking problem for an electric vehicle (EV) which has four electromechanical wheel systems. With considering wheel slip constraints and certain faults, a controller based on low-high gain control is developed to maintain the system's stability and guarantee the acceptable tracking performance. Then based on the designed controller, an active fault diagnosis approach is introduced for this typical over-actuated system to isolate and evaluate faults more precisely. With the diagnosed information, an accommodated fault-tolerant controller is designed to maintain the tracking performance as best as possible.

Based on existing researches, this thesis gives a different view of the FTC design for systems with actuator saturation. However, because of lack of time and knowledge, some problems are still not solved in the thesis. They are presented as follows:

The objective $r(t)$ in Problem 1 and Problem 2 is assumed to be a constant value in this thesis, even in the application for the electric vehicle, a simple trajectory is chosen for simplicity. For a time-varying tracking objective $r(t)$, new methods could be developed to analyse systems' attraction region and performance region.

The proposed method used to estimate the stability region, which has the same result as in [114]. It is not the optimal one. Estimating the stability region by using convex theory and by adopting linear/nonlinear programming could be investigated.

In the proposed FTC scheme based on the reference adjustment technique, the problem of choosing suitable degraded references arise. It is not a simple task, especially for a system with various possible faults. A satisfactory reference should be able to capture most of the control requirements but without violating the physical constraints. It is related to the designed controller, the considered worst fault case and also the defined performance set Ω_{deg}. In future research, a systematical method should be developed to find these suitable references.

Linear systems are considered in this thesis. A natural extension of this work is to deal with nonlinear systems. The general principles of our approach can be kept but the system analysis and design methods would be different. The FTC design for nonlinear system with input constraints has greater meaning to be researched.

Finally, the application of the FTC methodology on a real system (as for instance the Robucar EV in CRIStAL Laboratory) is still a challenging issue.

Bibliography

[1] Y. M. Zhang and J. Jiang. Bibliographical review on reconfigurable fault-tolerant control systems. *Annual Reviews in Control*, 32(2):229 – 252, December 2008.

[2] M. Kang. *Studies on Failure Diagnose and Reconfigurable Technique of Fault-tolerant Control System*. PhD thesis, University BeiHang, 2004.

[3] D. H. Zhou and X. Ding. Theory and application of fault tolerant control. *Acta Automatica Sinica*, 26(06):788 – 797, 2000.

[4] A. Bartoszewicz. *Robust Control, Theory and Applications*. InTech, 2011.

[5] M. Blanke, M. Kinnaert, J. Lunze, and M. Staroswiecki. *Diagnosis and Fault-tolerant Control*. Springer Science, 2003.

[6] D. D. Siljak. Reliability control using multiple control systems. *Int. J. Control*, 31(2):303 – 329, 1980.

[7] Y. J. Cho, Z. Bien, and B. K. Kim. Reliable control via additive redundant adaptive controller. In *Proc. of 1989 Amer. Contr. Conf*, pages 1899 – 1904, Pittsburgh, PA, 1989.

[8] A. N. Gundes and M. G. Kabuli. Reliable decentralized control. In *Proc. of 1994 Amer. Contr. Conf*, pages 3359–3363, Baltimore, MD, 1994.

[9] N. Sebe and T. Kitamori. Reliable stabilization based on a multi-compensator configuration. In *Proc. of 12th IFAC World Congress*, volume 4, pages 5–8, 1993.

[10] N. Sebe and T. Kitamori. Passive fault tolerant servo control against one device failure out of sensors and actuators. In *Proc. of 14th European Control Conference*, pages 644–651, Strasbourg, France, 2014.

[11] J. Ackermann. *Sampled-Data Control Systems: Analysis and Synthesis,Robust System Design*. Springer-Verlag, 1985.

[12] S. M. Joshi. Design of failure accommodating multiloop LQG-type controllers. *IEEE Transactions on Automatic Control*, 32(8):740 – 741, 1987.

[13] E. Shimemura and M. Fujita. A design method for linear state feedback systems possessing integrity based on a solution of a Riccati-type equation. *Int. J. Control*, 42(4):887 – 899, 1985.

[14] L. S. Shieh, H. M. Dib, S. Ganesan, and R. E. Yates. Optimal pole-placement for state feedback systems possessing integrity. *Int. J. Systems Science*, 19 (8):1419–1435, 1988.

[15] Z. D. Wang and J. S. Sun. Studies on the design of state feedback control systems possessing integrity. *Control Theory and Application*, 14(5):754–758, 1997.

[16] R. Seaks and J. Murray. Fractional representation, algebraic geometry and the simultaneous stabilization problem. *IEEE Transactions on Automatic Control*, 27(4):895–903, 1982.

[17] K. J. Åström and B. Wittenmark. Adaptive control. *Addison-Wesley*, (343 - 371), 1989.

[18] J. S. Shamma and M. Athans. Gain scheduling: Potential hazards and possible remedies. *Control Systems Magazine, IEEE*, 12(3):101 – 107, 1992.

[19] D. Lawrence and W. Rugh. Gain scheduling dynamic linear controllers for a nonlinear plant. *Automatica*, 31(3):381 – 390, 1995.

[20] I. Kaminer, A. Pascoal, P. Khargonekar, and E. Coleman. A velocity algorithm for the implementation of gain-scheduled controllers. *Automatica*, 31: 1185–1191, 1995.

[21] D. P. Looze, J. L. Weiss, J. S. Eterno, and N. M. Barrett. An automatic redesign approach for restructureable control systems. *IEEE Con. Sys. Mag.*, 5(2):16–22, 1985.

[22] C. Y. Huang and R. F. Stengel. Restructurable control using proportional-integral implicit model-following. *Journal of Guidance Control and Dynamics*, 13(2):303 – 309, 1990.

[23] S. S. Hu and J. Cheng. The fault-tolerant control based on model reference for aircraft. *Acta Aeronautica et Astronautica Sinica*, 12(5):279–286, 1991.

[24] J. Jiang. Design of reconfigurable control systems using eigenstructure assignments. *Int. J. Control*, 59(2):395–410, 1994.

[25] A. K. Caglayan, S. M. Allen, and K. Wehmuller. Evaluation of a second generation reconfiguration strategy for aircraft fight control systems subjected to actuator failure surface damage. In *Proc. of 1988 National Aero. and Electron. Conference*, pages 520–529, Dayton, 1988.

[26] Z. Q. Gao and P. J. Antsaklis. Stability of the pseudo-inverse method for reconfigurable control systms. *Int. J. Control*, 53(3):717 – 729, 1991.

[27] S. M. Guo, S. H. Tsai, Y. C. Lin, Tzong-Jiy Tsai, and C. W. Chen. Intelligent-based PID fault tolerant tracking control for unknown nonlinear mimo systems. In *IEEE International Conference on Control and Automation*, pages 331 – 336, Christchurch, New Zealand, 2009.

[28] D. Ichalal, B. Marx, D. Maquin, and J. Ragot. New fault-tolerant control strategy for nonlinear systems with multiple model approach. In *Conference on Control and Fault Tolerant Systems*, pages 607– 611, Nice, France, 2010.

[29] Q. K. Shen, B. Jiang, and V. Cocquempot. Adaptive fuzzy observer-based active fault-tolerant dynamic surface control for a class of nonlinear systems with actuator faults. *IEEE Transactions on Fuzzy Systems*, 22(2):338 – 349, April 2014.

[30] P. M. Frank. Fault diagnosis in dynamic systems using analytical and knowledge-based redundancy: A survey and some new results. *Automatica*, 26(3):459 – 474, 1990.

[31] V. Venkatasubramanian, R. Rengaswamy, K. W. Yin, and S. N. Kavuri. A review of process fault detection and diagnosis part i: Quantitative model-based methods. *Computers and Chemical Engineering*, 27:293–311, 2003.

[32] V. Venkatasubramanian, R. Rengaswamy, K. W. Yin, and S. N. Kavuri. A review of process fault detection and diagnosis part ii: Quantitative models and search strategies. *Computers and Chemical Engineering*, 27:313–326, 2003.

[33] C. C. Ma and X. D. Gu. Fault diagnosis with fault gradation using neural network group. *Journal of Systems Engineering and Electronics*, 31(1):225 – 228, 2009.

[34] H. A. Talebi, K. Khorasani, and S. Tafazoli. A recurrent neural-network-based sensor and actuator fault detection and isolation for nonlinear systems with application to the satellite's attitude control subsystem. *IEEE Transactions on Neural Networks*, 20(1):45 – 60, Jan 2009.

[35] S. Peng, J. S. Yuan, X. L. An, Z. Li, and et al. Diagnosis method of transformer faults based on rough set theory. *Techniques of Automation and Applicaitons*, 24(3):56 – 59, 2008.

[36] L. L. Jin. Study on spacecraft fault diagnosis expert system based on fault tree. Master's thesis, Nanjing University of Aeronuatics and Astronautics, 2008.

[37] S. S. Hu and Y. Wang. Support vector machine based fault diagnosis for nonlinear dynamics systems. *Control And Decision*, 16(5):617 – 620, 2011.

[38] Y. Zhang, Y. Yang, S. X. Ding, and L. Lin. Data-driven design and optimization of feedback control systems for industrial applications. *IEEE Transactions on Industrial Electronics*, 61:6409 – 6417, 2014.

[39] S. Yin, S. X. Xie, and H. Luo. A review on basic data-driven approaches for industrial process monitoring. *IEEE Transactions on Industrial Electronics*, 61:6418 – 6428, 2014.

[40] Z. T. Cao, G. G. He, H. P. Chen, and E.Ritchie. Multiple bandwith wavelet analysis for fault diagnosis elgenvalue in squirrel-cage induction motor. *Proceedings of The Chinese Society for Electrical Egineering*, 23(7):112–116, 2003.

[41] R. Dunia, S. J. Qin, T. F. Edgar, and T. J. McAvoy. Identification of fault sensors using principal component analysis. *American Institute of Chemical Engineers Journal*, 42(10):2797 – 2812, 1996.

[42] Y. Seongkyu and J. F. MacGregor. Principal-component analysis of multiscale data for process monitoring and fault diagnosis. *American Institute of Chemical Engineers Journal*, 50(11):2891–2903, 2004.

[43] K. Kumamaru. Robust fault detection using index of kullback discrimination information. *In Proc. of IFAC World congress*, pages 205–210, 1996.

[44] H. W. Cho. Diagnosis of multivariate process via nonlinear kernel method combined with qualitative representation of fault patterns. *World Academy of Science, Engineering and Technology*, 6(12):107–110, 2012.

[45] S. X. Ding, Y. Yang, Y. Zhang, and L. Li. Data-driven realizations of kernel and image representations and their application to fault detection and control system design. *Automatica*, 50:2615–2623, 2014.

[46] A. Shumsky. Robust analytical redundancy relations for fault diagnosis in nonlinear systems. *Asian Journal of Control*, 4(2):159 – 170, June 2002.

[47] V.Cocquempot, T. EL Mezyani, and M. Staroswiecki. Hybrid dynamical systems monitoring using structured analytical redundancy relations. In *17th IMACS World Congress*, Paris, France, 2005.

[48] A. Medvedev. Disturbance attenuation enhancement in continuous parity space methods. In *European Control Conference ECC 97*, pages 641 – 647, Sweden, 1997.

[49] E. Y. Chow and A. S. Willsky. Analytical redundancy and the design of robust fauilure detection systms. *IEEE Transactions on Automatic Control*, AC-29:603–614, 1984.

[50] D. N. Yu, D. Williams, D. N. Shields, and J. B. Gomm. A parity space method of fault detection for bi-linear systems. In *Proc. of the American Control Conference*, pages 1132 – 1133, Seattle, 1995.

[51] G. Comtet-Varga, J. Ph, and M. Staroswiecki. Analytic redundancy relations for state affine systems. In *Proc. of 4th European Control Conference (ECC'97)*, Brussels, Belgium, 1997.

[52] M. Staroswiecki and G. Comtet-Varga. Analytic redundancy relations for fault detection and isolation in algebraic dynamic systems. *Automatica*, 37: 687–699, 2001.

[53] V. Cocquempot, T. EL Mezyani, and M. Staroswiecki. Fault detection and isolation for hybrid systems using structured parity residuals. In *IEEE/IFAC-ASCC 2004: Asian Control Conference*, Melbourne, Victoria, Australia, Juil 2004.

[54] S. Diop. Elimination in control theory. *Mathematical Control Signals Systems*, 4:17–32, 1991.

[55] J. C. Faugere, P. Gianni, D. Lazard, and T. Mora. Efficient computation of grobner bases by change of orderings. *Journal of Symbolic Computations*, 16:329–344, 1993.

[56] Q. Zhang, M. Basseville, and A. Benveniste. Fault detection and isolation in nonlinear dynamic systems: A combined input-output and local approach. *Automatica*, 34(11):1359 – 1374, 1998.

[57] H. Hammouri, M. Kinnaert, and E. H. El-Yaagoubi. Observer-based approach to fault detection and isolation for nonlinear systems. *IEEE Transactions on Automatic Control*, 44:1879–1884, 1999.

[58] K. Zhang, B. Jiang, and P. Shi. *Observer-based Fault Estimation and Accomodation for Dynamic Systems*. Springer, Berline, 2012.

[59] H. Yang, B. Jiang, and V. Cocquempot. Observer-based fault tolerant control for constrained switched systems. *International Journal of Control, Automation and Systems: IJCAS*, 5(6):707–711, 2007.

[60] W. Chen, A. Q. Khan, M. Abid, and S. X. Ding. Integrated design of observer based fault detection for a class of uncertain nonlinear systems. *Int. J. Appl. Math. Comput. Sci.*, 20(3):423–430, 2011.

[61] G. R. Duan and R. J. Patton. Robust fault detection using luenberger-type unknown input observers - a parametric approach. *International Journal of Systems Science*, 32:533–540, 2001.

[62] B. Brumback. A chi-square test for fault detection in kalman filters. *IEEE Transactions on Automatic Control*, 32:552–554, 1987.

[63] C. Edwards, S. K. Spurgeon, and R. J. Patton. Sliding mode observers for fault detection and isolation. *Automatica*, 36:541–553, 2000.

[64] B. Jiang, M. Staroswiecki, and V. Cocquempot. Fault estimation in nonlinear uncertain systems using robust/sliding mode observers. *IEE Control Theory and Application (IJCAS)*, 151(1):29–37, January 2004.

[65] C. D. Qu and H. Y Zhang. The fault diagnosis of momentum close-loop system used in satellite based on the UIO double observers. *Aerospace Control*, 23(6):66 – 71, 2005.

[66] B. Jiang, M. Staroswiecki, and V. Cocquempot. Fault diagnosis based on adaptive observer for a class of nonlinear systems with unknown parameters. *Int. Journal of Control (IJC)*, 77(4):415 – 426, 2004.

[67] X. Ding and P. M. Frank. On-line fault detection for uncertain dynamical systems using adaptive observers. *European J. of Diagnosis and Safety in Automation*, 3(1):7 – 21, 1993.

[68] P. Tadic, Z. Durovic, B. Kovacevic, and V. Papic. Fault diagnosis for steam separators based on parameter identification and cusum classification. In *2012 IEEE International Conference on Industrial Technology (ICIT)*, pages 248–253, Athens, March 19-21 2012.

[69] T. Jiang, K. Khorasani, and S. Tafazoli. Parameter estimation-vased fault detection, isolation and recovery for nonlinear satellite models. *IEEE Transactions on Control System Technology*, 16(4):799–808, 2008.

[70] P. Young. Parameter estimation for continuous time models - a survey. *Automatica*, 17(1):23–39, 1981.

[71] J. H. Fan, Z. Q. Zheng, and M. LV. Linear optimal fault-tolerant invariant set for saturating system. *Journal of National University of Defense Technology*, 32(6):158–162, 2010.

[72] S. S. Keerthi and E. G. Gilbert. Computation of minimum-time feedback control laws for discrete-time systems with state-control constraints. *IEEE Transactions on Automatic Control*, 32:432–435, 1987.

[73] K. J. Astrom and L. Rundowist. Integrated windup and how to avoid it. In *Proceedings of the American Control Conference*, pages 1693–1698, Pennsylvania, USA, 1989.

[74] S. Tarbouriech, G. Garciea, and et al. *Stability and Stabilization of Linear Systems with Saturating Actuators*. Springer-Verlag London, 2011.

[75] T. Hu and Z. L. Lin. *Control Systems with Actuator Saturation: Analysis and Design*. Birkhauser, 2001.

[76] P. Gutman and P. Hagander. A new design of constrained controllers for linear systems. *IEEE Transactions on Automatic Control*, 30:2–33, 1985.

[77] S. Tarboriech and M. Turner. Anti-windup design: an overview of some recent advances and open problems. *Control Theory and Applications, IET*, 9:1–19, Jnuary 2009.

[78] L. Zaccarian and A. R. Teel. Nonlinear scheduled anti-windup design for linear systems. *IEEE Transactions on Auto. Control*, 15:2055–2061, Nov 2004.

[79] H. C. Bang, M. J. Tahk, and H. D. Choi. Large angle attitude control of spacecraft with actuator saturation. *Control Engineering Practice*, 11: 989–997, 2003.

[80] L. Show, J. Juang, Y. W. Jan, and et al. Spacecraft robust attitude control with saturation nonlinearity. In *AIAA Guidance, Navigation and Control Conference and Exhibit*, Monterey, 2002.

[81] R. F. Wang, T. G. Jia, and Y. G. Niu. Sliding-mode control for uncertain systems with input saturation. *Control Theory and Application*, 28(9):1154–1158, Sep 2011.

[82] A. R. Wei and Y. Z. Wang. Adaptive control of uncertain port- controlled hamiltonian systems subject to actuator saturation. *International Journal of Control, Automation, and Systems*, 9(6):1–7, 2011.

[83] E. D. Sontag and H. J. Sussmann. Nonlinear output feedback design for linear systems with saturating controls. *Proc. of 29th IEEE Conf. Decision and Control*, pages 3414–3416, 1990.

[84] A. Saberi, Z.L. Lin, and A.R. Teel. Control of linear systems with saturation actuators. *IEEE Transactions on Automatic Control*, 41(3):368–378, March 1996.

[85] Z. L. Lin and A. Saberi. Semi-global exponential stabilization of linear systems subject to input saturation via linear feedbacks. *Systems and Control Letters*, 21:225–239, 1993.

[86] Z. L. Lin, A. Saberi, and A. A. Stoorvogel. Semi-global exponential stabilization of linear discrete-time systems subject to input saturation via linear feedback- an are-based approach. *IEEE Transactions on Automatic Control*, 41(8):1203–1207, 1996.

[87] J. A. De Dona and G. C. Goodwin. A general scheme that combines piecewise-linear control, low-high-gain control and over-saturation to achieve high performance in the presence of input saturation. In *Proceedings of the American Control Conference*, pages 745–749, Chicago, Illinois, June 2000.

[88] F. Blanchini. Set invariance in control. *Automatica*, 35:1747–1767, 1999.

[89] S. T. Hu and Z. L. Lin. Exact characterization of invariant ellipsoids for linear systems with saturating actuators. *Proceedings of 40th IEEE Conference on Decision and Control*, pages 4669–4674, 2001.

[90] A. Benzaouia and A. Hmamed. Regulator problem for linear continuous-time systems with nonsymmetrial constrained control. *IEEE Transactions on Automatic Control*, 38(10):1556–1560, 1993.

[91] E. B. Castelan and J. Hennet. Eigenstructure assignment for state constrained linear continuous time systems. *Automatica*, 28(3):605–611, 1992.

[92] S. Tarbouriech and E. B. Castelan. An eigenstructrue assignment approach for constrained linear continuous-time singular systems. *Systems and Control Letters*, 24:333–343, 1995.

[93] A. Bemporad and M. Morari. Robust model predictive control: A survey. *Lecture Notes in Control and Information Sciences*, pages 207–226, September .

[94] V. T. Minh and N. Afzulpurkar. Robust model predictive control for input saturated and softened state constraints. *Asian Journal of Control*, 7(3): 323–329, September 2005.

[95] H. J. Lee. Recent advances in model predictive control and other related areas. In *presented at the CPC V*, Lake Tahoe, CA, 1996.

[96] P. J. Campo and M. Morad. Robust model predictive control. In *Proceedings of the American Control Conference*, pages 1021–1026, 1987.

[97] Z. Q. Zheng. *Robust Control of Systems subject to Constraints*. PhD thesis, California Institute of Technology Pasadena, CA, 1995.

[98] Z. Y. Wan and K. V Mayuresh. Robust output feedback model predictive control using off-line linear matrix inequalities. In *Proceedings of the American Control Conference*, pages 25–27, Arlington, VA, June 2001.

[99] I. Boyd and P. Stephen. *Linear Matrix Inequalities in System and Control Theory*, volume 15. SIAM Studies in Applied Mathematics, 1994.

[100] C. S. Jiang, L. H. Sun, Q. X. Wu, and W. H. Chen. *Control Theory and Robust Control*. Aviation Industry Press, 1998.

[101] B. Boussaid, C. Aubrun, M. N. Abdelkrim, and M. K. B. Gayed. Performance evaluation based fault tolerant control with actuator saturation avoidance. *Int. J. Appl. Math. Comput. Sci.*, 21(3):457–466, 2011.

[102] J. H. Fan, Y. M. Zhang, and Z. Q. Zheng. Robust fault-tolerant control against time-varying actuator faults and saturation. *IET Control Theory and Applications*, 6(14):2198–2208, July 2012.

[103] W. Guan and Z. F. Sun. Design of state feedback controller for systems with input constrains and actuator faults. In *2009 Chinese Control and Decision Conference (CCDC 2009)*, pages 476–481, 2009.

[104] W. Guan and G. Yang. Adaptive fault-tolerant control of linear systems with actuator saturation and L2 distrubances. *J. Control Theory Appl.*, 7 (2):119–126, 2009.

[105] S. Gayaka and B. Yao. Adaptive robust actuator fault-tolerant control in presence of input saturation. In *Proc. American Control Conference*, San Francisco, CA, USA, 2011.

[106] Q. Hu, B. Xiao, and M.I.Friswell. Robust fault-tolerant control for spacecraft attitude stabilisation subject to input saturation. *IET Control Theory and Applications*, 5(2):271–282, 2011.

[107] B. Xiao, Q. L. Hu, and Y. M. Zhang. Adaptive sliding mode fault-tolerant attitude tracking control for flexible spacecraft under actuator saturation. *IEEE Transactions on Control System Technology*, 2011.

[108] J. H. Fan, Z. Q. Zheng, and Y. M. Zhang. Stabilization of observed-based actuator fault-tolerant control systems with uncertainties, actuator saturation and disturbances: an lmi approach. In *Proc. 23rd Canadian Congress of Applied Mechanics*, Vancouver, BC, Canada, 2011.

[109] J. H. Richter. *Reconfigurable Control of Nonlinear Dynamical Systems: A Fault-hiding Approach*. Springer-Verlag, Berlin, Heidelberg, 2011.

[110] J. H. Fan, Z. Q. Zheng, and Y. M. Zhang. Control allocation-based fault-tolerant control for over-actuated systems with saturation and imperfect fault information. In *AIAA Infotech Aerospace: Unleashing Unmanned Systems*, St. Louis, Missouri, USA, 2011.

[111] A. Yetendje, M. Seron, and J. De Dona. Robust multisensor fault-tolerant model-following mpc design for constrained systems. *Int. J. Appl. Math. Comput. Sci.*, 22(1):211–223, 2012.

[112] J. H. Fan, Y. M. Zhang, and Z. Q. Zheng. Hybrid fault-tolerant flight control against actuator faults and input constraints: A set invariance approach. In *AIAA Guidance, Navigation and Control Conference*, Minneapolis, MN, USA, 2012.

[113] J. Jiang and Y. M. Zhang. Graceful performance degradation in active fault-tolerant control systems. In *15th Triennial World Congress*, Barcelona, Spain, 2002.

[114] B. Boussaid, C. Aubrun, J. Jiang, and M. N. Abdelkrim. FTC approach with actuator saturation avoidance based on reference management. *International Journal of Robust and Nonlinear Control*, (17):2724–2740, 2014.

[115] Lyubomir T. Gruyich. *Tracking Control of Linear Systems*. CRC Press, 2013.

[116] P. Y. Li. Reference input tracking: Feedforword control. Technical report, University of Minnesota, 2014.

[117] G. F. Wredenhagen and P. R. Belanger. Piecewise-linear LQ control for systems with input constraints. *Automatica*, 30(3):403–616, 1994.

[118] P. Y. Li. Linear quadratic optimal control. Technical report, University of Minnesota, 2014.

[119] T. S. Hu, Z. L. Lin, and B. M. Chen. Analysis and design for discrete-time linear systems subject to actuator saturation. *Systems and Control Letters*, 45:97–112, 2002.

[120] M. C. Turner and I. Postlethwaite. Guaranteed stability regions of linear systems with actuator saturation using the low-and-high gain technique. *International Journal of Control*, 74(14):1425–1434, December 18 2001.

[121] Q. Gao. Robust control of systems subject to actuator saturation and disturbance. In *Proceedings of the 25th Chinese Control Conference*, pages 151–155, Harbin, Heilongjiang, August 7-11 2006.

[122] S. Weissenberger. Application of results from the absolute stability to the computation of finite stability domains. *IEEE Transactions on Automatic Control*, 13:124–125, 1968.

[123] H. Khalil. *Nonlinear Systems*. Upper Saddle River NJ Prentice Hall, 1996.

[124] W. Chen, D. Ballance, and J. Oreilly. Optimisation of attraction domains of nonlinear MPC via LMI methods. In *Proceedings of the ACC*, 2001.

[125] J. M. Gomes da Silva Jr and S. Tarbouriech. Anti-windup design with guaranteed regions of stability: an lmi-based approach. *IEEE Transactions on Automatic Control*, 50(1):106–111, 2005.

[126] T. Hu and Z. L. Lin. On enlaging the basin of attraction for linear systems under saturated linear feedback. *System and Control Letters*, 40:59–69, 2000.

[127] H. Hindi and S. Boyd. Analysis of linear systems with saturation using convex optimization. In *Proceedings of the 37th IEEE Conference on Decision and Control*, pages 903–908, Tampa, Florida USA, December 1998.

[128] A. A. Stoorvogel, X. Wang, A. Saberi, and P. Sannuti. Control of linear systems with input saturation and matched uncertainty and disturbance. In *Proceedings of the American Control Conference*, pages 4380 – 4385, O'Farrell Street, San Francisco, CA, USA, June 29 - July 01 2011.

[129] K. J. Åström and T. Hägglund. *PID controllers: Theory, Design and Tuning*. Instrument Society of America, 1995.

[130] H. M. Do, J. Y. Choi, and J. H. Kyung. Design of reference governor for a class of nonlinear systems with input constraints. In *Proc. 11th International Conference on Control, Automation and Systems*, KINTEX, Gyeonggi-do, Korea, Oct. 26-29 2011.

[131] T. Jain. *Behavioral System-theoretic Approach to Fault-tolerant Control*. PhD thesis, University of Lorraine, 2012.

[132] M. R. Woods and J. Katupitiya. Modelling of a 4WS4WD vehicle and its control for path tracking. *2013 IEEE Symposium on Computational Intelligence in Control and Automation (CICA)*, pages 155–162, 2013.

[133] S. T. Peng, J. J. Sheu, and C. C. Chang. A control scheme for automatic path tracking of vehicle subject to wheel slip constraint. In *The 2004 American Control Conference*, pages 804 – 809, Boston, Massachusetts, June 30 - July 2 2004.

[134] S. T. Peng. On one approach to constraining the combined wheel slip in the autonomous control of a 4WS4WD vehicle. *IEEE Transactions on Control System Technology*, 15(1):168–175, 2007.

[135] P. E. Dumont, A. Aitouche, R. Merzouki, and M. Bayart. Fault tolerant control on an electric vehicle. pages 2450 – 2455, December 15 - 17 2006.

[136] A. Casavola and E. Garone. Enhancing the actuator fault tolerance in autonomous overactuated vehicle via adaptive control allocation. pages 1–6, May 27-29 2008.

[137] X. Huo, Q. L. Hu, B. Xiao, and G. F. Ma. Variable-structure fault-tolerant attitude control for flexible satellite with input saturation. *Control Theory and Application*, 28(9):1063 – 1068, 2011.

[138] Q. L. Hu, B. Xiao, and M. I. Friswell. Robust fault-tolerant control for spacecraft attitude stabilisation subject to input saturation. *IET Control Theory and Applications*, 5(2):271–281, 2011.

[139] I. Sadeghzadeh, A. Chamseddine, Y. M. Zhang, and D. Theilliol. Control Allocation and Re-Allocation for a Modified Quadrotor Helicopter against Actuator Faults. In *8th IFAC Symposium on Fault Detection, Supervision and Safety of Technical Processes, SAFEPROCESS 2012*, page CDROM, Mexico City, Mexico, August .

[140] Y. M. Zhang and D. Theilliol. Reconfigurable control allocation against partial control effector faults in aircraft. In *3rd International Conference on Advances in Vehicle Control and Safety, AVCS 2007*, page CDROM, Buenos Aires, Argentina, February .

[141] R. Wang and J. M. Wang. Fault-tolerant control with active fault diagnosis for four-wheel independently-driven electric ground vehicles. In *2011 American Control Conference*, O'Farrell Street, San Francisco, CA, USA, June 29-July 01 2011.

[142] J. Y. Shin and C. M. Belcastro. Performance analysis on fault tolerant control system. *IEEE Transactions on Control System Technology*, 14(5), September 2006.

[143] J.Jiang and Y. M. Zhang. Graceful performance degradation in active fault-tolerant control systems. In *15th Triennial World Congress*, Barcelona, Spain, 2002.

[144] N. Chatti, A. L. Gehin, O. B. Belkacem, and R. Merzouki. Functional and behavior models for the supervision of an intelligent and autonomous system. *IEEE Transactions on Automation Science and Engineering*, 10(2): 431 – 445, April 2013.

[145] H. Yang, V. Cocquempot, and B. Jiang. Optimal fault tolerant path tracking control for 4WD4WS electric vehicle. *IEEE Transactions on Intelligent Transportation Systems*, 11(1):237 – 243, 2010.

[146] C. F. Chen, Y. M. Jia, J. P. Du, and F. S. Yu. Lane keeping control for autonomous 4WS4WD vehicles subject to wheel slip constraint. In *2012 American Control Conference*, Fairmont Queen Elizabeth, Montral, Canada, June 27 - 39 2012.

[147] U. Kiencke and A. Daiβ. Estimation of tyre friction for enhanced abs-system. pages 515–520, Tokyo, Japan, 1994.

[148] R. Potluri and A. K. Singh. Path-tracking control of an autonomous 4WS4WD electric vehicle using its natural feedback loops. In *2013 IEEE Multi-conference on System and Control (Conference on Control Application)*, Hyderabad, India, August 28-30 2013.

[149] R. Potluri and A. K. Singh. Path-tracking control of an autonomous 4WS4WD electric vehicle driving motors' dynamics. In *The 7th IEEE International Conference on Industrial and Informantion Systems (ICIIS)*, pages 1 – 2, Indian Institute of Technology Madras, Chennai, India, 2012.

Publications

Xian ZHANG, V. COCQUEMPOT. Fault Tolerant Control Scheme based on Active Fault Diagnosis for the Path Tracking Control of a 4WD Electric Vehicle, IEEE MSC 2014, Multi - Conference on Systems and Control: ISIC International Symposium on Intelligent Control, Antibes, France. October 8 - 10, 2014.

Xian ZHANG, V. COCQUEMPOT. Fault Tolerant Control for an Electric 4WD Vehicle's Path Tracking with Active Diagnosis, 19th IFAC World Congress, IFAC WC 2014, Cape Town, South Africa, 24-29 August 2014.

Xian ZHANG, V. COCQUEMPOT, Bin JIANG and Hao YANG. Active Fault Diagnosis based on Fault Tolerant Control with Control Constraints for an Electric 4WD, 10th IEEE International Conference on Control and Automation, ICCA 2013, Hangzhou, China, June 12-14, 2013.

Xian ZHANG, V. COCQUEMPOT. Passive Fault Tolerant Control for an Electric 4WD vehicle subject to Input Contraints, 11th International Conference on Diagnosis of Processes and Systems, DPS 2013, Lagow Lubuski, Poland, 8-11 September 2013.

Résumé : Cette thèse s'intéresse à la conception de lois de commandes tolérantes aux fautes d'actionneurs pour des systèmes linéaires en tenant compte de la saturation de ces actionneurs. Pour le système nominal, un contrôleur à "faible-grand" gain est déterminé en utilisant la théorie de stabilité de Lyapunov et en résolvant une équation linéaire matricielle (LMI). Un algorithme itératif, basé sur des équations de Ricatti, est proposé pour trouver ce contrôleur. L'analyse du système linéaire commandé, soumis à la saturation des actionneurs et en présence de défauts, est réalisée en calculant les ellipsoïdes d'attraction (régions de stabilité) et de performance. Dans le cas où l'état initial n'est pas dans la région d'attraction, une technique d'ajustement des références est proposée. Ceci permet d'agrandir la région de stabilisation. En présence de certains défauts d'actionneurs, l'influence de la faute est analysée afin de savoir si le système reste stable ou non, et si les performances sont influencées par le défaut. Deux principales méthodes de commande tolérante, l'une passive, l'autre active sont utilisées pour tolérer les défauts, en évitant de saturer l'actionneur. Le contrôleur tolérant passif est en fait un contrôleur robuste à certains défauts, il peut garantir que le système fonctionne avec des performances dégradées dans une petite région de la stabilité qui est fixée par le pire des cas de défaut. Le contrôleur actif utilise l'estimation du défaut fournie par un observateur pour tolérer le défaut. Il est cependant difficile d'analyser la région de stabilité du système lorsque la commande active est utilisée du fait que cette commande dépend du défaut. Un nouveau schéma de FTC basé sur la technique de réglage de référence est proposé afin de garantir les performances du système dans une région acceptable. Plusieurs exemples académiques sont traités tout au long de la thèse pour illustrer les méthodes. Enfin, la méthodologie est appliquée au problème de suivi de trajectoire d'un véhicule électrique (EV) qui a 4 roues motrices (4WD). En tenant compte des contraintes de glissement de la roue, un contrôleur est proposé pour maintenir la stabilité du système et garantir les performances de suivi acceptables. Enfin, une méthode de diagnostic actif de défaut est proposée pour ce système suractionné afin d'isoler et d'évaluer plus précisément les défauts. Avec cette information précise de diagnostic, une FTC est synthétisée afin de maintenir au mieux les performances de poursuite.

Abstract: In this thesis, we deal with the FTC design problem for a linear system with both input constraints and actuator faults. For the nominal system, a low-high gain controller is designed based on the Lyapunov stability theory and the solution of LMI. An iterative Ricatti equation algorithm is given to find such controller. Based on the designed controller, with the analysis of the linear system subject to actuator saturation, the invariant ellipsoids of attraction and performance regions are calculated. For the case that the initial state is not within the attraction region, a novel methodology based on the reference adjustment technique is proposed in the thesis to achieve large-region stabilization. For the system with certain actuator faults, the fault's influence is analysed first, its size and the time when it happens will decide whether the system is stable or not and will influence the system's performance. Then two main FTC design methods (PFTC and AFTC) are used to cope with faults and actuator saturation together. The proposed PFTC and AFTC methods have both their restrictions when dealing with the input saturation problem: Since the passive fault-tolerant controller is designed for presumed faults, it can guarantee that the system operates with degraded performance in a small stability region which is decided by the worst fault case. For the AFTC method, the degraded performance caused by faults will be recovered by designing an observer to obtain the fault information. However, its control capability will be reduced due to the fault, and it is hard to analyse the system's stability region. Based on the existing performance analysis principle and the implementation results of PFTC and AFTC, a novel fault-tolerant control scheme based on the reference adjustment technique is proposed to guarantee the system's performance in an acceptable region. Several academic examples are taken all along the thesis to illustrate the methods. Finally, the methodology is applied to the path tracking problem of an electric vehicle (EV) which has four electromechanical wheel-driven (4WD vehicle) systems under normal and faulty conditions.